

FLEXURAL AND SHEAR BEHAVIOUR OF FRP-RC MEMBERS

BY

CARLOS P. MOTA

A Thesis submitted to
The Faculty of Graduate Studies
In Partial Fulfillment of the Requirements for the Degree of

MASTER OF SCIENCE

Department of Civil Engineering
University of Manitoba
Winnipeg, Manitoba

© Carlos P. Mota, July 2005

500 University Centre, University of Manitoba
Winnipeg, Manitoba, R3T 2N2

THE UNIVERSITY OF MANITOBA
FACULTY OF GRADUATE STUDIES

COPYRIGHT PERMISSION

“Flexural and Shear Behaviour of FRP-RC Members”

BY

Carlos P. Mota

**A Thesis/Practicum submitted to the Faculty of Graduate Studies of The University of
Manitoba in partial fulfillment of the requirement of the degree
Of
MASTER OF SCIENCE**

Carlos P. Mota © 2005

Permission has been granted to the Library of the University of Manitoba to lend or sell copies of this thesis/practicum, to the National Library of Canada to microfilm this thesis and to lend or sell copies of the film, and to University Microfilms Inc. to publish an abstract of this thesis/practicum.

This reproduction or copy of this thesis has been made available by authority of the copyright owner solely for the purpose of private study and research, and may only be reproduced and copied as permitted by copyright laws or with express written authorization from the copyright owner.

Abstract

The design of fibre-reinforced polymer reinforced concrete (FRP-RC) is typically governed by serviceability limit state requirements rather than ultimate limit state requirements as conventional reinforced concrete is. Thus, a method is needed that can predict the expected service load deflections of fibre-reinforced polymer (FRP) reinforced members with a reasonably high degree of accuracy.

A need to develop an accurate equation which can predict the concrete contribution to shear has also arisen as a result of the differences between the behaviour of FRP-RC members and conventional steel reinforced concrete (RC) members. The objective of the thesis is to evaluate existing formulas for predicting the deflection and concrete shear capacity of FRP reinforced concrete beams.

An experimental investigation was undertaken to test FRP-RC beams which contained no stirrups and failed in shear. These beams allowed for a direct calculation of the concrete contribution to shear to be made since no stirrups were present. Based upon the experimental results, code equations of determining the concrete contribution to shear and the midspan deflection of the beams were evaluated. Here, it was found that the JSCE equation was the most accurate for predicting the concrete contribution to shear, while the CSA S806-02 was the most accurate for predicting the deflection behaviour.

A parametric study was completed to increase the number of members being analyzed. Eleven methods of deflection calculation are compared to the experimental deflection of

197 beams tested by other investigators, while eight methods of shear calculation are compared to the experimental failure load of 89 beams that failed in shear and did not contain stirrups. These beams are reinforced longitudinally with aramid FRP (AFRP), glass FRP (GFRP), or carbon FRP (CFRP) bars, have different reinforcement ratios, geometric and material properties. All beams were tested under monotonically applied load in four point bending configuration. The analysis revealed that the equation proposed in this thesis is well suited to deflection calculation at the service load level, while the equation proposed by the JSCE is well suited for calculating the concrete shear capacity of a member.

Acknowledgements

The author would like to express his sincerest gratitude and appreciation toward Dr. Dagmar Svecova. This work could not have been done without her continual guidance and support and the author is extremely thankful to have had the opportunity to work with her.

The author would also like to express his gratitude and appreciation toward Dr. Aftab Mufti for his support with this thesis. His support is appreciated and the author is thankful to have been able to work with him.

The author would also like to express his gratitude towards the lab technicians at the University of Manitoba, Mr. Moray McVey, Mr. Grant Whiteside and Mr. Chad Klowak, for their assistance during the experimental program of the thesis. The assistance of Ms. Sandee Alminar, Mr. Marc Lanoie and Mr. Rahul Bhattacharyya is also gratefully acknowledged.

The author would also like to gratefully acknowledge the Cement Association of Canada for their financial support throughout the entirety of the project.

Finally, the author would like to express his gratitude towards his family and friends for their support and continual encouragement. In particular, a special thank you goes out to Ms. Jocelyn Mamchur for her unending support over the duration of this thesis.

Table of Contents

Abstract	ii
Acknowledgements	iv
Table of Contents	v
List of Figures	ix
List of Tables	xii
Notation	xiii
Chapter 1 - Introduction	1
1.1 - General	1
1.2 - Objectives	2
1.3 - Scope	2
Chapter 2 - Background	4
2.1 - Shear Capacity of Concrete	4
2.1.1 - Concrete Shear Capacity of Conventional RC Beams	4
2.1.1.1 - CSA A23.3-94 Simplified Method (1998)	5
2.1.1.2 - CSA A23.3-94 General Method (1998)	5
2.1.2 - Concrete Shear Capacity of FRP-RC Beams	6
2.1.2.1 – The JSCE Method (1997)	7
2.1.2.2 - Equations Proposed by Deitz (1998)	8
2.1.2.3 – The ISIS M03-01 Method (2001)	9
2.1.2.4 – The CSA S806-02 Method (2002)	10
2.1.2.5 – The ACI 440.1R-03 Method (2003)	10
2.1.2.6 - Proposed Revision to the ACI 440.1R (2004)	11

2.1.2.7 - Equation Proposed by Razaqpur (2004).....	11
2.1.3 – Inclusion of Member Weight in Shear Analysis.....	12
2.2 - Deflection Behaviour.....	13
2.2.1 - Deflection Behaviour of Conventional RC Beams.....	13
2.2.1.1 - CSA A23.3-94 (1998) Effective Moment of Inertia Equation	14
2.2.1.2 - CSA A23.3-94 (1998) Bi-Linear Method.....	14
2.2.2 - Deflection Behaviour of FRP-RC Beams.....	15
2.2.2.1 - Equation Proposed by Faza and GangaRao (1992).....	16
2.2.2.2 - Equation Proposed by Benmokrane et al. (1996).....	17
2.2.2.3 - Equation Proposed by Brown and Bartholomew (1996).....	17
2.2.2.4 - Equation Proposed by Toutanji and Saafi (2000).....	18
2.2.2.5 – The ISIS M03-01 Method (2001)	18
2.2.2.6 – The CSA S806-02 Method (2002).....	19
2.2.2.7 – The ACI 440.1R-03 Method (2003)	20
2.2.2.8 - Equation Proposed by Yost et al. (2003).....	20
2.2.2.9 - Proposed Revision to the ACI 440.1R (2004).....	21
2.2.2.10 - Equation Proposed by Bischoff (2005)	21
2.2.3 – Inclusion of Member Weight in Deflection Analysis.....	22
Chapter 3 - Experimental Program	23
3.1 - Overview	23
3.2 - Beam Details.....	23
3.3 - Instrumentation and Testing	26
3.4 – Test Results.....	27

3.4.1 - Failure Loads	27
3.4.2 - Deflection Behaviour.....	31
3.4.2.1 – Steel RC Beams	32
3.4.2.2 - FRP-RC Beams.....	35
Chapter 4 - Parametric Study	39
4.1 - Introduction	39
4.2 - Statistical Analysis	43
4.3 - Analysis of Cracking Load	45
4.4 - Shear Analysis	46
4.5 - Deflection Analysis	56
4.5.1 - Derivation of Proposed Deflection Equation.....	59
4.5.2 - Deflection Analysis at Service	65
4.5.3 - Deflection Analysis at Load Levels close to Cracking.....	71
4.5.4 - Deflection Analysis at 50% of Failure Load	79
4.5.5 - Deflection Analysis at 80% of Failure Load	86
Chapter 5 - Summary and Conclusions	93
5.1 - Experimental Program.....	93
5.2 - Parametric Study.....	95
References.....	99
Appendix I – Properties of Members used in the Parametric Study.....	110
AFRP-RC Deflection Members.....	111
CFRP-RC Deflection Members	112
GFRP-RC Deflection Members.....	117

AFRP-RC Shear Members.....	129
CFRP-RC Shear Members.....	130
GFRP-RC Shear Members.....	134
Appendix II – Details of Members tested by Mota (2004).....	139

List of Figures

Figure 1.1 - Stress versus Strain Curves for Steel and FRP.....	1
Figure 2.1 - Shear Failure in Beam # 4L-C	4
Figure 2.2 - Comparison of FRP-RC Beams and Steel RC Beams (Michaluk, 1995)	7
Figure 2.3 - Idealized Curvature According to Faza and GangaRao (1992)	16
Figure 2.4 – Idealized Curvature According to the CSA S806-02 (2002).....	19
Figure 3.1 - Test Setup.....	24
Figure 3.2 – Coring of Concrete Cylinders.....	25
Figure 3.3 – Beam Instrumentation	27
Figure 3.4 –Shear Failure for Beams 3A, 4L-C, and 4S-20-A	29
Figure 3.5 – Effect of Reinforcement Type on Flexural Behaviour	32
Figure 3.6 - Load Deflection Behaviour for Beam # 4S-20-A	34
Figure 3.7 - Load Deflection Behaviour for Beam # 4S-20-B	34
Figure 3.8 - Load Deflection Behaviour for Beam # 3A	35
Figure 3.9 - Load Deflection Behaviour for Beam # 4L-A	36
Figure 3.10 - Load Deflection Behaviour for Beam # 4L-B.....	36
Figure 3.11 - Load Deflection Behaviour for Beam # 4L-C.....	37
Figure 3.12 - Load Deflection Behaviour for Beam # 4L-D	37
Figure 4.1 - Screenshot for data Entry form in Shear Database for ROD reinforcement.	40
Figure 4.2 - Screenshot for data Entry form in Shear Database for MESH reinforcement	41
Figure 4.3 – Screenshot for data Entry form in Deflection Database for ROD reinforcement	41

Figure 4.4 - Screenshot for data Entry form in Deflection Database for MESH reinforcement	42
Figure 4.5 - Effect of Modulus on Concrete Shear Prediction for GFRP-RC	48
Figure 4.6 - Effect of Modulus on Concrete Shear Prediction for CFRP-RC	50
Figure 4.7 - Effect of Modulus on Concrete Shear Prediction for CFRP-RC without Outlier Point.....	51
Figure 4.8 - Effect of Effective Depth on Shear Prediction.....	52
Figure 4.9 - Effect of Slenderness on Shear Prediction.....	55
Figure 4.10 - Effect of Concrete Strength on Shear Prediction.....	55
Figure 4.11 - Moment-Curvature Relationship for Beam BC2H (Theriault et al., 1997)	58
Figure 4.12 - Effect of Applied Moment on Deflection Prediction.....	59
Figure 4.13 - Load Deflection Behaviour for Beam # 3A	62
Figure 4.14 - Load Deflection Behaviour for Beam # 4L-A	63
Figure 4.15 - Load Deflection Behaviour for Beam # 4L-B.....	63
Figure 4.16 - Load Deflection Behaviour for Beam # 4L-C.....	64
Figure 4.17 - Load Deflection Behaviour for Beam # 4L-D	64
Figure 4.18 - Effect of Modulus on Deflection Prediction at Service for GFRP-RC.....	66
Figure 4.19 - Effect of Modulus on Deflection Prediction at Service for CFRP-RC	66
Figure 4.20 - Effect of Slenderness on Deflection Prediction at Service	70
Figure 4.21 - Effect of Relative Reinforcement Ratio on Deflection Prediction at Service	70
Figure 4.22 - Effect of Modulus on Deflection Prediction at $1.1P_{cr}$ for GFRP-RC.....	72
Figure 4.23 - Effect of Modulus on Deflection Prediction at $1.1P_{cr}$ for CFRP-RC.....	72

Figure 4.24 - Effect of Relative Reinforcement Ratio on Deflection Prediction for Over-Reinforced Members at $1.1P_{cr}$ 75

Figure 4.25 - Effect of Relative Reinforcement Ratio on Deflection Prediction for Under-Reinforced Members at $1.1P_{cr}$ 76

Figure 4.26 - Effect of Modulus on Deflection Prediction at $0.5P_{max}$ for GFRP-RC 80

Figure 4.27 - Effect of Modulus on Deflection Prediction at $0.5P_{max}$ for CFRP-RC 80

Figure 4.28 - Effect of Relative Reinforcement Ratio on Deflection Prediction for Over-Reinforced Members at $0.5P_{max}$ 83

Figure 4.29 - Effect of Relative Reinforcement Ratio on Deflection Prediction for Under-Reinforced Members at $0.5P_{max}$ 84

Figure 4.30 - Effect of Modulus on Deflection Prediction at $0.8P_{max}$ for GFRP-RC 86

Figure 4.31 - Effect of Modulus on Deflection Prediction at $0.8P_{max}$ for CFRP-RC 88

Figure 4.32 - Effect of Relative Reinforcement Ratio on Deflection Prediction for Over-Reinforced Members at $0.8P_{max}$ 89

Figure 4.33 - Effect of Relative Reinforcement Ratio on Deflection Prediction for Under-Reinforced Members at $0.8P_{max}$ 90

List of Tables

Table 3.1 - Beam Properties for Steel Reinforced Beams	24
Table 3.2 - Beam Properties for CFRP Reinforced Beams	24
Table 3.3 - Properties of Concrete Cylinders.....	26
Table 3.4 – Beam Failure Loads	28
Table 3.5 – Comparison between Experimental and Theoretical Cracking Moments	29
Table 3.6 – Summary of the Concrete Shear Capacities (kN) of the FRP-RC Beams	31
Table 3.7 - Ratio of Experimental over Predicted Concrete Shear Capacity.....	31
Table 4.1 - Ranges of Properties Present in the Database	42
Table 4.2 - Comparison of Typical Statistics to Log Transform Statistics.....	44
Table 4.3 - Accuracy of Design Methods for Calculating Modulus of Rupture.....	46
Table 4.4 - Statistical Analysis of the Predicted Shear Capacity.....	49
Table 4.5 - Further Analysis of the Predicted Shear Capacity.....	54
Table 4.6 - Correlation Analysis at Service Load.....	60
Table 4.7 - Statistical Analysis of the Predicted Deflections at Service.....	67
Table 4.8 - Statistical Analysis of the Predicted Deflections at $1.1P_{cr}$	73
Table 4.9 - Further Analysis of the Predicted Deflections at $1.1P_{cr}$	78
Table 4.10 - Statistical Analysis of the Predicted Deflections at $0.5P_{max}$	81
Table 4.11 - Further Analysis of the Predicted Deflections at $0.5P_{max}$	85
Table 4.12 - Statistical Analysis of the Predicted Deflections at $0.8P_{max}$	87
Table 4.13 - Further Analysis of the Predicted Deflections at $0.8P_{max}$	92

Notation

The following symbols are used in this thesis

AFRP	=	aramid fibre-reinforced polymer
A_{frp}	=	area of FRP reinforcement in the longitudinal direction [mm^2]
A_s	=	area of steel reinforcement in the longitudinal direction [mm^2]
a	=	shear span [mm]
a/d	=	slenderness ratio
b	=	beam width [mm]
CFRP	=	carbon fibre-reinforced polymer
c	=	depth of neutral axis [mm]
d	=	effective depth [mm]
d_b	=	bar diameter [mm]
E_c	=	modulus of elasticity of concrete [MPa]
E_{frp}	=	modulus of elasticity of FRP [MPa]
E_s	=	modulus of elasticity of steel [MPa]
FRP	=	fibre-reinforced polymer
f_c	=	concrete compressive strength [MPa]
f_{frpu}	=	ultimate strength of FRP reinforcement [MPa]
f_r	=	modulus of rupture of concrete [MPa]
f_{vcd}	=	compressive strength coefficient used in the JSCE (1997) equation for shear [MPa]
f_y	=	yield strength of steel reinforcement [MPa]
GFRP	=	glass fibre-reinforced polymer

h	=	beam height [mm]
I	=	moment of inertia [mm^4]
I_{cr}	=	moment of inertia of cracked section transformed to concrete [mm^4]
I_e	=	effective moment of inertia [mm^4]
I_g	=	moment of inertia of gross section [mm^4]
I_g/I_{cr}	=	ratio of the gross moment of inertia to the cracked moment of inertia
I_T	=	moment of inertia of section transformed to concrete [mm^4]
k_a	=	slenderness coefficient used in Razaqpur et al. (2004) shear equation
k_s	=	size effect coefficient used in Razaqpur et al. (2004) shear equation
L	=	span of the beam [mm]
L_{cr}	=	uncracked span of the beam [mm]
LVDT	=	linear variable displacement transducer
M_a	=	applied moment [Nmm]
M_{cr}	=	cracking moment [Nmm]
M_f	=	factored moment [Nmm]
M_n	=	nominal moment capacity [Nmm]
M_{serv}	=	service moment [Nmm]
M_{ult}	=	ultimate moment capacity [Nmm]
m	=	order coefficient used in Toutanji and Saafi (2000) I_e equation
n	=	number of samples present in statistical analysis
P	=	applied load [N]
P_{cr}	=	cracking load [N]
P_{max}	=	failure load [N]

P_{serv}	=	service load [N]
RC	=	reinforced concrete
V_c	=	concrete shear capacity [N]
V_f	=	factored shear force [N]
y_t	=	distance from the centroid of the beam to outmost compressive fibre [mm]
α_1	=	CSA A23.3-94 (1998) concrete stress block factor
β	=	reduction coefficient used in ACI 440.1R-03 (2003), Yost et al. (2003), Proposed ACI 440.1R (2004), and Mota deflection equations
β_1	=	CSA A23.3-94 (1998) concrete stress block factor
$\beta_{1,ACI}$	=	ACI 318 (1999) concrete stress block factor
β_d	=	size effect coefficient used in JSCE (1997) shear equation
β_E	=	FRP type coefficient used in Mota deflection equation
β_n	=	FRP modulus coefficient used in JSCE (1997) shear equation
β_p	=	prestressing coefficient used in JSCE (1997) shear equation
β_ρ	=	relative reinforcement coefficient used in Mota deflection equation
γ_{sw}	=	density of the beam [N/mm ³]
Δ	=	immediate deflection under a given load [mm]
ϵ_c	=	strain in the extreme concrete compressive fibre
ϵ_c'	=	strain in the extreme concrete compressive fibre at peak concrete stress
ϵ_{cu}	=	strain in the extreme concrete compressive fibre when concrete crushing begins
ϵ_{frp}	=	strain in the FRP reinforcement

ε_{frps}	=	strain in the FRP reinforcement at the service load level
ε_{frpu}	=	rupture strain in the FRP reinforcement
ε_y	=	strain in the steel reinforcement when yielding commences
η	=	coefficient used in the CSA S806-02 (2002) deflection equation
η_{frp}	=	FRP modular ratio
κ	=	ratio of the neutral axis at cracking to the effective depth
μ_y	=	mean of the ratios in the natural log scale
ρ	=	reinforcement ratio
ρ_{bal}	=	balanced reinforcement ratio
ρ_{frp}	=	FRP reinforcement ratio
ρ/ρ_{bal}	=	relative reinforcement ratio
ρ_s	=	steel reinforcement ratio
σ_y	=	standard deviation of the ratios in the natural log scale
Ψ_{serv}	=	curvature in the member at the service load level [mm ⁻¹]
Ψ_{ult}	=	curvature in the member at the ultimate load level [mm ⁻¹]

Chapter 1 - Introduction

1.1 - General

Fibre-reinforced polymer (FRP) reinforcing bars are currently available as a substitute for steel reinforcement in concrete structures that may be vulnerable to attack by aggressive corrosive agents. In addition to superior durability, FRP reinforcing bars have a much higher strength than conventional mild steel. However, FRP bars exhibit elastic stress-strain behaviour and a brittle failure. This is quite different from the behaviour of steel, as can be seen in Figure 1.1. Thus, different design methodologies are required than for conventional reinforced concrete.

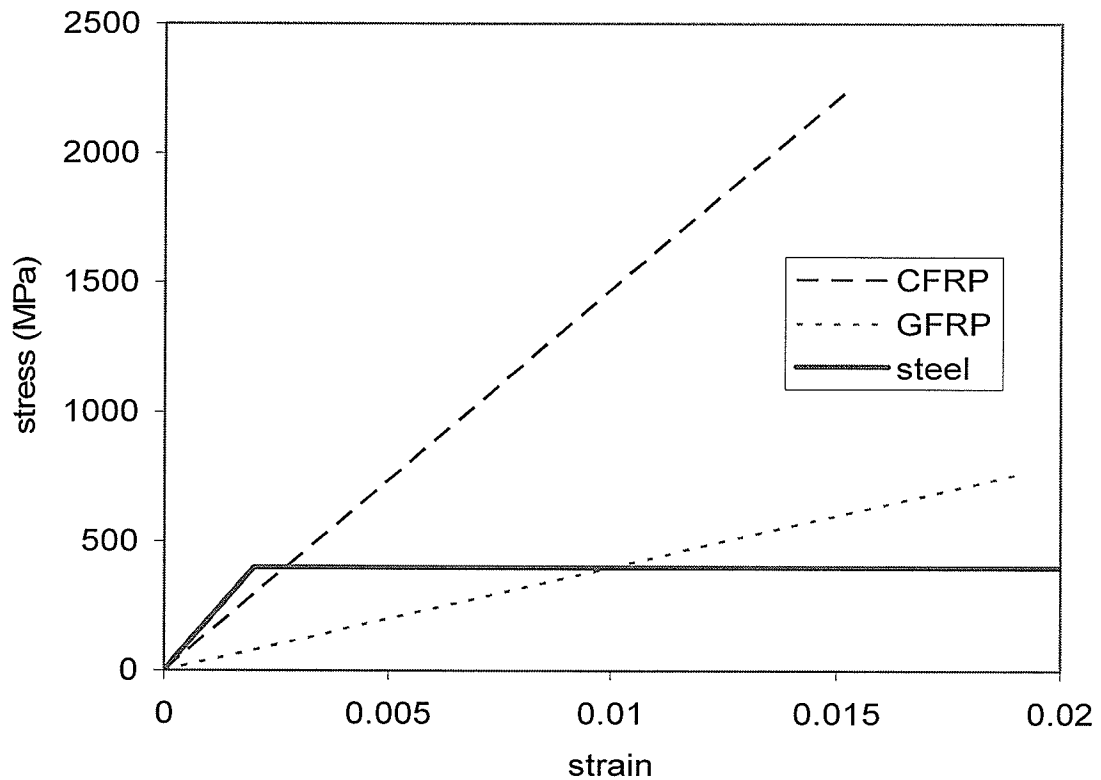


Figure 1.1 - Stress versus Strain Curves for Steel and FRP

1.2 - Objectives

With the acceptance of FRP materials as a viable substitute for steel reinforcement in reinforced concrete (RC) structures, the need to develop a code with accurate equations for designing concrete structures reinforced with FRP materials has arisen. The main objective of this thesis is to aid in the progression of a design code for FRP reinforced concrete (FRP-RC). The specific objectives of this thesis are:

1. To determine an equation that is both accurate and conservative for predicting the immediate deflection of FRP-RC beams.
2. To determine an equation that is both accurate and conservative for predicting the concrete contribution to shear strength.

1.3 - Scope

The scope of this investigation was limited to the shear and flexural behaviour of reinforced concrete beams. The research program consisted of an experimental investigation of FRP-RC beams. A database containing information from 197 FRP-RC members was assembled and statistical analysis of the deflection behaviour of the members was performed. Similarly, a database containing information from 89 FRP-RC members, which failed in shear and contained no stirrups, was assembled and statistical analysis of the concrete shear capacity of the members was performed. Both steel and FRP reinforced concrete beams have been used in the experimental program and the beams were tested under monotonic four-point bending. Fatigue performance and long-term deflection of the reinforced beams have not been investigated. The shear behaviour of beams containing transverse reinforcement has also not been considered, nor have

shear deformations. Furthermore, to avoid the effects of arching action in the shear analysis, only slender members were considered. Based upon the results of the parametric study, existing models that predict the shear strength and deflection behaviour were evaluated.

Chapter 2 - Background

2.1 - Shear Capacity of Concrete

A well designed reinforced concrete beam should never fail in shear when exposed to the ultimate failure conditions as shear failures provide very little warning of an impending failure and can be quite violent in nature. A shear failure can be characterized by a diagonal crack propagating through the entire depth of a beam towards the applied load and can be avoided by providing adequate transverse reinforcement in a beam. An example of a shear failure can be seen in Figure 2.1.

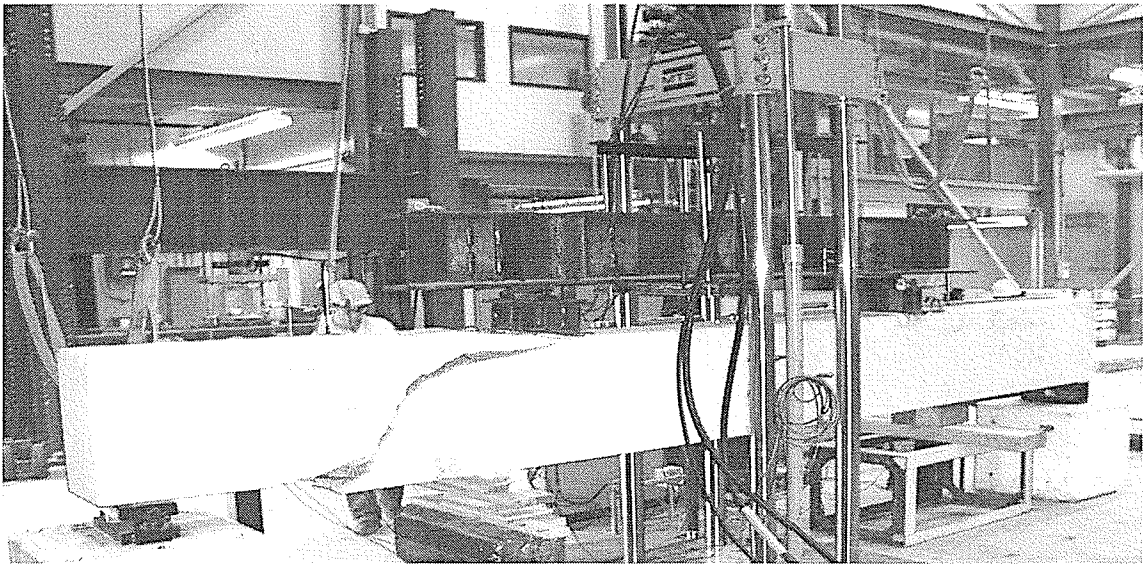


Figure 2.1 - Shear Failure in Beam # 4L-C

2.1.1 - Concrete Shear Capacity of Conventional RC Beams

Given the complexity of the nature of shear failures, the shear capacity of a reinforced concrete beam is typically found empirically. Since the various codes all have slightly different equations for determining the shear capacity of a beam, several codes were used to determine the shear capacity of the beams and the accuracy of each formula when

compared to experimental results. Various equations proposed by independent researchers were also considered in this research. To study the concrete contribution to the shear capacity V_c , the beams tested in the laboratory did not contain any stirrups. Here, material resistance factors were not applied to give an accurate comparison to the experimental results. In the following, different methods used to calculate V_c will be discussed.

2.1.1.1 - CSA A23.3-94 Simplified Method (1998)

Based on an assumption that the shear crack propagates at an angle of 45° , the CSA A23.3-94 (1998) has derived empirical formulas for the concrete shear capacity that are dependant only on the cross-sectional area and the concrete strength. These equations were derived primarily to give conservative estimates of the capacity of the concrete. The CSA A23.3-94 (1998) has noted that there is a size effect factor that influences the concrete contribution to shear and has thus limited the use of Equation 2.1 to sections with an effective depth not exceeding 300 mm. The shear capacity of sections larger than this should be calculated with the use of Equation 2.2.

$$V_c = 0.2\sqrt{f'_c}bd \quad d \leq 300mm \quad \text{Equation 2.1}$$

$$V_c = \left(\frac{260}{1000 + d} \right) \sqrt{f'_c}bd \geq 0.1\sqrt{f'_c}bd \quad d > 300mm \quad \text{Equation 2.2}$$

2.1.1.2 - CSA A23.3-94 General Method (1998)

The CSA A23.3-94 (1998) has derived a more accurate method for calculating the concrete contribution to shear known as the General Method. This method not only predicts the concrete shear capacity, but also predicts the angle of the shear failure. The

downfall to the General Method is that the method requires the use of various tables and figures and cannot be summarized by a formula. Given that the objective of this thesis was to determine a simple formula for calculating the concrete shear resistance, the General Method was not considered.

2.1.2 - Concrete Shear Capacity of FRP-RC Beams

If the reinforcement is FRP, intuition may lead to the belief that since Equations 2.1 and 2.2 are only predicting the concrete contribution to shear, that these equations are independent on the type of reinforcement used. However, given the empirical nature of these formulas, this is not the case. In studying the differences between the behaviour of steel reinforced concrete and FRP reinforced concrete, it can be better understood why the concrete shear strength would be greater for beams reinforced by steel than beams reinforced by FRP.

Testing has repeatedly shown that beams reinforced by FRP materials experience fewer cracks than beams reinforced by steel. Given that FRP materials have a lower modulus of elasticity than steel, it is a known fact that the curvature must be greater for beams reinforced with FRP. Thus, the crack widths in beams reinforced with FRP must be greater than those present in similar steel reinforced concrete beams to allow for this increase in curvature. This effect can better be seen in Figure 2.2. Here, the second beam from the bottom is reinforced with steel reinforcing bars, while the other beams are all reinforced with CFRP bars at the same reinforcement ratio. It can easily be seen that the beam reinforced with steel has many more cracks than those reinforced with CFRP, even though the same amount of reinforcement was used.

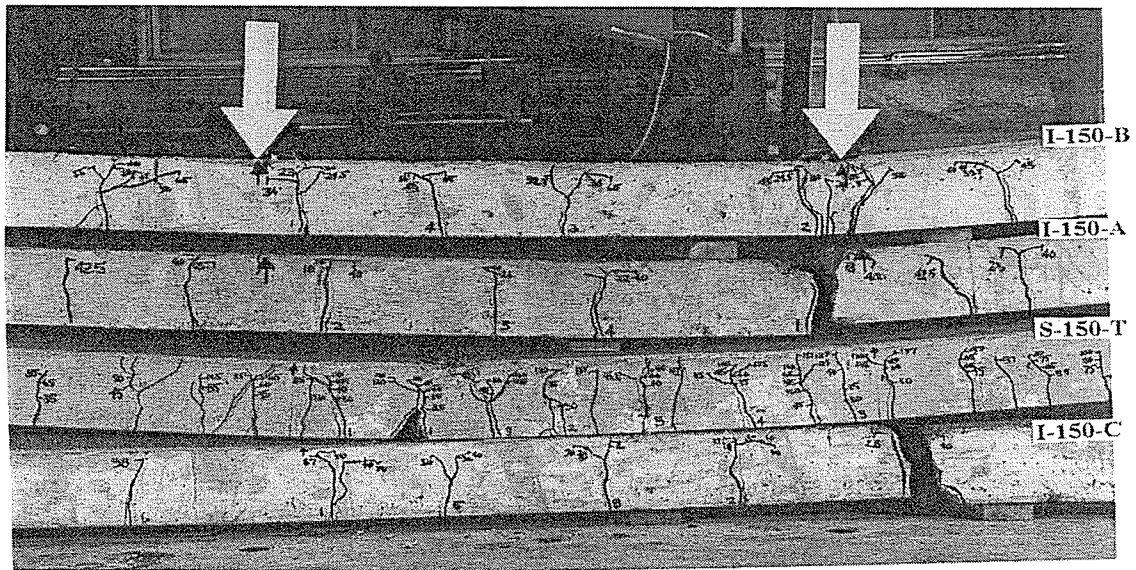


Figure 2.2 - Comparison of FRP-RC Beams and Steel RC Beams (Michaluk, 1995)

Wider cracks present in FRP-RC beams as compared to steel reinforced beams reduce the concrete contribution to shear by minimizing the amount of aggregate interlock present between the cracks of the beam. The increased curvature also means that the neutral axis must be higher in beams reinforced with FRP than in beams reinforced with steel. This effect eliminates some concrete contribution to shear by reducing the amount of uncracked concrete in the compression zone. The final reduction in shear capacity comes from the poor dowel action from the reinforcing bars when FRP reinforcement is used since FRP is relatively weak in the transverse direction. Since the concrete contribution to shear is less when FRP is the flexural reinforcement rather than steel, new equations have been developed to determine the concrete contribution to shear.

2.1.2.1 – The JSCE Method (1997)

The Japanese Society for Civil Engineers (JSCE) has developed an equation to calculate the concrete contribution to shear based on multiplying the cross-sectional area by a number of factors. The equation accounts for the size effect with a factor β_d , the modulus

of the FRP with a factor β_p , and any prestressing effects with a factor β_n . With the use of a factor f_{vcd} , the equation also assumes that there is a limit on the shear strength of concrete and that higher strength concrete does not guarantee a higher shear resistance. The JSCE (1997) formula for the concrete contribution to shear has thus included a great deal of parameters in its derivation and is presented in Equations 2.3 to 2.7.

$$V_c = \beta_d \beta_p \beta_n f_{vcd} b d \quad \text{Equation 2.3}$$

$$\beta_d = (1000 / d)^{1/4} \leq 1.5 \quad \text{Equation 2.4}$$

$$\beta_p = (100 \rho_{frp} E_{frp} / E_s)^{1/3} \leq 1.5 \quad \text{Equation 2.5}$$

$$\beta_n = 1 \text{ for non-prestressed member} \quad \text{Equation 2.6}$$

$$f_{vcd} = 0.2(f'_c)^{1/3} \leq 0.72 \quad \text{Equation 2.7}$$

2.1.2.2 - Equations Proposed by Deitz (1998)

The derivations of the equations proposed by Deitz (1998) are based on empirical relationships which were found for the shear strength of FRP-RC slabs tested and failed in shear. In this method, the primary reason for the reduction in shear capacity when FRP is used as opposed to steel reinforcement is the lower modulus of elasticity of FRP. Thus, equations were derived which included a ratio of these terms to predict the concrete shear capacity of FRP-RC beams. These formulas come in both a simplified and a detailed form.

Simplified Method

The simplified method proposed by Deitz (1998) is derived from Equation 2.1 and has been modified slightly to include the ratio of the FRP modulus to the steel modulus. The simplified formula proposed can be found in Equation 2.8.

$$V_c = \frac{1}{2} \sqrt{f'_c} b d \frac{E_{frp}}{E_s} \quad \text{Equation 2.8}$$

Detailed Method

The detailed method proposed by Deitz (1998) also includes the ratio of the modulus of the FRP to the steel modulus. However, unlike the simplified method, the detailed method also accounts for the amount of flexural reinforcement present in the beam, as well as the slenderness of the beam. The detailed method for calculating the concrete shear capacity can be found in Equation 2.9.

$$V_c = \frac{3}{7} \left(\sqrt{f'_c} + 120 \rho_{frp} \frac{V_f d}{M_f} \right) b d \frac{E_{frp}}{E_s} \leq 0.9 \sqrt{f'_c} b d \frac{E_{frp}}{E_s} \quad \text{Equation 2.9}$$

2.1.2.3 – The ISIS M03-01 Method (2001)

ISIS M03-01 (2001) has noted that the basic form of Equations 2.1 and 2.2 could remain the same if they were modified to account for the use of FRP materials, rather than steel. According to ISIS M03-01 (2001), the primary reason for the concrete shear capacity to be lower in FRP-RC beams when compared to conventional RC beams is because FRP has a lower modulus of elasticity. Thus, Equations 2.1 and 2.2 were modified to include a ratio of the modulus of FRP divided by the modulus of steel. After comparing the results of the modified formulas to experimental results, it was found that the formulas would be

better modified with the square root of this ratio, which was contrary to what Deitz (1998) had previously found. As such, ISIS M03-01 (2001) has recommended the use of Equations 2.10 and 2.11 to calculate the concrete contribution to shear.

$$V_c = 0.2\sqrt{f'_c}bd\sqrt{E_{frp}/E_s} \quad d \leq 300mm \quad \text{Equation 2.10}$$

$$V_c = \left(\frac{260}{1000+d}\right)\sqrt{f'_c}bd\sqrt{E_{frp}/E_s} \geq 0.1\sqrt{f'_c}bd\sqrt{E_{frp}/E_s} \quad d > 300mm \quad \text{Equation 2.11}$$

2.1.2.4 – The CSA S806-02 Method (2002)

The CSA S806-02 (2002) has used the same assumption as the CSA A23.3-94 (1998) that the shear crack propagates at an angle of 45^0 to develop empirical formulas for the concrete shear capacity that are dependant only on the cross-sectional area and the concrete strength. Similar in form to Equations 2.1 and 2.2, the CSA S806-02 (2002) has reduced the concrete contribution to shear strength when FRP is the reinforcing bar. The CSA S806-02 (2002) has also noted that there is a size effect factor that influences the concrete contribution to shear and has thus developed Equations 2.12 and 2.13 to be dependent upon the effective depth, d , of the beam.

$$V_c = 0.035\left(f'_c \rho_{frp} E_{frp} \frac{V_f d}{M_f}\right)^{1/3} \quad bd \geq 0.1\sqrt{f'_c}bd \leq 0.2\sqrt{f'_c}bd \quad d \leq 300mm \quad \text{Equation 2.12}$$

$$V_c = \left(\frac{130}{1000+d}\right)\sqrt{f'_c}bd \geq 0.08\sqrt{f'_c}bd \quad d > 300mm \quad \text{Equation 2.13}$$

2.1.2.5 – The ACI 440.1R-03 Method (2003)

The ACI 440.1R-03 (2003) has developed an equation to calculate the concrete contribution to shear in a very simple manner which is dependent upon both the modulus

of elasticity of the FRP reinforcement as well as the reinforcement ratio. The ACI 440.1R-03 (2003) has recommended the use of Equation 2.14 to calculate the concrete contribution to shear.

$$V_c = \frac{1}{6} \frac{\rho_{frp} E_{frp} b d}{90 \beta_{1,ACI} \sqrt{f'_c}} \leq \frac{1}{6} \sqrt{f'_c} b d \quad \text{Equation 2.14}$$

$$\beta_{1,ACI} = 1.05 - 0.05 \left(\frac{f'_c}{6.895} \right) \geq 0.65 \leq 0.85 \quad \text{Equation 2.15}$$

2.1.2.6 - Proposed Revision to the ACI 440.1R (2004)

Equation 2.14 was found to be extremely conservative for calculating the concrete contribution to shear. Therefore, the ACI 440.1R (2004) revisited their equation and simplified it further, while achieving more accurate results than Equation 2.14 had. To do this, the ACI 440.1R (2004) related the term κ , which is the ratio of the neutral axis at cracking divided by the effective depth, to Equation 2.1 and added a modification factor. The new formula, given by Equation 2.16, became more accurate than Equation 2.14, while still giving conservative estimates.

$$V_c = 5\kappa \sqrt{f'_c} b d; \quad V_c \text{ [lbs]}, f'_c \text{ [psi]}, b \text{ [in]}, d \text{ [in]} \quad \text{Equation 2.16}$$

$$\kappa = \sqrt{2\rho_{frp}\eta_{frp} + (\rho_{frp}\eta_{frp})^2} - \rho_{frp}\eta_{frp} \quad \text{Equation 2.17}$$

2.1.2.7 - Equation Proposed by Razaqpur (2004)

The equation proposed by Razaqpur et al. (2004) is similar in nature to the equation given by the JSCE (1997) in that it has a central equation with attached modification factors. The equation proposed by Razaqpur et al. (2004) accounts for the size effect with the

factor K_s , and also accounts for the slenderness of the beam with the introduction of the factor K_a . The equation for calculating the concrete contribution to shear of FRP-RC beams can be found in Equation 2.18, with equations for K_s and K_a , in Equations 2.19 and 2.20, respectively.

$$V_c = 0.035K_sK_a \left[1 + (\rho_{frp} E_{frp})^{1/3} \right] \sqrt{f'_c} \left(\frac{V_f d}{M_f} \right)^{2/3} bd \leq 0.2K_s \sqrt{f'_c} bd \quad \text{Equation 2.18}$$

$$K_s = \frac{750}{450 + d} \leq 1 \quad \text{Equation 2.19}$$

$$K_a = \frac{2.5(V_f d)}{M_f} \geq 1 \quad \text{Equation 2.20}$$

2.1.3 – Inclusion of Member Weight in Shear Analysis

From preliminary analysis, it became apparent that the added shear due to the self-weight of the members could be vital in the analysis of members with large cross-sections. Thus, the self weight of the member is considered in the analysis by assuming a concrete density, γ_{sw} , of 23.5kN/m³, and assuming that the critical section occurs at a distance “d” away from the support. Using these assumptions, the applied shear can be set equal to the concrete shear capacity. Solving for the failure load, P_{max} , Equation 2.21 is derived. This is the expected failure load which would occur due to a shear failure.

$$P_{max} = V_c - \gamma_{sw} bh \left(\frac{L}{2} - d \right) \quad \text{Equation 2.21}$$

2.2 - Deflection Behaviour

Deflections should be within acceptable limits imposed by the use of the structure (for example, supporting attached nonstructural elements without damage). Deflections must be limited from an aesthetic point as well, as large deflections are not aesthetically pleasing and give a sense of insecurity amongst the users of the structure. Thus, it is important to be able to accurately predict the deflections that a beam will incur under a given load. Typically, deflections are considered only at service loads since limiting deflections is a serviceability limit state criterion.

When subjected to four-point bending, the midspan deflection of a beam can be found using Equation 2.22 (CSA A23.3-94). The difficulty in calculating the deflection for RC sections arises from the fact that both the modulus of elasticity, E_c , and the moment of inertia, I , vary with the load.

$$\Delta = \frac{Pa}{24E_c I} (3L^2 - 4a^2) \quad \text{Equation 2.22}$$

2.2.1 - Deflection Behaviour of Conventional RC Beams

Given the complexity of predicting the modulus of elasticity, E_c , and the moment of inertia, I , the deflection behaviour of a reinforced concrete beam is typically found empirically. The most common approach to determining the deflection of a RC beam is to assume that the modulus of elasticity is constant, while only the moment of inertia is changing. An empirical relationship can then be determined to develop an appropriate equation to predict the effective moment of inertia, I_e , to be used in place of I in Equation

2.22. The assumption that the modulus of elasticity is constant is well warranted within service loads but at elevated loads, the same relationship may not be true.

2.2.1.1 - CSA A23.3-94 (1998) Effective Moment of Inertia Equation

The CSA A23.3-94 (1998) Code for designing RC structures has adopted the effective moment of inertia approach for calculating the deflection of a RC beam. The effective moment of inertia, I_e , is based on semi-empirical considerations, and despite some doubt about its applicability to conventional reinforced concrete members subjected to complex loading and boundary conditions, it has yielded satisfactory results in most practical applications over the years. Better known as Branson's formula (1965), the effective moment of inertia can be calculated with the use of Equation 2.23.

$$I_e = \left(\frac{M_{cr}}{M_a} \right)^3 I_g + \left[1 - \left(\frac{M_{cr}}{M_a} \right)^3 \right] I_{cr} \leq I_g \quad \text{Equation 2.23}$$

$$M_{cr} = \frac{f_r I_g}{y_t} \quad \text{Equation 2.24}$$

$$f_r = 0.6 \sqrt{f'_c} \quad \text{Equation 2.25}$$

2.2.1.2 - CSA A23.3-94 (1998) Bi-Linear Method

The CSA A23.3-94 (1998) has also derived a bi-linear method of predicting the deflection. For the bi-linear method, it is assumed that the moment of inertia to be used in Equation 2.22 is the gross moment of inertia, I_g until cracking. After cracking, any load above cracking should be used in place of P in Equation 2.22 and the moment of inertia to be used should be the moment of inertia of the cracked section, I_{cr} . This deflection

should then be added to the deflection at the onset of cracking for the total deflection. The bilinear method of calculating deflection can be summed up by Equations 2.26 and 2.27.

$$\Delta = \frac{Pa}{24E_c I_g} (3L^2 - 4a^2) \quad P \leq P_{cr} \quad \text{Equation 2.26}$$

$$\Delta = \frac{P_{cr} a}{24E_c I_g} (3L^2 - 4a^2) + \frac{(P - P_{cr}) a}{24E_c I_{cr}} (3L^2 - 4a^2) \quad P > P_{cr} \quad \text{Equation 2.27}$$

2.2.2 - Deflection Behaviour of FRP-RC Beams

Knowing that the moment of inertia of FRP-RC is smaller than that of steel RC after cracking, and that deflection is inversely proportional to the moment of inertia, it can be accepted that the deflection for FRP-RC beams is higher than in conventionally reinforced concrete beams at the same load level. Given that Equation 2.23 incorporates the cracked moment of inertia, I_{cr} , in its form, which is dependant upon the modulus of the reinforcing material, it is commonly thought that Equation 2.23 can also be used to predict the deflection of FRP-RC beams. However, given the empirical nature of the formula, this is not the case and Branson's formula (1965) will typically under-predict the deflection when FRP reinforcement is used. Thus, an effort has been made to find an equation which can accurately predict the post cracking deflection for FRP-RC beams. Prior to cracking, a general agreement has been made that the deflection should be calculated with the use of Equation 2.26.

2.2.2.1 - Equation Proposed by Faza and GangaRao (1992)

Faza and GangaRao (1992) used a theoretical approach based on an assumed moment-curvature relationship of FRP-RC to estimate deflections with the use of virtual work. Faza and GangaRao (1992) made the assumption that for 4-point bending, the member would be fully cracked between the load points and partially cracked everywhere else. A deflection equation could thus be derived by assuming that the moment of inertia between the load points was the cracked moment of inertia, and the moment of inertia elsewhere was the effective moment of inertia defined by Equation 2.23. Through the integration of the moment curvature diagram proposed by Faza and GangaRao (1992) in Figure 2.3, the deflection for 4-point loading is defined according to Equation 2.28.

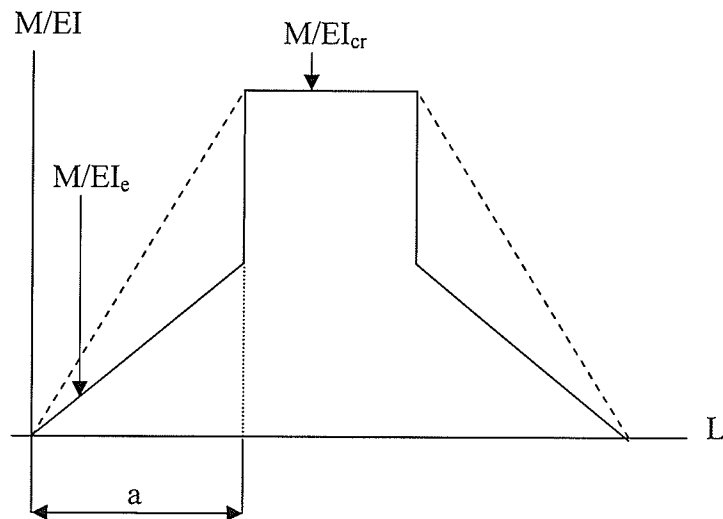


Figure 2.3 - Idealized Curvature According to Faza and GangaRao (1992)

$$\Delta = \frac{Pa}{24E_c I_e I_{cr}} [8a^2 I_{cr} + 3L^2 I_e - 12a^2 I_e] \quad \text{Equation 2.28}$$

Equation 2.28 has limited use as it is not clear what assumptions for the application of the effective moment of inertia should be used for other load cases. However, it worked quite

accurately for predicting the deflection of the beams in Faza and GangaRao (1992) who subjected the beams to 4-point bending at the third spans of the beams.

2.2.2.2 - Equation Proposed by Benmokrane et al. (1996)

Benmokrane et al. (1996) suggested that in order to improve the performance of Equation 2.23, a modification would be needed in order to account for the use of FRP materials as the longitudinal reinforcement. Constants to modify the equation were developed through a comprehensive experimental program and the effective moment of inertia was defined according to Equation 2.29.

$$I_e = \frac{1}{7} \left(\frac{M_{cr}}{M_a} \right)^3 I_g + 0.84 \left[1 - \left(\frac{M_{cr}}{M_a} \right)^3 \right] I_{cr} \leq I_g \quad \text{Equation 2.29}$$

2.2.2.3 - Equation Proposed by Brown and Bartholomew (1996)

Brown and Bartholomew (1996) suggested that the basic form of Equation 2.23 should remain unchanged, but that the effective moment of inertia should converge to the cracked moment of inertia quicker than the cubic equation when FRP reinforcement is used. They proposed that the basic form of Equation 2.23 could be used with reasonable accuracy to find the service deflections of FRP reinforced concrete beams if a fifth order equation was used rather than a cubic. The modified equation proposed by Brown and Bartholomew (1996) is presented in Equation 2.30.

$$I_e = \left(\frac{M_{cr}}{M_a} \right)^5 I_g + \left[1 - \left(\frac{M_{cr}}{M_a} \right)^5 \right] I_{cr} \leq I_g \quad \text{Equation 2.30}$$

2.2.2.4 - Equation Proposed by Toutanji and Saafi (2000)

Similar in nature to the research of Brown and Bartholomew (1996), a further investigation of the effective moment of inertia was performed by Toutanji and Saafi (2000). It was found that the order of the equation depends on both the modulus of elasticity of the FRP, as well as the reinforcement ratio. Based on their research, Toutanji and Saafi (2000) have recommended that Equations 2.31 and 2.32 be used to calculate the deflection of FRP reinforced concrete.

$$I_e = \left(\frac{M_{cr}}{M_a} \right)^m I_g + \left[1 - \left(\frac{M_{cr}}{M_a} \right)^m \right] I_{cr} \leq I_g \quad \text{Equation 2.31}$$

$$m = 6 - 10 \frac{E_{frp}}{E_s} \rho_{frp} \geq 3 \quad \text{Equation 2.32}$$

2.2.2.5 – The ISIS M03-01 Method (2001)

The ISIS Design Manual M03-01 (2001) has suggested the use of an effective moment of inertia which is derived from equations given by the CEB-FIP MC-90 (1990). Ghali et al. (2001) have verified that I_e calculated by Equation 2.33 gives good agreement with experimental deflection of numerous beams reinforced with different types of FRP materials. Quite different in form from the previous effective moment of inertia equations discussed, ISIS M03-01 (2001) suggests Equation 2.33 for calculating the effective moment of inertia of FRP-RC.

$$I_e = \frac{I_T I_{cr}}{I_{cr} + \left[1 - 0.5 \left(\frac{M_{cr}}{M_a} \right)^2 \right] (I_T - I_{cr})} \leq I_g \quad \text{Equation 2.33}$$

2.2.2.6 – The CSA S806-02 Method (2002)

The CSA S806-02 (2002) design code uses a theoretical approach based on the moment-curvature relationship of FRP-RC to estimate deflections. The moment-curvature method of calculating deflection is well suited for FRP-RC because the moment-curvature diagram can be approximated by two linear regions: one before the concrete cracks, and the second one after the concrete cracks (Razaqpur et al. 2000). Therefore, there is no need of calculating curvature at different sections along the length of the beam as for steel reinforced concrete. There are only three moments with corresponding curvature that define the entire moment-curvature diagram: at cracking, immediately after cracking, and at ultimate. With the use of the virtual work method for calculating deflection, deflection equations for various load configurations based on the integration of moment-curvature diagrams are given. For example, Equation 2.34 calculates the post cracking deflection at midspan in FRP-RC members subjected to symmetric four-point bending through the integration of the curvature diagram given in Figure 2.4.

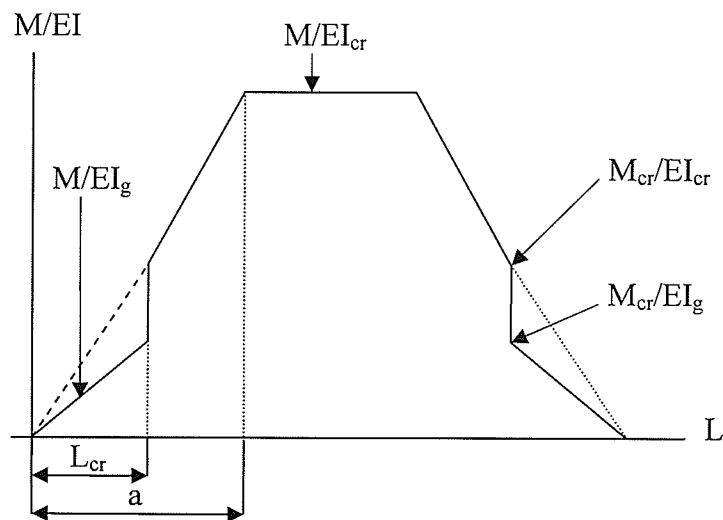


Figure 2.4 – Idealized Curvature According to the CSA S806-02 (2002)

$$\Delta = \frac{Pa}{24E_c I_{cr}} (3L^2 - 4a^2 - \eta a^2) \quad \text{Equation 2.34}$$

$$\eta = 8 \left(\frac{M_{cr}}{M_a} \right)^3 \left(1 - \frac{I_{cr}}{I_g} \right) \quad \text{Equation 2.35}$$

2.2.2.7 – The ACI 440.1R-03 Method (2003)

In order for a deflection equation to be accepted for use by industry, it has to take on a familiar form and be easy to use. The ACI 440.1R-03 (2003) have thus suggested that the basic form of Equation 2.23, which calculates the effective moment of inertia of steel RC, can remain the same for predicting the deflection of FRP-RC beams if a modification factor is used. The ACI 440.1R-03 (2003) found that the effective moment of inertia equation for FRP-RC is dependent on the modulus of elasticity of the FRP and recommended the use of Equations 2.36 and 2.37 for I_e to calculate the deflection of FRP reinforced beams

$$I_e = \beta \left(\frac{M_{cr}}{M_a} \right)^3 I_g + \left[1 - \left(\frac{M_{cr}}{M_a} \right)^3 \right] I_{cr} \leq I_g \quad \text{Equation 2.36}$$

$$\beta = 0.5 \left[\frac{E_{frp}}{E_s} + 1 \right] \quad \text{Equation 2.37}$$

2.2.2.8 - Equation Proposed by Yost et al. (2003)

Upon finding that the ACI 440.1R-03 (2003) equation often under predicted the service load deflection of FRP-RC members, Yost et al. (2003) attempted to modify Equation 2.37 in order to give more accurate deflection predictions. Realizing that the accuracy of Equation 2.37 was dependent on the relative reinforcement ratio, ρ/ρ_{bal} , a regression

analysis was performed on a series of beams tested by Yost et al. (2003). From the analysis, it was found that Equation 2.37 could be modified slightly to better account for the effects of FRP. Similar in form to Equation 2.37, the researchers determined that both the modulus and the relative reinforcement ratio are important for determining the deflection and recommended the use of Equation 2.38 for determining β , while still using the same form for I_e as shown in Equation 2.36.

$$\beta = \left[0.064 \left(\frac{\rho_{frp}}{\rho_{bal}} \right) + 0.13 \right] \left[\frac{E_{frp}}{E_s} + 1 \right] \quad \text{Equation 2.38}$$

2.2.2.9 - Proposed Revision to the ACI 440.1R (2004)

Upon finding that the ACI 440.1R-03 (2003) equation often under predicted the service load deflection of FRP reinforced concrete members, the ACI 440 Committee (2004) has proposed revisions to the design equation in ACI 440.1R-03 (2003). The moment of inertia equation has retained the same familiar form as that of Equation 2.36 in these revisions. However, the form of the reduction coefficient, β , to be used in place of Equation 2.37 was modified. The new reduction coefficient has changed the key variable in the equation from the modulus of elasticity to the relative reinforcement ratio as shown in Equation 2.39.

$$\beta = \frac{1}{5} \left[\frac{\rho_{frp}}{\rho_{bal}} \right] \leq 1.0 \quad \text{Equation 2.39}$$

2.2.2.10 - Equation Proposed by Bischoff (2005)

Bischoff (2005) developed a rational equation for the effective moment of inertia to be used in Equation 2.22 based on tension stiffening relationships found from tension tests.

Unlike any other method presented for computing the deflection of FRP-RC, the method given by Bischoff (2005) can also be used to calculate the deflection of conventional steel RC. According to Bischoff (2005), the effective moment of inertia, I_e , should be found using Equation 2.40.

$$I_e = \frac{I_{cr}}{1 - \left(1 - \frac{I_{cr}}{I_g}\right) \left(\frac{M_{cr}}{M_a}\right)^2} \quad \text{Equation 2.40}$$

2.2.3 – Inclusion of Member Weight in Deflection Analysis

The deflection equations are all sensitive to the value of the cracking moment. To improve the accuracy of the predicted cracking moment, the equation used to calculate the applied load was modified in order to account for the respective self weights of the members. Without accounting for the moment due to the self weight, the calculated cracking moment of the section would be larger than the cracking moment measured during the test and would cause incorrect estimates of deflection. The self weight was accounted for in the analysis by including the moment due to the self weight, as well as the moment caused by the 4-point loading in the applied moment M_a , terms found in each equation as can be seen by Equation 2.41. The cracking load, P_{cr} , found in Equations 2.26 and 2.27 was also adjusted in the analysis to account for the self weight of the members, being defined according to Equation 2.42.

$$M_a = Pa + \frac{\gamma_{sw}bhL^2}{8} \quad \text{Equation 2.41}$$

$$P_{cr} = \frac{M_{cr}}{a} - \frac{\gamma_{sw}bhL^2}{8a} \quad \text{Equation 2.42}$$

Chapter 3 - Experimental Program

3.1 - Overview

An experimental program was carried out to study the shear behaviour of CFRP-RC beams without stirrups and with an effective depth greater than 300 mm. Through the completion of the literature review, it was believed that there was a definite lack of knowledge in this particular area. This experimental program was conducted to partially fill in that missing void. To do this, 7 beams were tested, 2 reinforced with steel and 5 reinforced with CFRP. These beams were tested monotonically under 4-point bending and the following parameters were studied as a part of the program:

1. the effect of the reinforcement type (steel or CFRP) on flexural and shear behaviour
2. the effect of the reinforcement ratio on flexural and shear behaviour
3. the accuracy of the FRP-RC code equations for predicting deflections and the concrete contribution to shear

3.2 - Beam Details

All beams were designed to fail in shear with a specified 28-day concrete compressive strength of 45 MPa. Beams 4S-20-A and 4S-20-B were reinforced with 20M steel bars, beam 3A was reinforced with 9 mm Aslan™ bars, while beams 4L-A, 4L-B, 4L-C, and 4L-D were reinforced with 9.5 mm ribbed Leadline™ bars. The material properties of the Aslan™ bars shown in Table 3.2 were determined by Vogel (2005) by means of tension tests and are not the values given by the manufacturer. The dimensions of the beams were constant with a height of 600 mm, a width of 350 mm, and a length of 5.4 m. However,

the effective depth of the reinforcement was altered slightly between beams, as well as the simply supported length. The shear span to depth ratio of the beams was greater than 2.5 for all specimens, to minimize the effect of arching action. No stirrups were provided in any of the beams to ensure that a shear failure occurred. A summary of the beam data is presented in Tables 3.1 and 3.2 and an explanation of the test parameters can be seen in Figure 3.1.

Table 3.1 - Beam Properties for Steel Reinforced Beams

Beam #	L (mm)	a (mm)	b (mm)	h (mm)	d (mm)	f'_c (MPa)	E_s (GPa)	f_y (MPa)	# bars	d_b (mm)
4S-20-A	5100	1550	350	600	550	57.25	200	400	4	20
4S-20-B	5400	1700	350	600	550	46.10	200	400	4	20

Table 3.2 - Beam Properties for CFRP Reinforced Beams

Beam #	L (mm)	a (mm)	b (mm)	h (mm)	d (mm)	f'_c (MPa)	E_{frp} (GPa)	f_{frpu} (MPa)	# bars	d_b (mm)
3A	5100	1550	350	600	550	59.18	174	2563	3	9.0
4L-A	5100	1550	350	600	565	45.10	147	2255	4	9.5
4L-B	5100	1550	350	600	550	57.25	147	2255	4	9.5
4L-C	5100	1550	350	600	550	57.25	147	2255	4	9.5
4L-D	5400	1700	350	600	550	46.10	147	2255	4	9.5

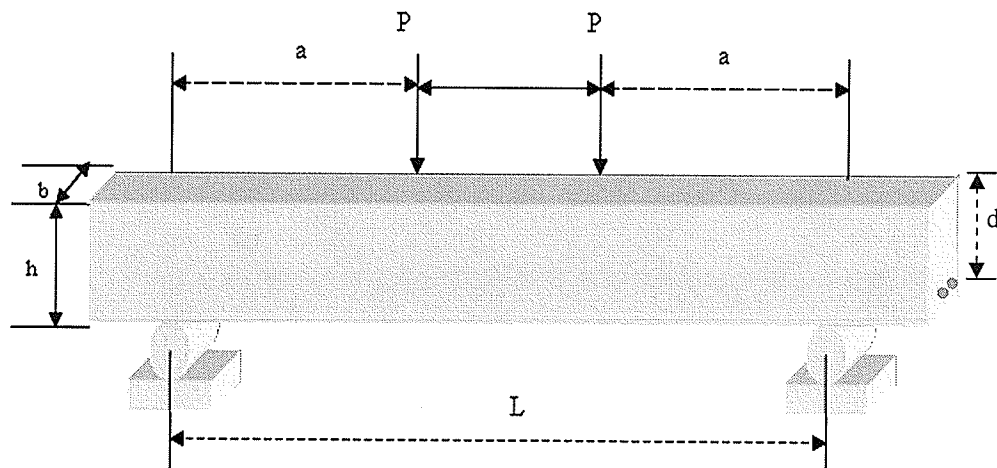


Figure 3.1 - Test Setup

For beams 4S-20-A, 4L-B, and 4L-C that were cast prior to the start of this experimental program, it was necessary to core cylinders out of the beams after testing to determine the concrete strength. This process can be seen in Figure 3.2. For the remaining beams, the concrete strength was determined through the testing of cylinders which were cast simultaneously with the beams. The concrete strength was determined by taking the average strength of the cylinders tested. This information, as well as the age of the concrete at testing, can be found in Table 3.3.

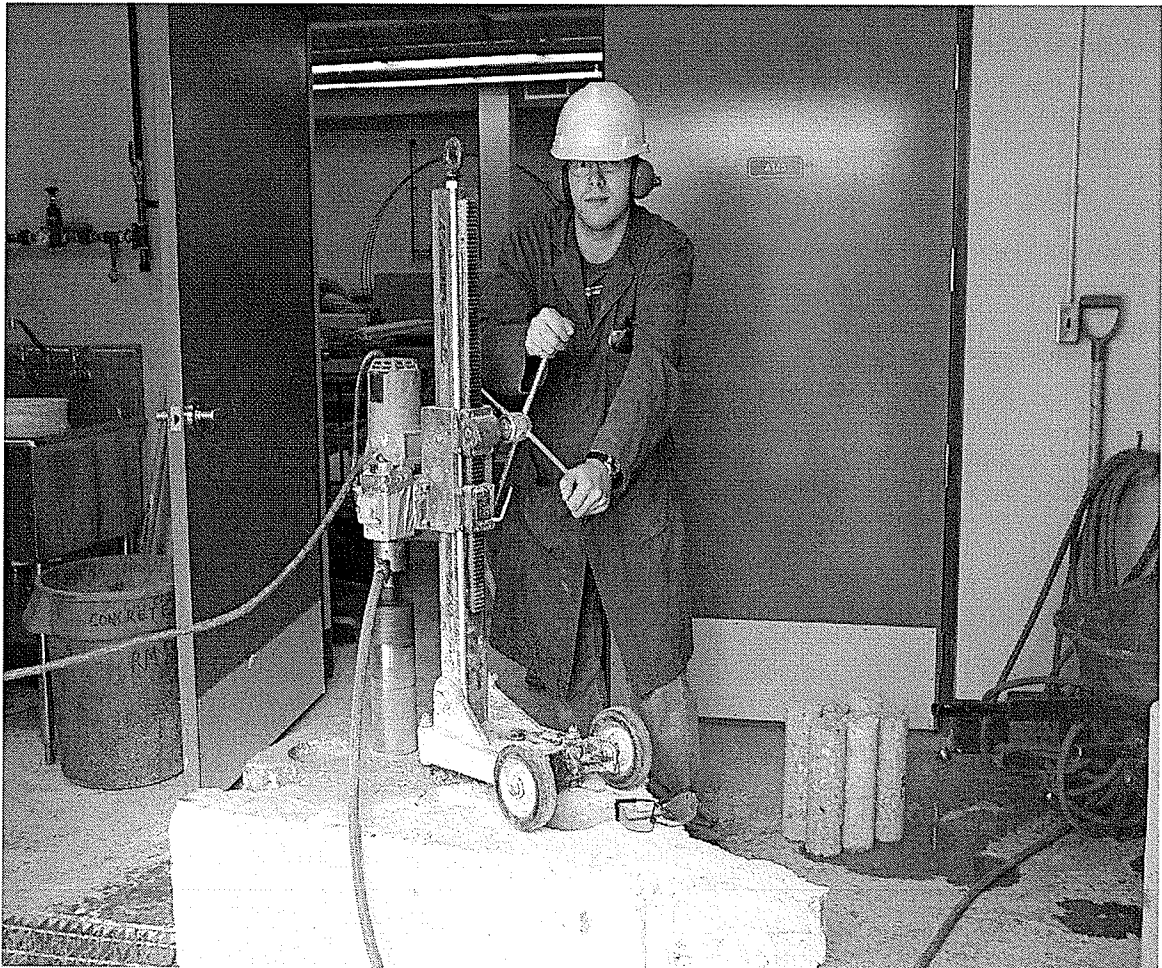


Figure 3.2 – Coring of Concrete Cylinders

Table 3.3 - Properties of Concrete Cylinders

Beam #	# Cylinders Tested	Age of Cylinders (days)	f'_c (MPa)
3A	4	98	59.18
4L-A	3	174	45.10
4L-B			
4L-C	9	697	57.25
4S-20-A			
4L-D	3	28	46.10
4S-20-B			

3.3 - Instrumentation and Testing

All beams were tested in four-point bending as shown in Figure 3.1. Pi gauges were mounted on the surface of the beams prior to testing at midspan to determine the depth of the neutral axis during testing, as well as to determine the strain in the reinforcement and the concrete at ultimate. One pi gauge was placed on top of the beam, while the other three were mounted at a depth of 185 mm, 370 mm, and 555 mm, respectively from the top of the beam. Linear variable displacement transducers (LVDTs) were used during testing to measure the deflection at various sections along the length of the beam. The LVDTs were placed at midspan, directly below the load points, and midway between the load points and the supports, for a total of 5 LVDTs.

The beams were loaded with the use of a 1000 kN capacity MTS testing machine at a rate of 2 mm/min. All instruments were calibrated and were continuously monitored with the use of a data acquisition system during the tests. An illustration of the instrumentation can be seen in Figure 3.3.

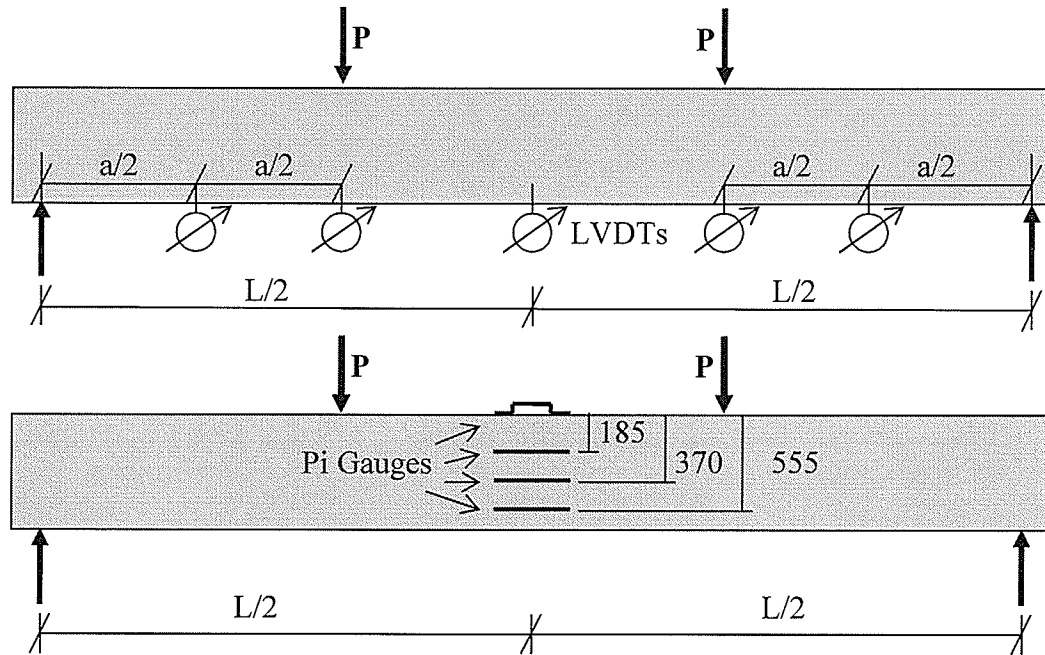


Figure 3.3 – Beam Instrumentation

3.4 – Test Results

3.4.1 - Failure Loads

The CSA A23.3-94 (1998) and CSA S806-02 (2002) code equations were used to determine both the shear resistance and the flexural resistance of the steel reinforced, and FRP reinforced beams, respectively. The mode of failure resulting in the lesser resistance was then deemed to be the predicted mode of failure. Table 3.4 gives a comparison between the predicted failure load of each beam and the experimental failure load.

Table 3.4 – Beam Failure Loads

Beam #	$P_{max,flexure}$ (kN)	$P_{max,hear}$ (kN)	Predicted Failure Mode	$P_{max,experimental}$ (kN)	Experimental Failure Mode
4S-20-A	155.13*	234.31*	Flexure (T)	153.77	Shear
4S-20-B	140.30*	233.56*	Flexure (T)	157.11	Shear
3A	157.90 ⁺	115.97 ⁺	Shear	84.16	Shear
4L-A	212.58 ⁺	101.95 ⁺	Shear	85.42	Shear
4L-B	208.51 ⁺	114.70 ⁺	Shear	105.51	Shear
4L-C	208.51 ⁺	114.70 ⁺	Shear	97.49	Shear
4L-D	187.75 ⁺	100.43 ⁺	Shear	93.00	Shear

* - Failure load according to CSA A23.3-94 (1998)

+ - Failure load according to CSA S806-02 (2002)

(T) - Flexural failure initiated in tension by the steel yielding prior to the concrete crushing

It can be seen in Table 3.4 that all FRP-RC beams failed at loads which were lower than anticipated. Thus, the CSA code formulas for calculating the concrete shear strength are not conservative and should be revised. What is even more alarming is that for the steel reinforced beams, a different failure mode was predicted. It must be noted however, that if the material resistance factors had been applied as is done in practice, the design would have still been satisfactory, giving predicted failure loads less than those experienced in the lab. The experimental shear failures from beams 3A, 4L-C, and 4S-20-A are shown below in Figure 3.4. The beams with similar reinforcement ratios to these all had very similar failures.

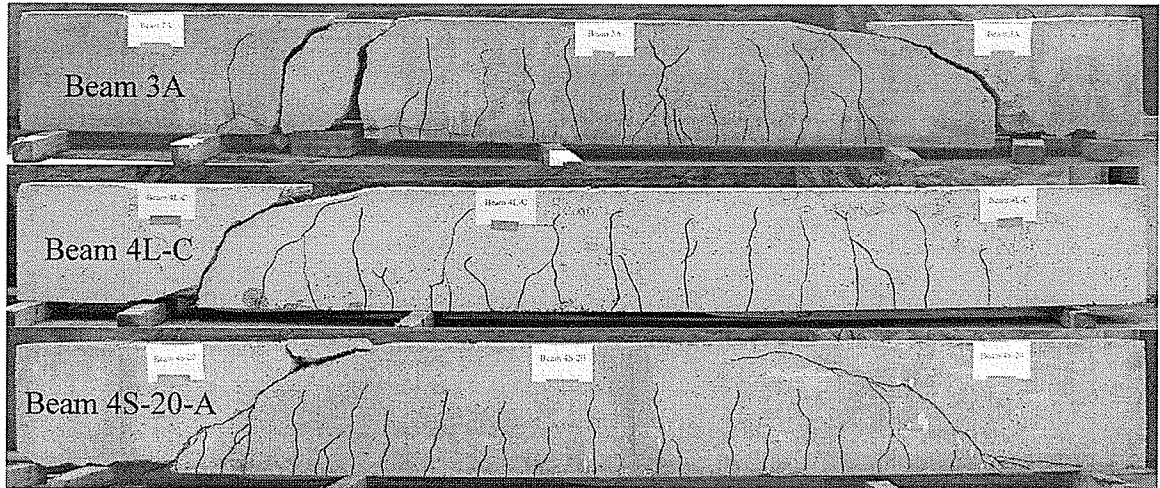


Figure 3.4 –Shear Failure for Beams 3A, 4L-C, and 4S-20-A

A large reason for the lower experimental than predicted loads arises from the fact that nearly all of the beams cracked much earlier than predicted using Equation 2.24. These are quite alarming results as the codes are not giving conservative estimates. A possible reason for this is that Equation 2.25, which calculates the modulus of rupture, f_r , is quite simple and does not take into account such variables as shrinkage and age of concrete. A summary of the experimental cracking moments versus those defined by Equations 2.24 and 2.25 is shown in Table 3.5.

Table 3.5 – Comparison between Experimental and Theoretical Cracking Moments

Beam #	$M_{cr,predicted}(kNm)$ (1)	$M_{cr,experimental}(kNm)$ (2)	(1)/(2)
4S-20-A	95.34	64.17	1.49
4S-20-B	85.55	114.82	0.75
3A	96.93	48.41	2.00
4L-A	84.62	57.77	1.46
4L-B	95.34	55.60	1.71
4L-C	95.34	54.51	1.75
4L-D	85.55	62.19	1.38

Since all of the beams failed in shear, an investigation was performed to see which of the codes most accurately predicted the concrete contribution to shear for FRP reinforced concrete beams. These equations are taken from the JSCE (1997), ISIS M03-01 (2001), CSA S806-02 (2002), ACI 440.1R-03 (2004), and the Proposed Revisions to the ACI 440.1R (2004). Only the code equations were checked here to determine which code was predicting the concrete contribution to shear most accurately. A summary of the predicted shear carrying capacities of these beams is shown in Table 3.6. A ratio of the experimental shear capacity to the predicted shear capacity, V_c , for each beam can be found in Table 3.7.

Table 3.7 shows that the ISIS M03-01 (2001) and CSA S806-02 (2002) equations always over predict the concrete contribution to the shear capacity of these beams. This could be catastrophic as it means that the beams will fail at lower loads than anticipated. The JSCE (1997) and the Proposed Revisions to the ACI 440.1R (2004) equations on the other hand are always conservative and are thus better equations for use in a design code. It can be seen in Table 3.7 that both the JSCE (1997) and the Proposed Revision to the ACI 440.1R (2004) equations work well but that the JSCE (1997) equation is the most accurate and also has a very low standard deviation. Thus, the JSCE (1997) equation seems to be a very good equation for predicting the concrete shear capacity of CFRP reinforced concrete beams. This will later need to be verified for a larger number of samples

Table 3.6 – Summary of the Concrete Shear Capacities (kN) of the FRP-RC Beams

Beam #	Experimental	JSCE (1997)	ISIS M03-01 (2001)	CSA S806-02 (2002)	ACI 440.1R-03 (2003)	Proposed ACI 440.1R (2004)
3A	94.03	76.96	231.70	124.20	12.29	58.54
4L-A	95.22	77.56	189.15	110.31	15.89	60.66
4L-B	115.39	82.11	209.46	122.16	15.69	64.86
4L-C	107.36	82.11	209.46	122.16	15.69	64.86
4L-D	103.61	76.69	187.96	109.62	15.88	60.22

Table 3.7 - Ratio of Experimental over Predicted Concrete Shear Capacity

Beam #	JSCE (1997)	ISIS M03-01 (2001)	CSA S806-02 (2002)	ACI 440.1R-03 (2003)	Proposed ACI 440.1R (2004)
3A	1.222	0.406	0.757	7.651	1.606
4L-A	1.228	0.503	0.863	5.992	1.570
4L-B	1.405	0.551	0.945	7.354	1.779
4L-C	1.308	0.513	0.879	6.843	1.655
4L-D	1.351	0.551	0.945	6.525	1.721
Average	1.303	0.505	0.878	6.873	1.666
St. Dev.	0.079	0.059	0.077	0.659	0.085

3.4.2 - Deflection Behaviour

Given that steel is a stiffer material than CFRP, and that the reinforcement ratio of the steel reinforced beams in this study was higher than those of the CFRP reinforced beams, it is no surprise that the steel reinforced beams had a much stiffer load versus deflection response than the CFRP reinforced beams as can be seen in Figure 3.5.

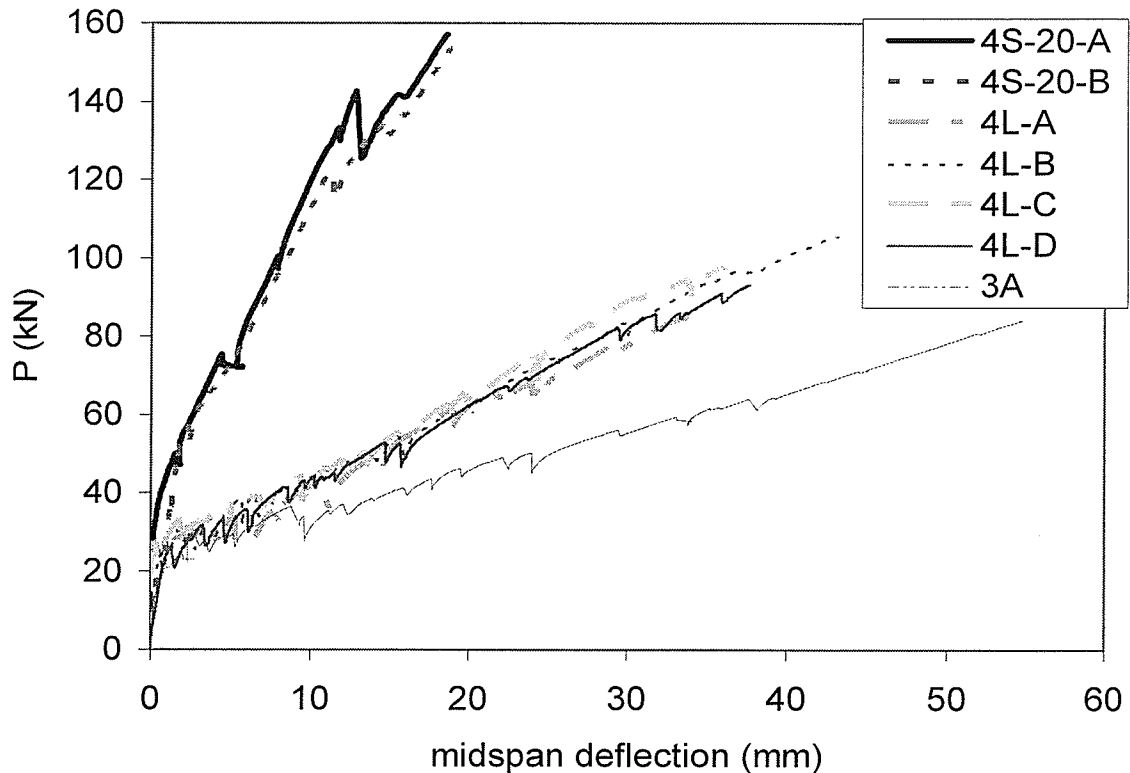


Figure 3.5 – Effect of Reinforcement Type on Flexural Behaviour

It can be seen in Figure 3.5 that the beams which contained the same amounts of reinforcement behaved very similarly as nearly identical load versus deflection responses for beams 4S-20-A and 4S-20-B and for beams 4L-A, 4L-B, 4L-C, and 4L-D were achieved. The main difference between the beams of the same reinforcement was the ultimate failure load, due to the varying concrete strengths between the beams. It can also be noted that as the reinforcement ratio decreased, the ultimate deflection was increased and the ultimate load was typically decreased.

3.4.2.1 – Steel RC Beams

An investigation was performed to see which of the CSA A23.3-94 (1998) deflection equations was the most accurate for predicting the deflection of the steel RC beams. The

experimental load deflection behaviours of beams 4S-20-A and 4S-20-B were compared against the predicted load deflection behaviours given by the CSA A23.3-94 (1998). These comparisons can be seen in Figures 3.6 and 3.7.

It can be seen in Figures 3.6 and 3.7 that the deflection can be predicted quite accurately using the effective moment of inertia equation given in the CSA A23.3-94 (1998). This can particularly be seen in Figure 3.7 as the predicted load deflection curve matches the experimental curve quite well. Although there are some discrepancies between the predicted and the experimental curves in Figure 3.6 resulting from the miscalculation of the cracking moment, it can be seen that the slope of the load deflection response given by the effective moment of inertia is the same as that of the experimental curve. Thus, the effective moment of inertia approach seems to work very well for predicting the deflection behaviour of RC beams. Based on the experimental program, the bi-linear equation presented by the CSA A23.3-94 (1998) is not working as well and tends to under predict the deflection at a given load.

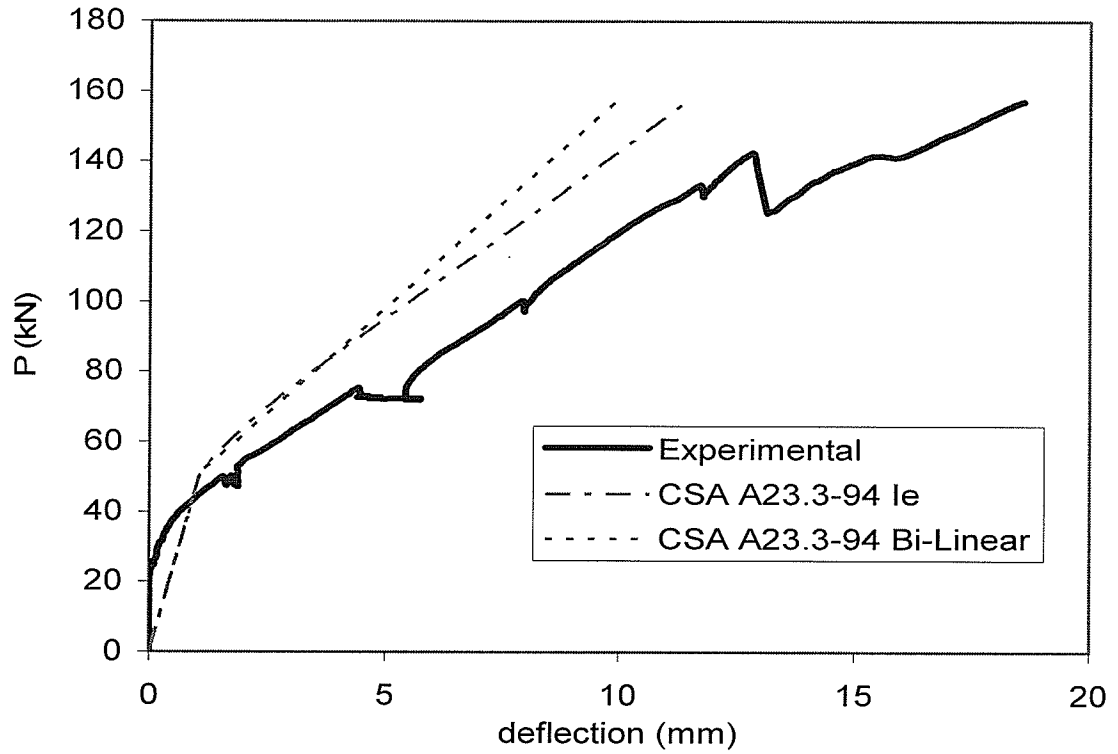


Figure 3.6 - Load Deflection Behaviour for Beam # 4S-20-A

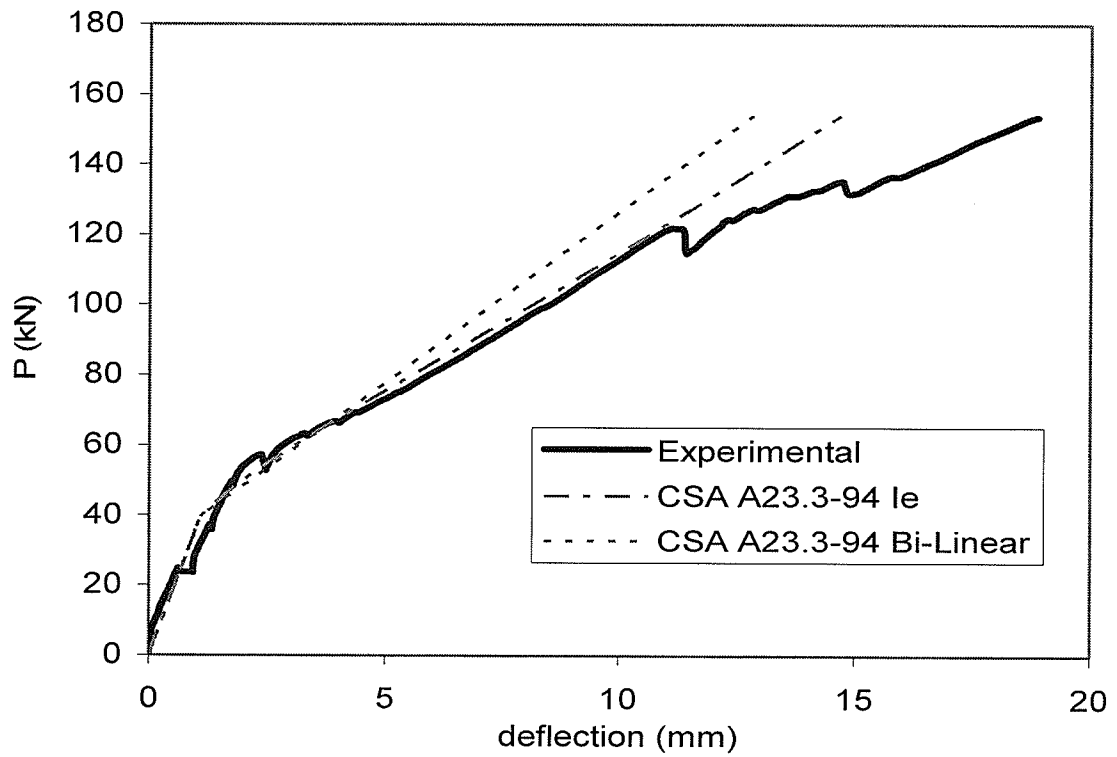


Figure 3.7 - Load Deflection Behaviour for Beam # 4S-20-B

3.4.2.2 - FRP-RC Beams

An investigation was also performed to see which of the codes most accurately predicted the deflection response for the FRP-RC beams tested. These equations are taken from ISIS M03-01 (2001), CSA S806-02 (2002), ACI 440.1R-03 (2003), and the Proposed Revisions to the ACI 440.1R (2004). The experimental deflection response, along with the predicted deflection response of each code, can be seen in Figures 3.8 to 3.12 for beams 3A, 4L-A, 4L-B, 4L-C, and 4L-D, respectively. This investigation only included the code equations, and did not check the accuracy of the other proposed deflection equations.

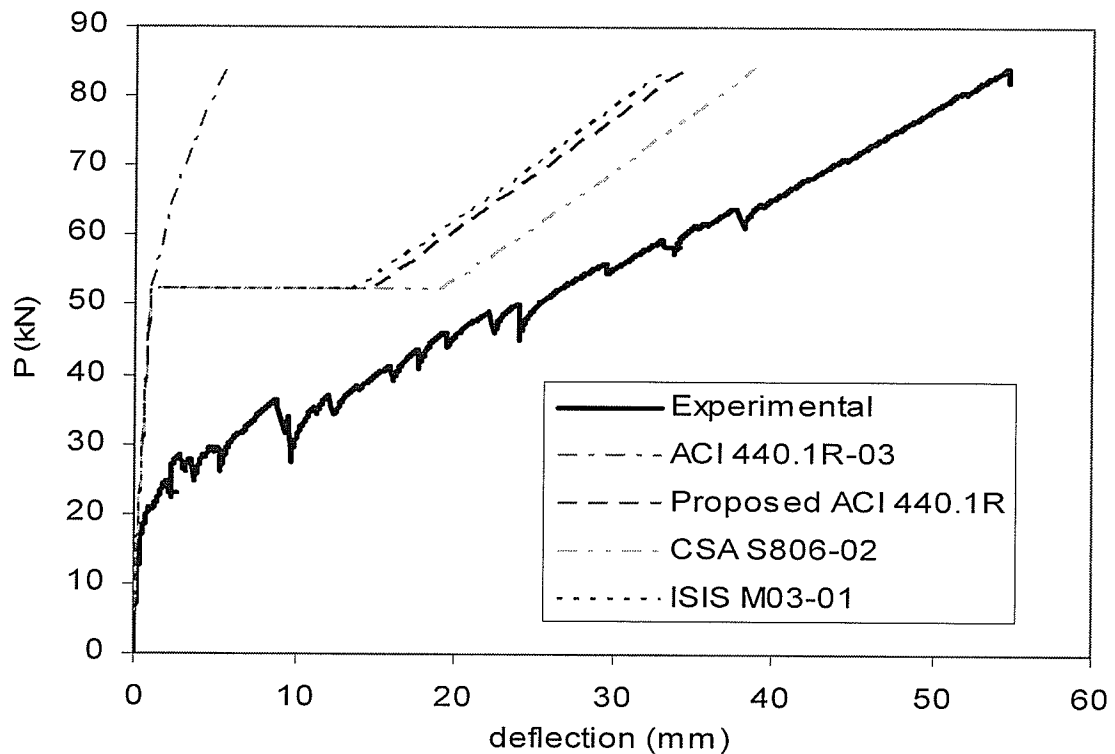


Figure 3.8 - Load Deflection Behaviour for Beam # 3A

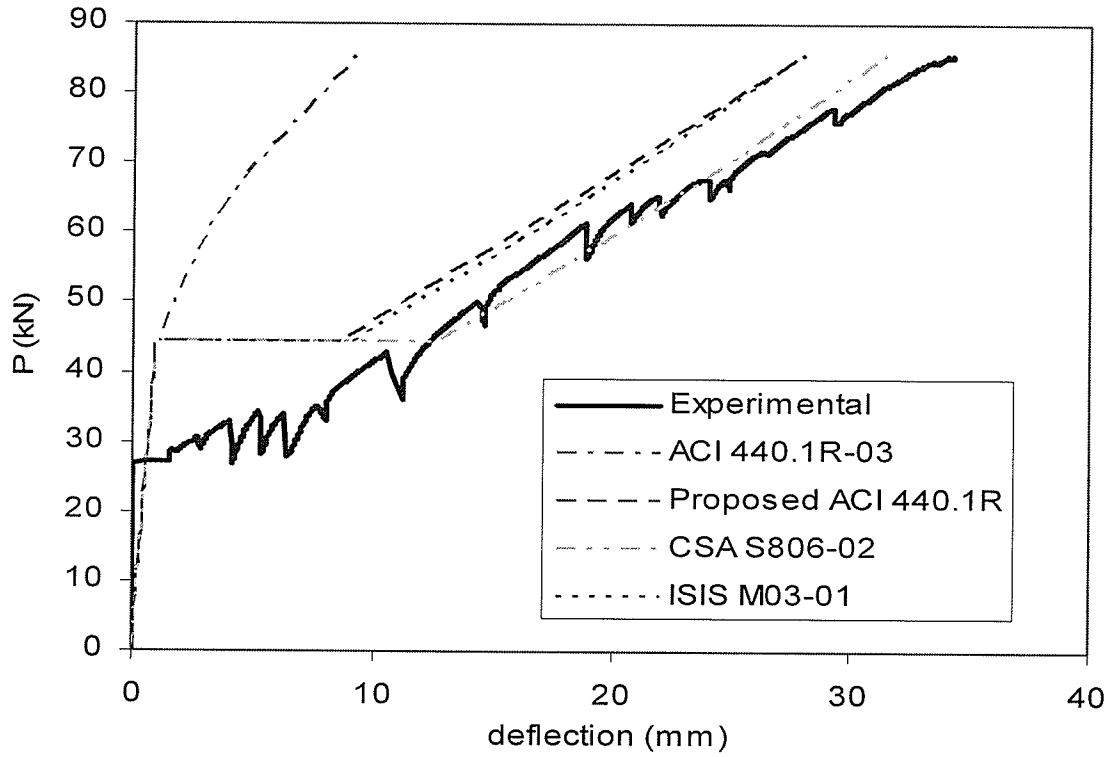


Figure 3.9 - Load Deflection Behaviour for Beam # 4L-A

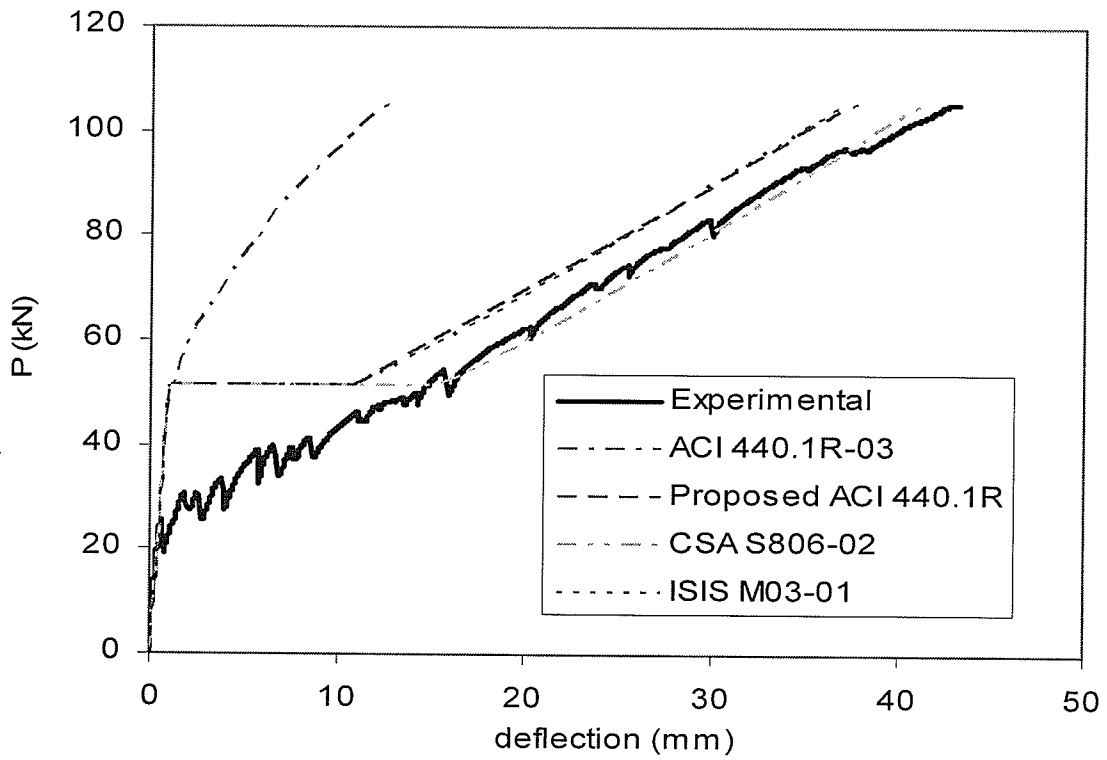


Figure 3.10 - Load Deflection Behaviour for Beam # 4L-B

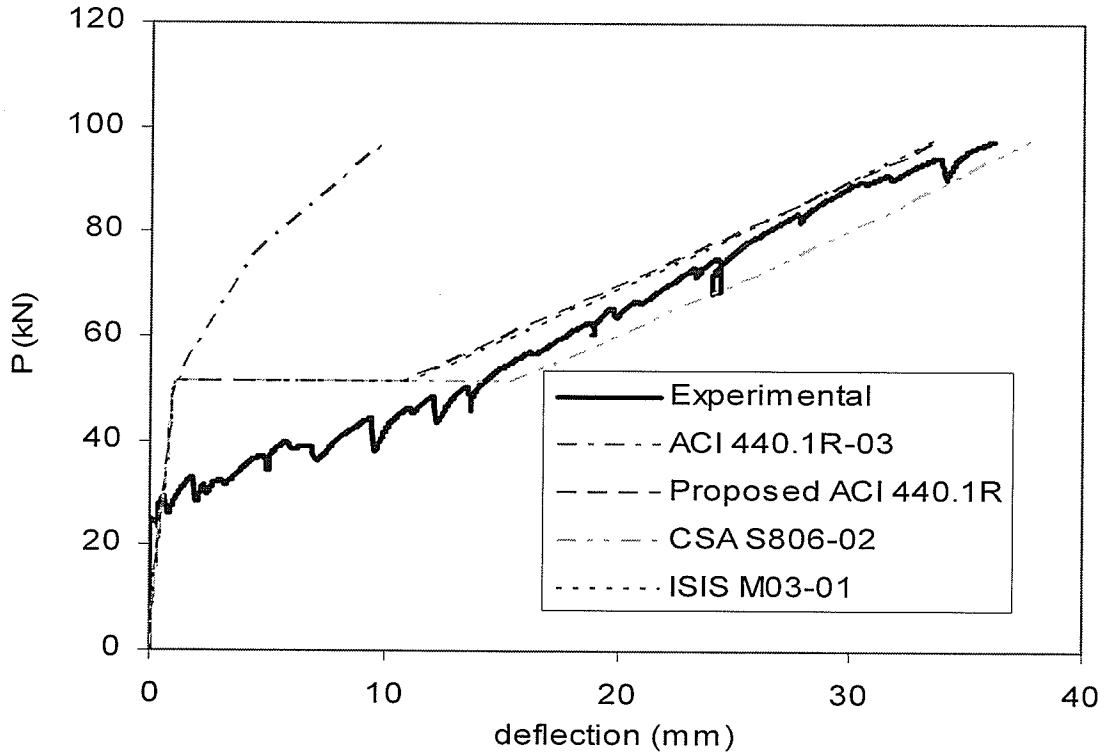


Figure 3.11 - Load Deflection Behaviour for Beam # 4L-C

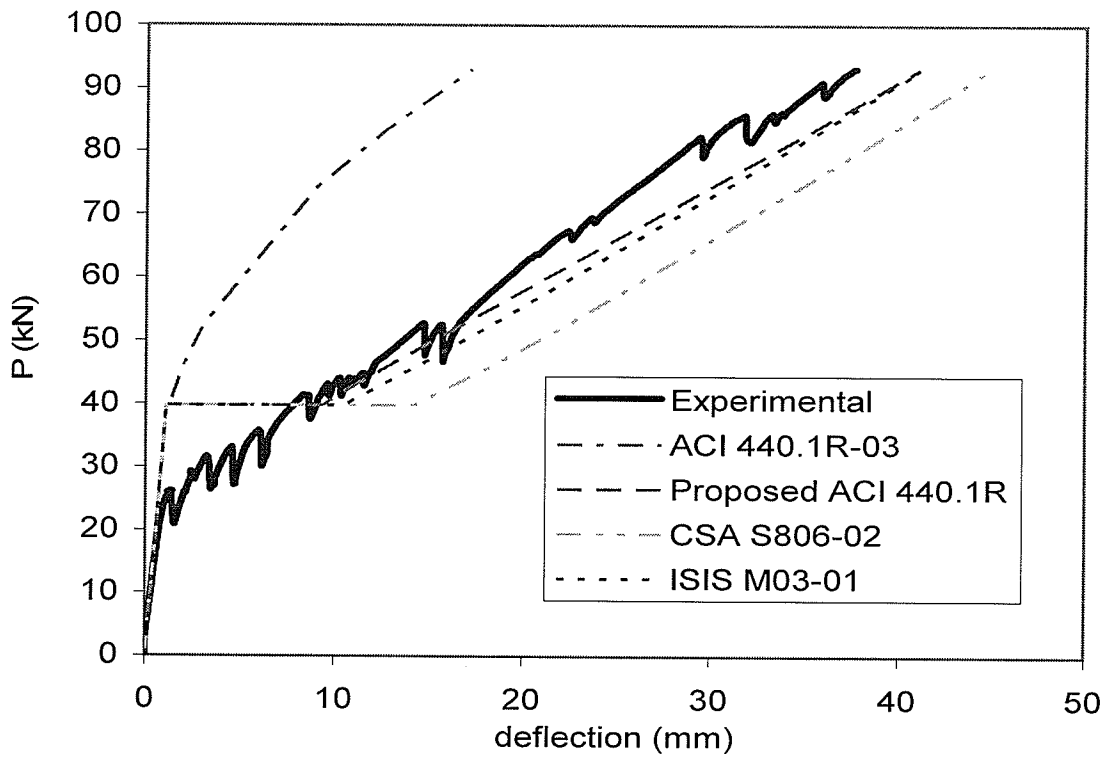


Figure 3.12 - Load Deflection Behaviour for Beam # 4L-D

It can be seen from Figures 3.8 to 3.12 that the deflection equations tend to predict the deflection much better for the beams with the 4 LeadlineTM bars (4L-A to D) than for the beam with the 3 AslanTM bars (3A). This may be because beam 3A was under reinforced, while beams 4L-A, 4L-B, 4L-C, and 4L-D were over-reinforced. Figures 3.8 to 3.12 also show that the cracking loads were predicted quite poorly from the use of Equations 2.24 and 2.25 for all of the FRP-RC beams tested. This led to very poor deflection prediction at low loads, typically where the service conditions lie for FRP-RC. Other trends include that the equation by the ACI 440.1R-03 (2003) consistently under predicted the deflection behaviour, while the CSA S806-02 (2002) equation typically predicted the deflection response very well after cracking for the over reinforced beams. The equations of the Proposed ACI 440.1R (2004) and ISIS M03-01 (2001) also predicted the response of the over reinforced beams accurately after cracking, but led to undesired, unconservative results.

Chapter 4 - Parametric Study

4.1 - Introduction

Two databases were compiled from published papers using Microsoft Access to increase the number of members analyzed. The database for shear analysis contained 89 beams containing no stirrups, to analyze the concrete contribution to shear, whereas the deflection analysis database consisted of 197 FRP-RC beams which were used to analyze the load deflection behaviour.

Microsoft Access had many benefits in its use for data basing these specimens. Mainly, the program allowed for a user friendly interface which only focused on the input of material and geometric properties of the tested specimens. All other parameters required for the comparison of the experimental results and the equation predicted results were done away from the input screens so that the final user of the database could not accidentally modify these formulas. This could not have been accomplished with the use of a spreadsheet. The program was also fully automated and performed all necessary calculations to arrive at the predicted results upon completion of the necessary input data. This led to quick, error-free, calculations that would not have been achieved with the use of a spreadsheet. Another large benefit to using a data basing software, such as Microsoft Access, was that queries could be done very quickly. For instance, if only the results of certain data were desired, these limitations could be entered in the program and the program would then only show these results. With the fully automated characteristics of the program, this allowed for a very quick and detailed analysis to be carried out.

The databases have similar input requirements. Both require the user to input any material and geometric properties of their test set-up. Furthermore, the database for shear analysis also requires that the user inputs the experimental failure load, while the deflection database requires the user to input the failure mode and experimental load versus deflection data. A large amount of time was spent creating a user friendly form for entering in this data. Figure 4.1 shows the input form for the shear database if the user were using reinforcing rods as the reinforcement, while Figure 4.2 shows the same input form if the user were using mesh reinforcement, such as NEFMAC. It should be noted that these are the same form but the input boxes describing the reinforcement only become visible once the user has selected a reinforcement type. Similarly, Figures 4.3 and 4.4 show the input forms for the deflection database.

Field Name	Value
Beam#	11-2-1
Year	2004
Researcher Name	Gross, Dinehart and Yost
L (mm)	1970
a (mm)	910
b (mm)	89
h (mm)	172
d (mm)	143
fc (MPa)	81.4
Ec (Mpa)	54600
Reinforcement	Rods
FRP	CFRP
Etrp (MPa)	139000
fty (MPa)	2640
# rods	2
Diameter (mm)	6.35
PMaxExp (KN)	8.76
Look Up Beam	

Figure 4.1 - Screenshot for data Entry form in Shear Database for ROD reinforcement

Microsoft Access - [Beam Data]

File Edit View Insert Format Records Tools Window Help

Type a question for help

Beam# f_c (MPa)

Year E_c (Mpa)

Researcher Name Reinforcement

L (mm) FRP

a (mm) E_{frp} (MPa)

b (mm) f_{frp} (MPa)

h (mm)

d (mm)

A_{frp} (mm²)

PMaxExp (KN)

Look Up Beam

Record: 14 of 98

Form View

start These Theads - Microsoft Word SHEAR - With self... Beam Data EN 11:49 AM

Figure 4.2 - Screenshot for data Entry form in Shear Database for MESH reinforcement

Microsoft Access - [Beam Data]

File Edit View Insert Format Records Tools Window Help

Type a question for help

Beam# f_c (MPa)

Year E_c (Mpa)

Researcher Name Reinforcement

L (mm) FRP

a (mm) E_{frp} (MPa)

b (mm) f_{frp} (MPa)

h (mm) # rods

d (mm) Diameter (mm)

Load (KN)	Deflection (mm)
0	0
2.4	1.524
2.41	1.547188
2.42	1.570376
2.46	1.663129
2.66	2.126893
4.38	6.115264
6.672	11.43
7	13.7
7.005	13.71592
8.51	18.50798
8.76	19.304

Stirrups Present?

Exp. Failure Mode

Look Up Beam

Record: 14 of 12

Form View

start These Theads - Microsoft Word Deflection - With self... Beam Data EN 11:03 AM

Figure 4.3 - Screenshot for data Entry form in Deflection Database for ROD reinforcement

The screenshot shows a Microsoft Access form titled "Beam Data". The form contains the following fields and values:

- Beam#: C3
- Year: 1995
- Researcher Name: Matthys and Taerve
- L (mm): 4000
- a (mm): 1000
- b (mm): 1000
- h (mm): 150
- d (mm): 126
- f_c (MPa): 28
- E_c (Gpa): 31400
- Reinforcement: Mesh
- FRP: CFRP
- E_{frp} (MPa): 98100
- f_{frp} (MPa): 1180
- A_{frp} (mm²): 650
- Stirrups Present?: NO
- Exp. Failure Mode: Compression
- Look Up Beam: (dropdown)

A table within the form displays the following data:

Load (kN)	Deflection (mm)
0	0
1	0.8
2.5	2
4.85	9.238373
4.86	9.269175
5.34	10.74765
8.01	18.97167
15.1	40.81
30.5	87.5
32.91	89.91
35	92
40	103
47	142

Record: 1 of 21

Figure 4.4 - Screenshot for data Entry form in Deflection Database for MESH reinforcement

Material and geometric properties of the beams used in this investigation can be found in Appendix I. The ranges of some of the important properties of the members in the databases are shown in Table 4.1.

Table 4.1 - Ranges of Properties Present in the Database

Minimum	Property	Maximum
520	f _{frpu} [MPa]	2640
26.2	E _{frp} [GPa]	174
25.5	f _c [MPa]	97.4
1.82	a/d	14.40
3.38	I _g /I _{cr}	64.42
0.001	ρ _{frp}	0.038
0.3	ρ _{frp} /ρ _{bal}	9.1

With the database in place, all formulas to be tested were input into the database and the results were compared against the experimental results. The database allowed for quick calculations to be made which were automated upon completion of the data entry form. This allowed for new members to be added to the database in a quick manner to increase the sample size present and improve the statistical analysis. The database also allowed for excellent organization and allowed for analysis to be completed on only a select group of members if desired. For instance, if only GFRP-RC members with an effective depth less than 300mm were to be analyzed, this could be specified by performing a simple query. All statistical information would automatically be adjusted to correspond to only the selected group, which allowed for an extensive study to be completed in a minimal time period.

4.2 - Statistical Analysis

To check the accuracy of formulas developed by other investigators, a statistical analysis has been performed. The most meaningful method for performing the statistical analysis was found to be applying a log transformation to the ratios of the experimental to calculated deflection or shear ratios. A log transformation was employed to give equal weight to those ratios which were below one and those which were above one. Without performing this transformation, more weight is given to the ratios above one and information is lost when statistics is applied as can be seen in Table 4.2.

Table 4.2 - Comparison of Typical Statistics to Log Transform Statistics

Exp. δ	Calc. δ	Exp./Calc.	Calc./Exp.	Ln (Exp./Calc.)	Ln (Calc./Exp.)
10	1	10	0.1	2.303	-2.303
0.1	1	0.1	10	-2.303	2.303
	average	5.05	5.05	0	0
	e^{average}			1.0	1.0

The example given in Table 4.2 demonstrates that although there are two ratios which are the inverse of each other, the statistics favors the higher ratio when computing the average ratio. After applying the log transformation to these ratios, it can be seen that equal weight has been given to each of these ratios and an average of 0 was obtained. Upon using an antilog to transform the average back into a real ratio, an average ratio of 1.0 was found, which is as expected for this dataset. Table 4.2 also demonstrates that prior to applying the log transformation on these ratios, an average ratio of 5.05 would be found, regardless of which way the ratio is calculated. This is very misleading as this number does not confirm that an equation is typically underestimating or overestimating the deflection. However, since the log transformation gives equal weight to inverse ratios, the average indicates whether the formula typically under predicts or over predicts the deflection.

In checking the performance of each of the equations, the limiting factor is determining whether or not the formula is consistently conservative. To do this, the 95% confidence interval was checked and only those formulas whose entire confidence interval was conservative were deemed to be acceptable. This will minimize the chance of a code equation under predicting either the deflection of a member, or the concrete shear

capacity. After completing the log transformation, the 95% confidence interval is defined by Equation 4.1. This 95% confidence interval is based on the Central Limit Theorem, which assumes a normal distribution with a sufficient number of samples.

$$\left[e^{\mu_y - 1.96\sigma_y / \sqrt{n}}, e^{\mu_y + 1.96\sigma_y / \sqrt{n}} \right] \quad \text{Equation 4.1}$$

When two confidently conservative methods were compared, the geometric mean and the variance were used to establish the most accurate one. Here the geometric mean should be as close to 1.0 as possible and the variance should be as small as possible. When using a log transformation, the geometric mean and variance, in terms of a real ratio, are as defined in Equations 4.2 and 4.3.

$$\text{mean} = e^{\mu_y} \quad \text{Equation 4.2}$$

$$\text{variance} = e^{\sigma_y^2} - 1 \quad \text{Equation 4.3}$$

4.3 - Analysis of Cracking Load

The accuracy of the calculated cracking moment, M_{cr} , is a key aspect to the accuracy of the deflection calculations. The controlling variable for predicting the cracking moment is the modulus of rupture of concrete, f_r . Thus, an analysis was done on the 197 members in the database to determine the most accurate formula for calculating f_r . The formulas were taken from Reda Taha and Hassanain (2003) and are given by Equations 4.4 to 4.10.

$$f_r = 0.7\sqrt{f'_c} \quad \text{ACI 318-99 (1999)} \quad \text{Equation 4.4}$$

$$f_r = 0.6\sqrt{f'_c} \quad \text{CSA A23.3-94 (1998), NZS 3101 (1995), AS 3600 (1994)} \quad \text{Equation 4.5}$$

$$f_r = 0.5\sqrt{f'_c} \quad \text{OHBC (1992)} \quad \text{Equation 4.6}$$

$$f_r = 1.4 \left(\frac{f'_c}{10} \right)^{2/3} \quad \text{CEB-FIP MC-90 (1990)} \quad \text{Equation 4.7}$$

$$f_r = 0.7 (f'_c)^{2/3} \quad \text{Raphael (1984)} \quad \text{Equation 4.8}$$

$$f_r = 0.214 (f'_c)^{0.69} \quad \text{Oluokun (1991)} \quad \text{Equation 4.9}$$

$$f_r = 0.5 (f'_c)^{2/3} \quad \text{Légeron and Paultre (2000)} \quad \text{Equation 4.10}$$

The accuracy of the formulas compared against the experimental modulus of rupture in the database can be seen in Table 4.3. These results were found using a logarithmic transformation as described in Section 4.2.

Table 4.3 - Accuracy of Design Methods for Calculating Modulus of Rupture

Statistical Property	Experimental / Calculated Modulus of Rupture						
	CSA A23.3 NZS 3101 AS 3600	ACI 318	OHBD	CEB-FIP MC-90	Raphael	Oluokun	Légeron and Paultre
mean	1.01	0.86	1.21	1.06	0.46	1.37	0.64
variance	0.39	0.39	0.39	0.39	0.39	0.40	0.39
95% conf. (-)	0.96	0.83	1.16	1.02	0.44	1.31	0.61
95% conf. (+)	1.06	0.91	1.27	1.11	0.48	1.44	0.67

It can be seen in Table 4.3 that the most accurate methods for calculating the cracking moment are given in the CSA A23.3-94 (1998), NZS 3101 (1995), AS 3600 (1994) and CEB-FIP MC-90 (1990) codes. Therefore, this equation has been used in the database to calculate the modulus of rupture.

4.4 - Shear Analysis

The shear analysis has been performed using members that contained no stirrups to analyze the concrete contribution to shear. Furthermore, to avoid the effects of arching

action in the analysis, only slender members were considered. A slender member is defined as a member with a slenderness ratio, a/d , of at least 2.5 (MacGregor and Bartlett, 2000). It is extremely important for the equations to under-predict the shear capacity of these members so that premature shear failures are avoided. Thus, only equations whose entire 95% confidence intervals were conservative are deemed to be acceptable for predicting the concrete shear capacity.

The database for shear analysis contained 89 beams with no stirrups, to analyze the concrete contribution to shear. These beams were all loaded under 4-point loading and all failed in shear. The failure loads of these beams were compared against the predicted shear failure loads given by Equations 2.3 to 2.20. These equations, which describe the shear failure due to 4-point loading, were reduced to account for the shear present on the members due to their respective self-weights. The shear force due to the self-weight of the members was accounted for in the analysis with the use of Equation 2.21.

The trend lines for the log of the experimental over predicted shear ratios versus the modulus of elasticity for GFRP-RC beams can be seen in Figure 4.5. In order for the formulas to be conservative, the log of the deflection ratio has to be greater than zero. Figure 4.5 shows that the formula proposed by Razaqpur et al. (2004) yields satisfactory results and its accuracy is not affected by changes in the modulus of elasticity. This is important since the modulus of elasticity changes rapidly among different types of FRP. Comparable results to those received by Razaqpur et al. (2004) can also be seen by the formulas proposed by the JSCE (1997) and the CSA S806-02 (2002). An advantage of

these formulas is that they are always conservative for GFRP-RC, whereas the formula given by Razaqpur et al. (2004) tends to be slightly unconservative when the modulus of elasticity of the GFRP is higher than 45 GPa. Table 4.4 shows the statistical analysis of each of the formulas. The formulas are conservative if the 95% confidence interval is greater than one. The formula given by Razaqpur et al. (2004) is the most accurate for GFRP-RC beams with a mean value of 1.03. However, the concern with this formula is that it can, at times, be unconservative and has a lower bound to its 95% confidence interval of 0.98. Thus, the use of either the JSCE (1997) or the CSA S806-02 (2002) formulas are preferential, as they are also accurate and have entirely conservative confidence intervals.

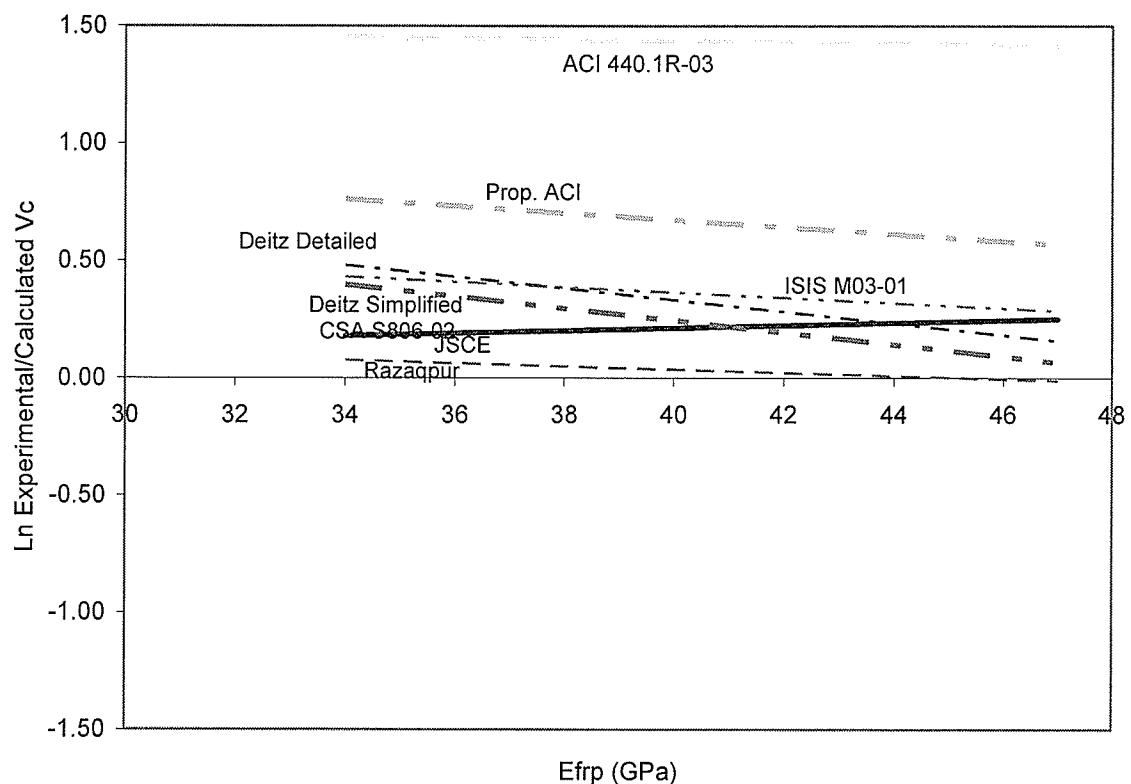


Figure 4.5 - Effect of Modulus on Concrete Shear Prediction for GFRP-RC

Table 4.4 - Statistical Analysis of the Predicted Shear Capacity

Method	Statistical Property	Experimental / Calculated Shear				All Members
		GFRP-RC	CFRP-RC	d≤300mm	d>300mm	
	Sample size	48	39	60	29	89
JSCE (1997)	mean	1.24	1.22	1.14	1.45	1.23
	variation	0.24	0.24	0.21	0.17	0.24
	95 % conf. (-)	1.16	1.14	1.08	1.37	1.18
	95 % conf. (+)	1.31	1.30	1.19	1.53	1.29
Deitz - Simplified (1998)	mean	1.25	0.41	0.77	0.76	0.77
	variation	0.35	0.62	0.93	1.08	0.97
	95 % conf. (-)	1.15	0.35	0.65	0.58	0.67
	95 % conf. (+)	1.36	0.47	0.91	0.99	0.88
Deitz - General (1998)	mean	1.37	0.46	0.85	0.84	0.85
	variation	0.32	0.57	0.87	1.03	0.92
	95 % conf. (-)	1.26	0.40	0.73	0.65	0.74
	95 % conf. (+)	1.48	0.53	1.00	1.09	0.97
ISIS M03-01 (2001)	mean	1.42	0.85	1.10	1.21	1.14
	variation	0.35	0.49	0.52	0.57	0.54
	95 % conf. (-)	1.31	0.75	0.99	1.03	1.04
	95 % conf. (+)	1.55	0.96	1.22	1.43	1.24
CSA S806-02 (2002)	mean	1.23	1.29	1.17	1.46	1.26
	variation	0.32	0.40	0.29	0.41	0.35
	95 % conf. (-)	1.14	1.16	1.10	1.29	1.18
	95 % conf. (+)	1.33	1.43	1.25	1.66	1.34
ACI 440.1R-03 (2003)	mean	4.21	3.28	3.66	3.99	3.76
	variation	0.53	0.61	0.57	0.61	0.58
	95 % conf. (-)	3.74	2.83	3.27	3.35	3.42
	95 % conf. (+)	4.75	3.81	4.10	4.74	4.14
Proposed ACI 440.1R (2004)	mean	1.94	1.72	1.83	1.86	1.84
	variation	0.24	0.19	0.23	0.20	0.22
	95 % conf. (-)	1.83	1.63	1.73	1.74	1.76
	95 % conf. (+)	2.06	1.82	1.93	1.99	1.92
Razaqpur et al. (2004)	mean	1.03	1.04	1.04	1.01	1.03
	variation	0.20	0.24	0.22	0.21	0.21
	95 % conf. (-)	0.98	0.97	0.99	0.94	0.99
	95 % conf. (+)	1.09	1.11	1.10	1.08	1.08

Figure 4.6 shows the trend lines for the shear ratio versus the modulus of elasticity for CFRP-RC members. In Figure 4.6, the accuracy of the methods by Razaqpur et al. (2004), and the CSA S806-02 (2002) vary much more than the accuracy of the formula given by the JSCE (1997). Furthermore, the JSCE (1997) formula also has the advantage of giving conservative shear predictions, regardless of the modulus of the reinforcement.

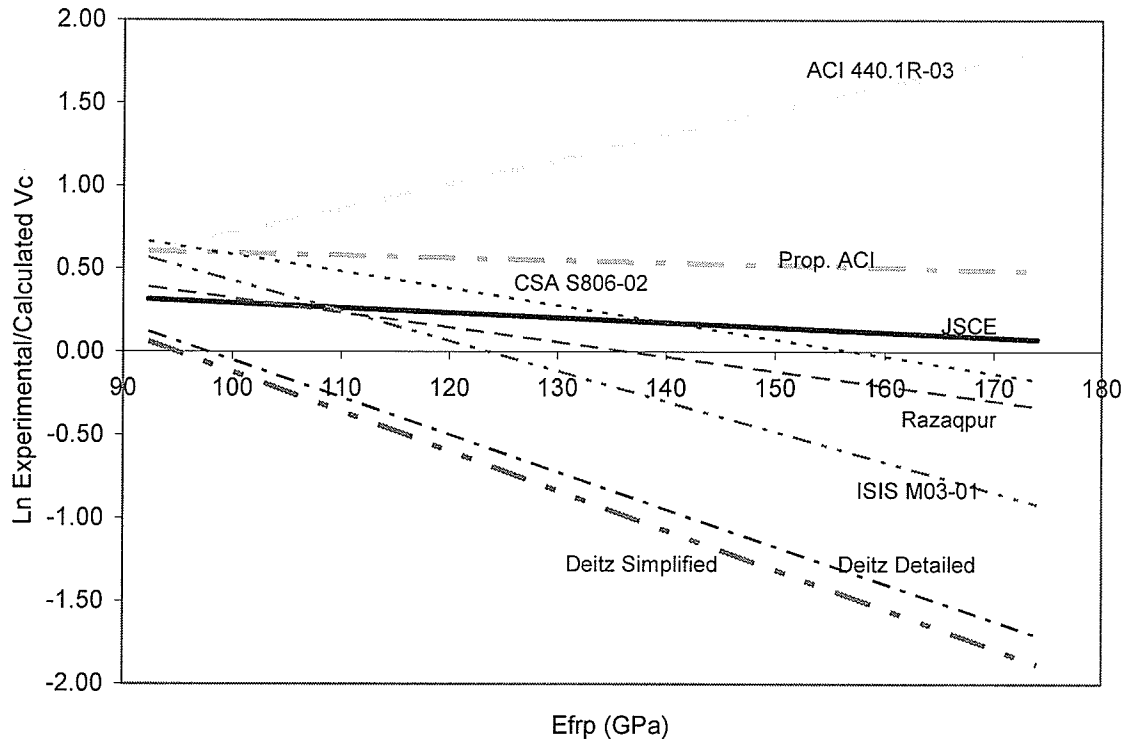


Figure 4.6 - Effect of Modulus on Concrete Shear Prediction for CFRP-RC

Since there was only one specimen with a modulus of elasticity greater than 150 GPa, a further analysis was completed which excluded this outlier from the analysis of the CFRP-RC members. Figure 4.7 shows the trend lines for the shear ratio versus the modulus of elasticity for CFRP-RC members excluding the outlier. In Figure 4.7, it is apparent that the method of the JSCE (1997) is still performing the most accurately and is always conservative. Table 4.4 shows that the equation given by Razaqpur et al. (2004) has the most accurate average ratio. However, upon reviewing Figure 4.6, it can be seen the formula tends to be conservative for members with a CFRP modulus less than 140 GPa, and unconservative when the CFRP modulus is greater than 140 GPa. Thus, the use of the formula given by the JSCE (1997) is the best suited for predicting the concrete shear strength of CFRP-RC. This formula is reasonably accurate and is conservative for its entire 95% confidence interval.

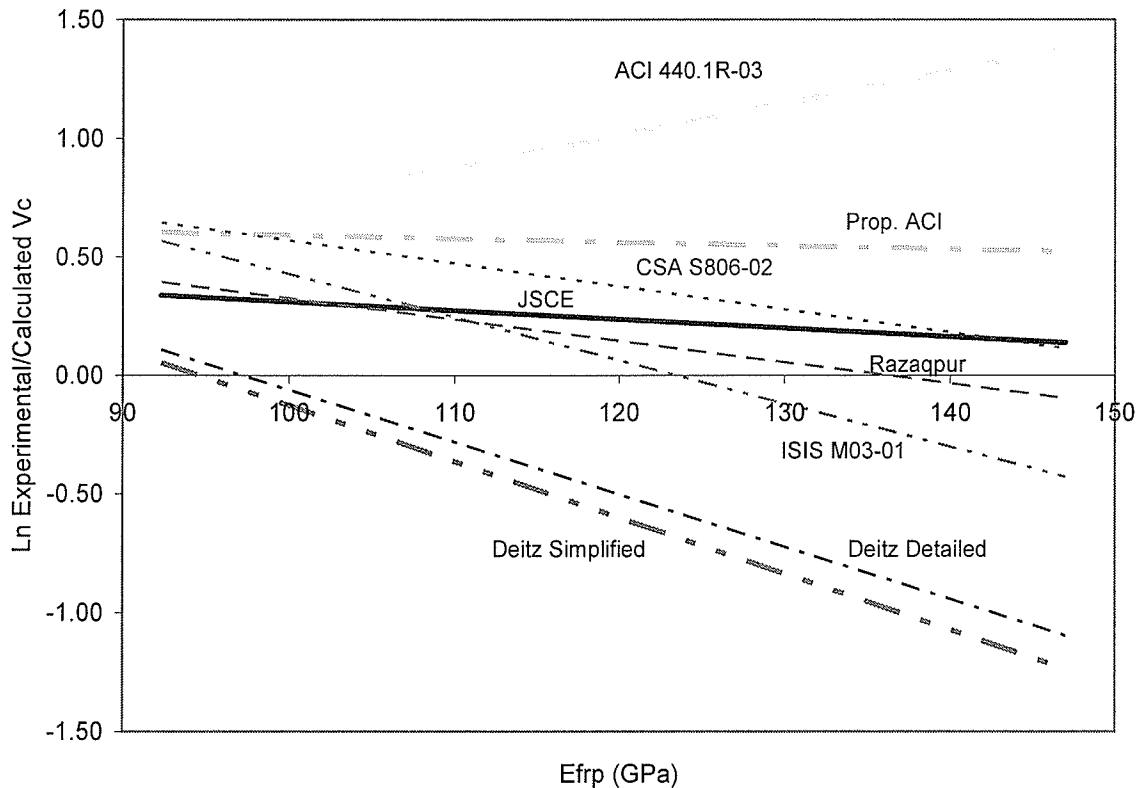


Figure 4.7 - Effect of Modulus on Concrete Shear Prediction for CFRP-RC without Outlier Point

All of the formulas for calculating the concrete shear capacity of FRP-RC are dependent upon the effective depth, d , of the member. The trend lines for the log of the experimental over predicted shear ratios versus the effective depth of the members can be seen in Figure 4.8. It can be seen that the equation given by Razaqpur et al. (2004) is typically quite accurate at predicting the shear capacity of the members. However, Figure 4.8 shows that the equation tends to be unconservative for members with an effective depth greater than 300 mm. This can be quite worrisome as this is often the case in practice. Figure 4.8 also shows that the equations given by ISIS M03-01 (2001) and CSA S806-02 (2002) are also quite accurate at predicting the concrete shear capacity, regardless of the effective depth. The formula given by the JSCE (1997) is conservative for all effective depth values and becomes increasingly conservative as the effective depth is increased.

This trend is desired as the designers of large structures will want an added insurance against a beam prematurely failing in shear. Since the formulas for predicting the shear capacity of both ISIS M03-01 (2001) and the CSA S806-02 (2002) vary depending on whether the effective depth is greater than or less than 300 mm, a statistical analysis has been performed on the accuracy of the equations in both of these ranges and can be found in Table 4.4. It can be seen in Table 4.4 that the equation given by Razaqpur et al. (2004) is quite accurate at calculating the shear capacity for either of the cases. However, as was also found in Figure 4.8, the formula is only consistently conservative for members with an effective depth less than 300 mm. Table 4.4 also shows that the ISIS M03-01 (2001) equation is performing accurately when grouped by the effective depth of the members. The concern with the ISIS M03-01 (2001) equation was that it is inconsistent with the modulus of elasticity of CFRP-RC as was shown in Figure 4.7.

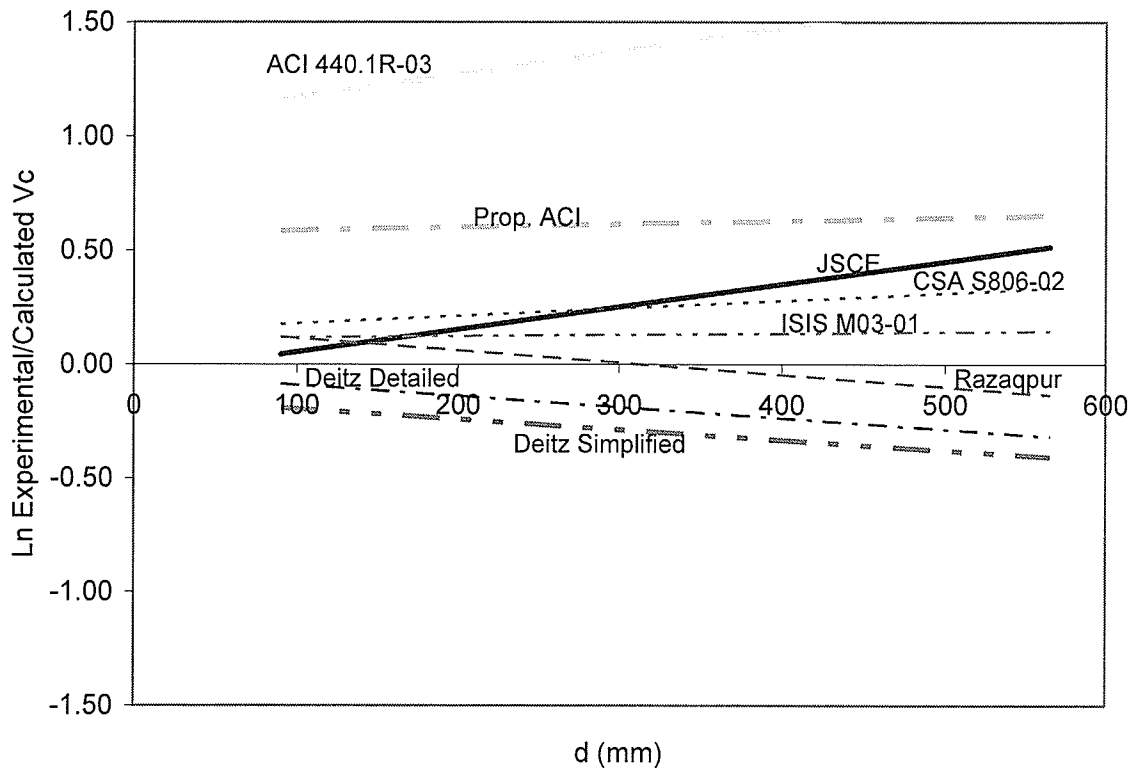


Figure 4.8 - Effect of Effective Depth on Shear Prediction

It has been shown that the accuracies of the shear formulas are dependent on both the effective depth as well as on the type of reinforcement used. For this reason, a further statistical analysis has been completed separating the members with an effective depth less than 300 mm from those with an effective depth greater than 300 mm, reinforced with either GFRP or CFRP in Table 4.5. According to Table 4.5, the equation given by Razaqpur et al. (2004) is the most accurate at predicting the concrete shear capacity in all of the categories presented. However, it can also be noticed that the formula given by Razaqpur et al. (2004) is not conservative over its entire 95% confidence interval in any of the categories presented in Table 4.5. Thus, the use of this formula is not recommended as it may not be safe in all cases. On the other hand, the use of either of the JSCE (1997) or the CSA S806-02 (2002) gives acceptable results for all of the categories, while still having conservative 95% confidence intervals. The only area of concern with the use of the CSA S806-02 (2002) formula was that it was shown to be inconsistent with the modulus of elasticity of CFRP-RC members in Figure 4.6. The JSCE (1997) formula on the other hand is always conservative, while still providing a reasonable accuracy.

Other areas of concern in predicting the concrete contribution to the shear capacity are revealed by Figures 4.9 and 4.10, which show the trend lines of each of the equations plotted against the beam slenderness ratio, a/d , and the concrete strength f'_c , respectively. It can be seen that the accuracy of all of the formulas presented varies as either the slenderness ratio or the concrete strength changes. It appears that in both cases, the equation given by the JSCE (1997) gives good results although it does become slightly unconservative in each case. However, neither case should be of great concern as

slenderness ratios rarely exceed 6.5 and concrete strengths greater than 70 MPa are also rarely used.

Table 4.5 - Further Analysis of the Predicted Shear Capacity

Method	Statistical Property	Experimental / Calculated Shear			
		GFRP-RC		CFRP-RC	
		d≤300mm	d>300mm	d≤300mm	d>300mm
	Sample size	35	13	25	14
JSCE (1997)	mean	1.16	1.47	1.11	1.43
	variation	0.20	0.22	0.23	0.12
	95 % conf. (-)	1.09	1.32	1.02	1.35
	95 % conf. (+)	1.23	1.64	1.20	1.52
Deitz - Simplified (1998)	mean	1.22	1.34	0.40	0.42
	variation	0.39	0.21	0.46	0.89
	95 % conf. (-)	1.10	1.21	0.34	0.30
	95 % conf. (+)	1.37	1.48	0.46	0.59
Deitz - General (1998)	mean	1.34	1.45	0.45	0.47
	variation	0.36	0.20	0.42	0.84
	95 % conf. (-)	1.21	1.32	0.39	0.34
	95 % conf. (+)	1.48	1.61	0.52	0.65
ISIS M03-01 (2001)	mean	1.38	1.56	0.81	0.93
	variation	0.39	0.21	0.39	0.66
	95 % conf. (-)	1.23	1.40	0.71	0.71
	95 % conf. (+)	1.53	1.73	0.92	1.21
CSA S806-02 (2002)	mean	1.17	1.41	1.17	1.52
	variation	0.33	0.22	0.23	0.57
	95 % conf. (-)	1.07	1.26	1.08	1.20
	95 % conf. (+)	1.29	1.57	1.27	1.93
ACI 440.1R-03 (2003)	mean	4.06	4.64	3.17	3.51
	variation	0.55	0.45	0.54	0.75
	95 % conf. (-)	3.51	3.80	2.67	2.61
	95 % conf. (+)	4.70	5.68	3.75	4.71
Proposed ACI 440.1R (2004)	mean	1.93	1.97	1.69	1.78
	variation	0.23	0.27	0.21	0.13
	95 % conf. (-)	1.80	1.73	1.57	1.67
	95 % conf. (+)	2.07	2.24	1.82	1.90
Razaqpur et al. (2004)	mean	1.04	1.02	1.05	1.00
	variation	0.20	0.21	0.25	0.23
	95 % conf. (-)	0.98	0.92	0.97	0.90
	95 % conf. (+)	1.10	1.12	1.15	1.12

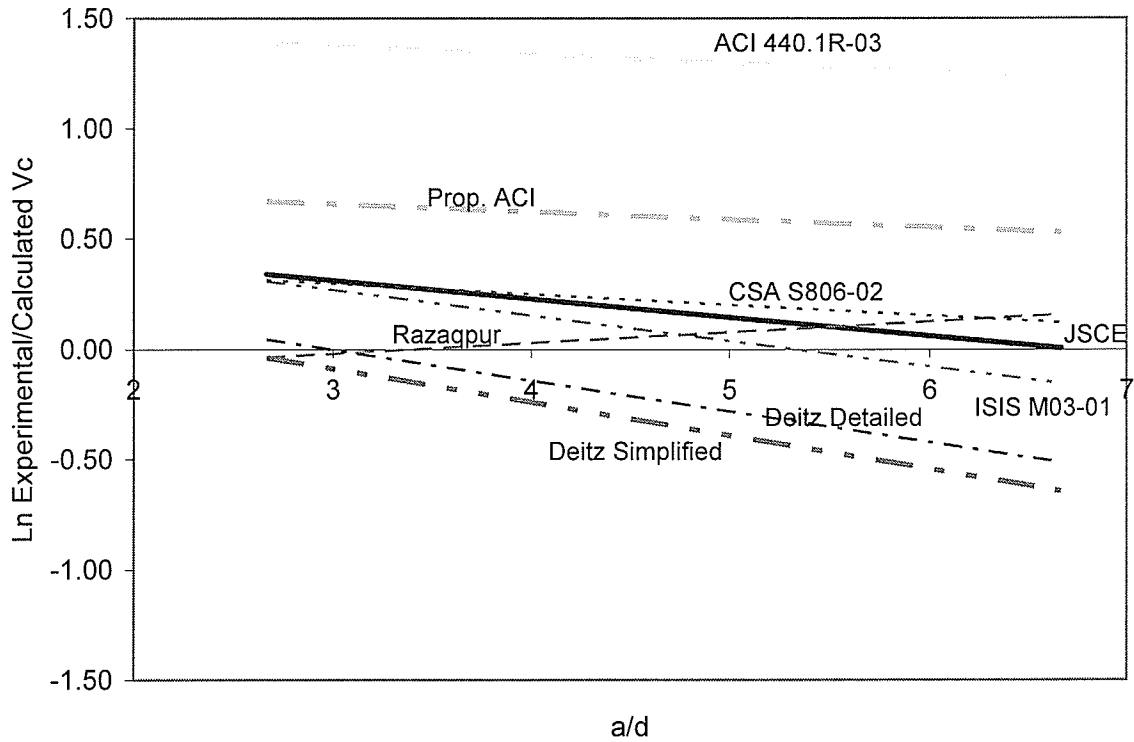


Figure 4.9 - Effect of Slenderness on Shear Prediction

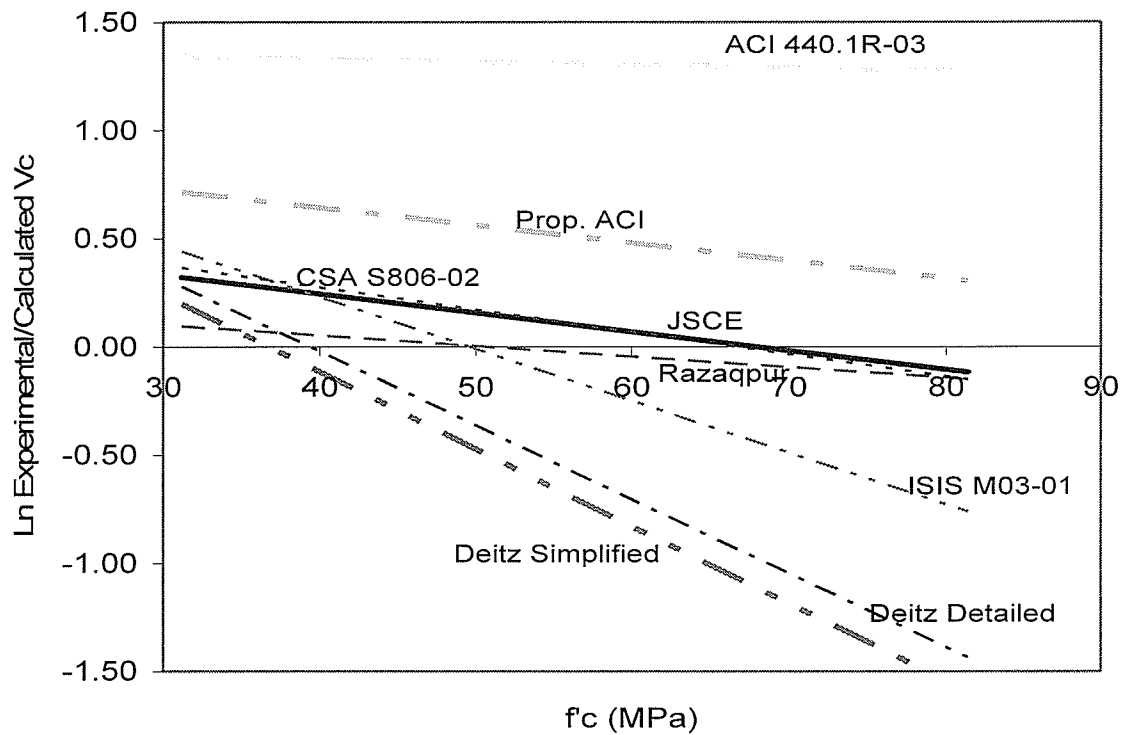


Figure 4.10 - Effect of Concrete Strength on Shear Prediction

4.5 - Deflection Analysis

It is desirable for the deflection equations to over-predict the deflection of the members to be conservative in the service analysis of the members. Typically, deflection behaviour is only checked at the service conditions. The only design manual in which the service conditions are explicitly stated is the ISIS M03-01 (2001). The service load of FRP-RC beams is referred to as the load at which the strain in the outermost FRP layer reaches a strain of ε_{frps} , equal to 2000×10^{-6} . The analysis to determine this service load is similar to finding the failure load of an under-reinforced FRP-RC beam and the neutral axis at service can be found by iterating for c using Equations 4.11 to 4.13.

$$\alpha_1 \beta_1 = \frac{\varepsilon_c}{\varepsilon_c'} - \frac{1}{3} \left(\frac{\varepsilon_c}{\varepsilon_c'} \right)^2 \quad \text{Equation 4.11}$$

$$\varepsilon_c = \frac{\varepsilon_{frps} c}{(d - c)} \quad \text{Equation 4.12}$$

$$c = \frac{A_{frp} E_{frp} \varepsilon_{frps}}{\alpha_1 \beta_1 f_c' b} \quad \text{Equation 4.13}$$

Once the neutral axis has been determined, Equations 4.14 and 4.15 can be used to find the service moment. Assuming a 4-point bending configuration and accounting for the self weight of the beam in the analysis, the service load P_{serv} , can be found with the use of Equation 4.16.

$$\beta_1 = \frac{4 - \varepsilon_c / \varepsilon_c'}{6 - 2 \varepsilon_c / \varepsilon_c'} \quad \text{Equation 4.14}$$

$$M_{serv} = \alpha_1 \beta_1 f'_c b c \left(d - \frac{\beta_1 c}{2} \right) \quad \text{Equation 4.15}$$

$$P_{serv} = \frac{M_{serv}}{a} - \frac{\gamma_{sw} b h L^2}{8a} \quad \text{Equation 4.16}$$

The service conditions proposed by ISIS M03-01 (2001) often led to instances where the service moment was smaller than the cracking moment, implying that the beam was not cracked. However, when the moment-curvature diagrams of these members were examined, all of these beams had curvature greater than the cracking curvature and therefore were cracked. A typical moment-curvature diagram for these members can be seen in Figure 4.11. The reason for this is the sudden decrease in stiffness immediately after cracking, when concrete in tension is not considered in calculating the capacity of the section. Since the cracking moment is greater than the service moment, all the formulas recommend the use of the gross moment of inertia to calculate the service deflection. This is incorrect and therefore, members that had service moments less than the cracking moment were not included in the service load analysis. This greatly reduced the number of members in the analysis and led to under-reinforced members not being analyzed, as they all encountered this phenomenon.

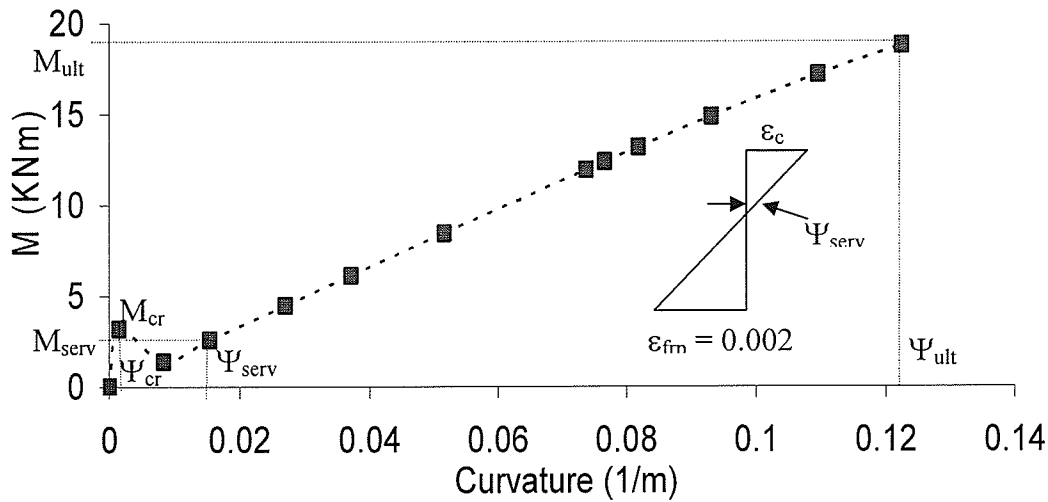


Figure 4.11 - Moment-Curvature Relationship for Beam BC2H (Theriault et al., 1997)

Since almost half of the beams in the database had, according to ISIS M03-01 (2001), service moments smaller than the cracking moment, it was desired to perform a statistical analysis at a load level which encompassed all of the beams in the database to improve the reliability of the statistical equations. Upon viewing a plot of the log of the deflection ratios versus the ratio of the applied moment to the cracking moment as shown in Figure 4.12, a funnel effect could be seen. All points plotted around the horizontal axis have been calculated correctly, while the others have not. An inspection of Figure 4.12 indicates that the consistency of the equations is improved dramatically at elevated loads of M_a/M_{cr} larger than 8 and that the greatest area of concern is slightly after cracking for all equations. Similar behaviour was also observed earlier in steel RC (Choi et al. 2004). Since all equations are accurate at higher loads, it was desired to perform an analysis of the behaviour of the equations at a lower load where there is a greater spread between the outputs of each equation. This load was chosen to be $1.1P_{cr}$.

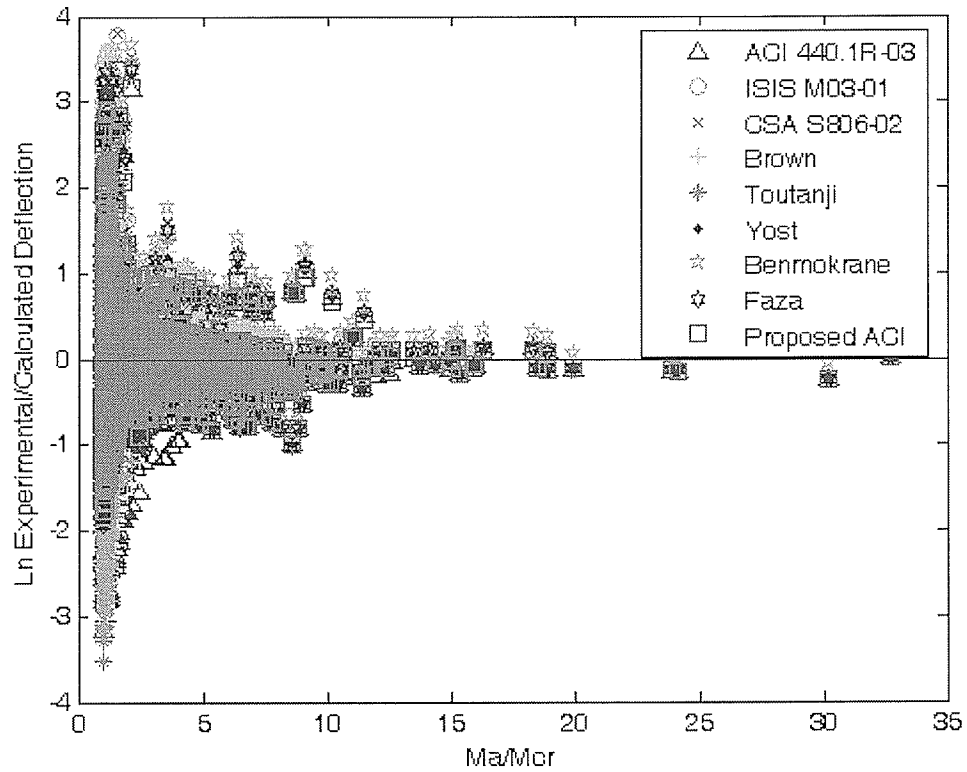


Figure 4.12 - Effect of Applied Moment on Deflection Prediction

A statistical analysis was also performed on each of the code equations at 50% and 80% of the maximum experimental loads to validate the equations for the entire loading range. This will allow the codes to choose a deflection equation that gives accurate results at the load level which most closely resembles their service conditions.

4.5.1 - Derivation of Proposed Deflection Equation

It is believed that the basic form of Equation 2.23 should remain unchanged, as it has had great success in predicting the deflection of conventional RC beams. Thus, an empirical modification factor was developed which can be used to have the deflection response converge to the cracked deflection response quicker when FRP is used as the longitudinal

reinforcement. The form of the equation has maintained the same form as that of Equation 2.36 with the only difference in the definition of β .

Through the completion of some preliminary analysis, it was found that the accuracy of Equation 2.23 relied both on the modulus of the reinforcement, as well as on the amount of reinforcement present. A correlation analysis was then completed at the service load level to determine which variables affected the accuracy of β the most, if an effective moment of inertia formula of the same form as Equation 2.36 was used. Contrary to what the ACI 440.1R (2004) had previously found, the accuracy of β was most dependant on the square root of the relative reinforcement ratio, rather than the relative reinforcement ratio. This can be seen in Table 4.6, which shows that this variable's correlation with β is the closest to 1.0 at the service load level.

Table 4.6 - Correlation Analysis at Service Load

Property	f'c (MPa)	Ec (MPa)	E_{frp} (MPa)	f_{frp} (MPa)	ρ	ρ/ρ_{bal}	$(\rho/\rho_{bal})^{1/2}$	l_{cr}/l_g	β
f'c (MPa)	1.000								
Ec (MPa)	0.833	1.000							
E_{frp} (MPa)	0.211	0.215	1.000						
f_{frp} (MPa)	0.341	0.375	0.908	1.000					
ρ	0.018	-0.041	-0.661	-0.668	1.000				
ρ/ρ_{bal}	-0.296	-0.288	-0.191	-0.050	0.453	1.000			
$(\rho/\rho_{bal})^{1/2}$	-0.299	-0.281	-0.180	-0.034	0.450	0.990	1.000		
l_{cr}/l_g	-0.303	-0.451	0.451	0.184	-0.027	0.209	0.214	1.000	
β	-0.037	-0.055	-0.107	-0.002	0.106	0.227	0.233	-0.079	1.000

Unlike the Proposed ACI 440.1R (2004) equation, it was further found that the coefficient for this term was dependent upon whether the reinforcement was GFRP or

CFRP. A regression analysis was completed at the service load level for both GFRP-RC and CFRP-RC beams, to determine that the coefficient should be 0.2 for GFRP-RC and 0.125 for CFRP-RC.

Since only over-reinforced members were able to be properly analyzed at the service conditions, a further correlation analysis was done at a load level of $1.1P_{cr}$ to determine which variables affected the accuracy of the deflection equations the most for the beams which were under-reinforced. Here, as the ACI 440.1R (2004) had previously found, it was determined that the accuracy of β was most dependant on the relative reinforcement ratio. Through the completion of a regression analysis, it was determined that the same coefficients found in the analysis at service could also be used for under-reinforced members, while still giving conservative deflection estimates. In summary, the proposed deflection equation follows the same format as Equation 2.36, with the difference arising in the definition of β . Here, β is defined according to Equations 4.17 to 4.19.

$$\beta = \beta_{\rho} \beta_E \quad \text{Equation 4.17}$$

$$\beta_{\rho} = \rho / \rho_{bal} \quad \text{if } \rho / \rho_{bal} < 1.0 \quad \text{Equation 4.18}$$

$$\beta_{\rho} = \sqrt{\rho / \rho_{bal}} \quad \text{if } \rho / \rho_{bal} \geq 1.0$$

$$\beta_E = 0.125 \quad \text{if CFRP-RC} \quad \text{Equation 4.19}$$

$$\beta_E = 0.2 \quad \text{if GFRP-RC}$$

To verify the use of the proposed formula, the deflection responses of the proposed formula were compared against the deflection responses received from the lab tests. The comparison between these responses can be seen in Figures 4.13 to 4.17.

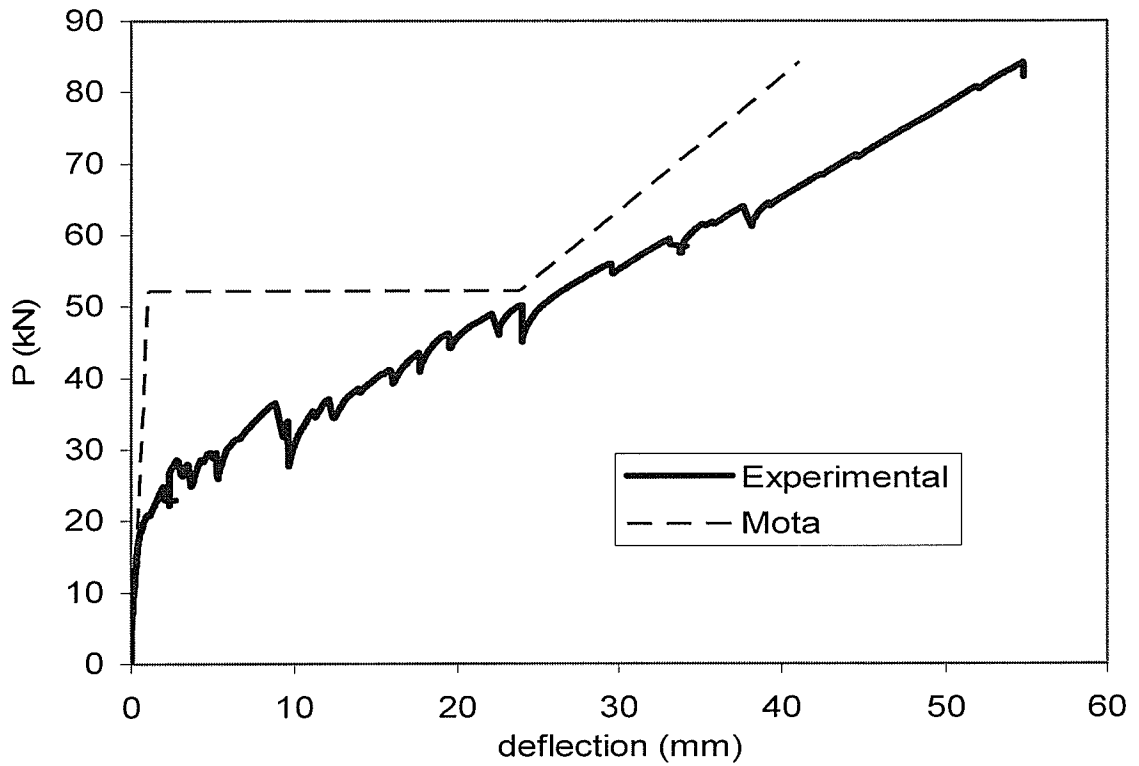


Figure 4.13 - Load Deflection Behaviour for Beam # 3A

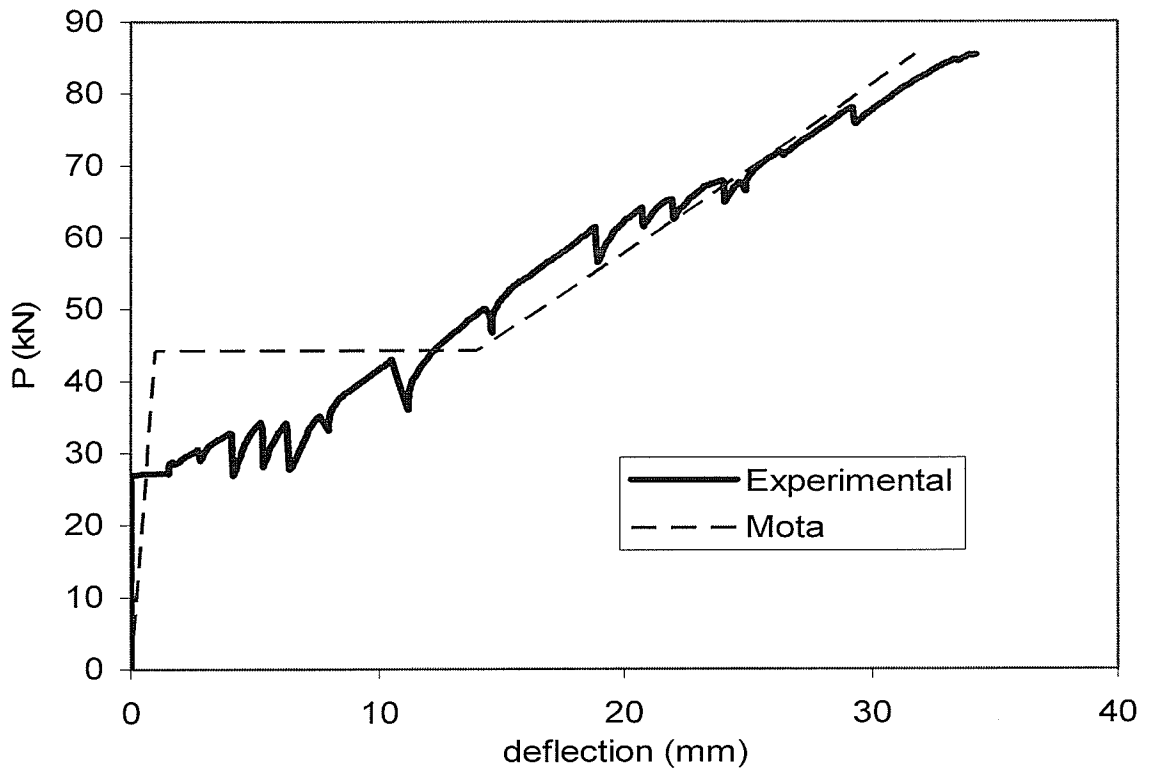


Figure 4.14 - Load Deflection Behaviour for Beam # 4L-A

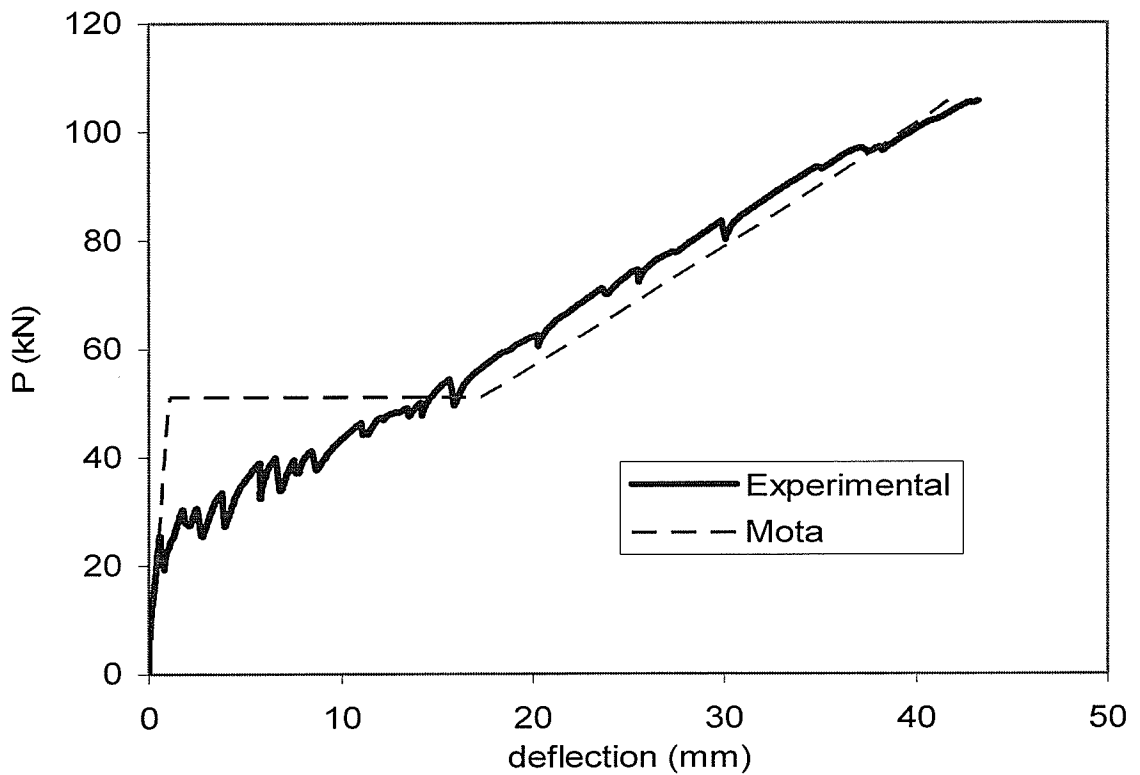


Figure 4.15 - Load Deflection Behaviour for Beam # 4L-B

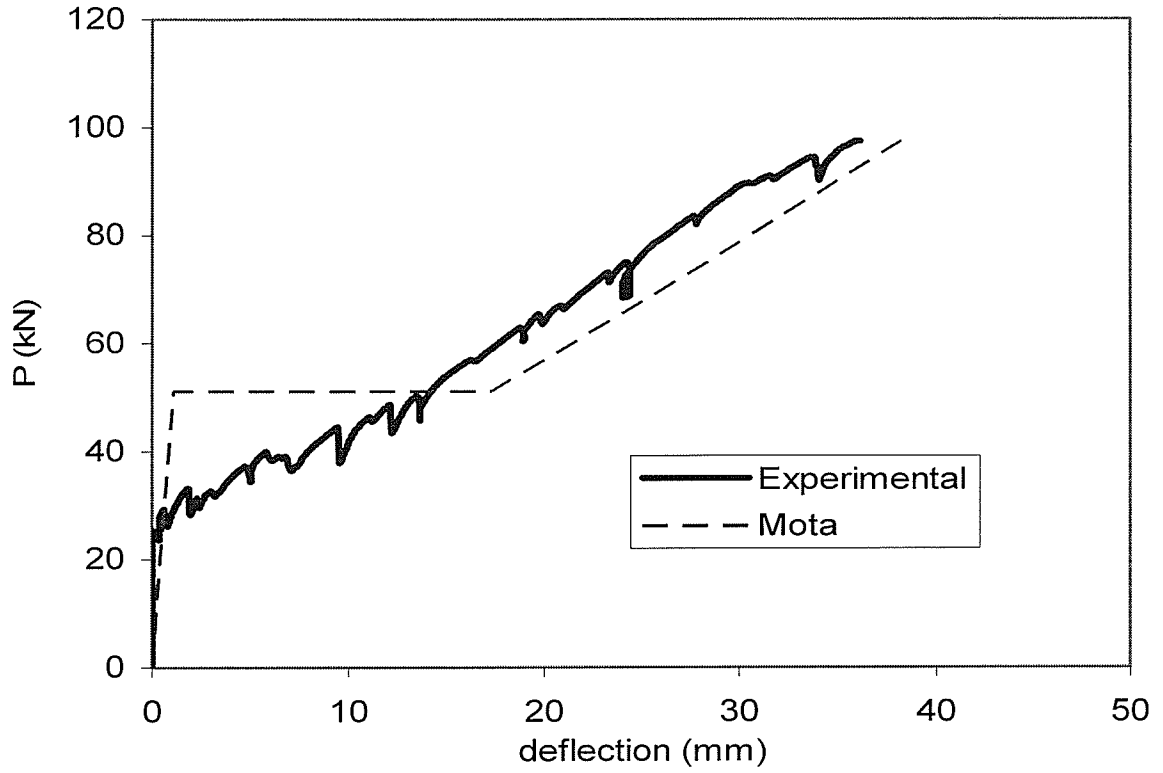


Figure 4.16 - Load Deflection Behaviour for Beam # 4L-C

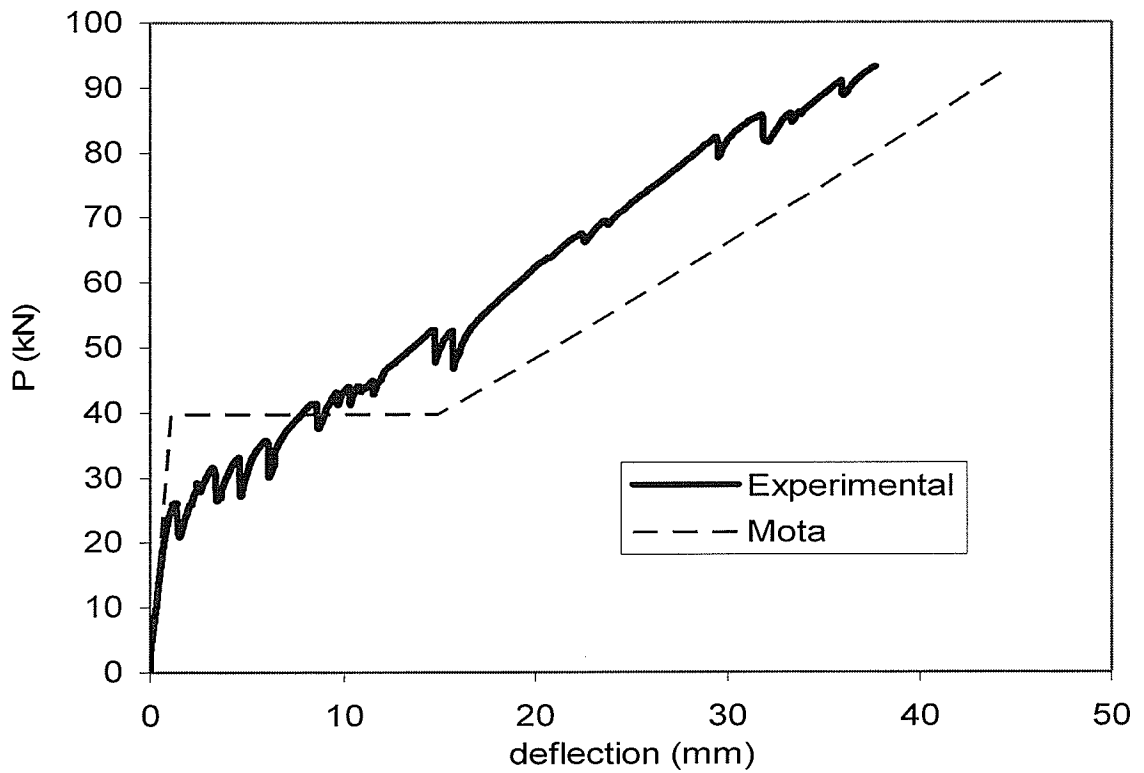


Figure 4.17 - Load Deflection Behaviour for Beam # 4L-D

In viewing Figures 4.13 to 4.17, it can be seen that the cracking loads were predicted quite poorly from the use of Equations 2.24 and 2.25 for all of the FRP-RC beams tested. This led to very poor deflection prediction at low loads. After the predicted cracking load however, the proposed deflection equation predicts the deflection responses of the beams tested quite well. In particular, the deflection responses of the over-reinforced beams (4L-A to 4L-D) were predicted quite well. The deflection response of the under-reinforced beam (3A) was not predicted as well and is likely a result of the poor calculation of the cracking load.

4.5.2 - Deflection Analysis at Service

The trend lines for the log of the deflection ratios versus the modulus of elasticity for GFRP-RC beams at the service load level can be seen in Figure 4.18. In order for the formulas to be conservative, the log of the deflection ratio has to be smaller than zero. Figure 4.18 shows that the formulas proposed by Yost et al. (2003) and Bischoff (2005) yield satisfactory results and their accuracies are not affected by changes in the modulus of elasticity. This is important since the modulus of elasticity changes rapidly among different types of FRP. Comparable results to those received by Yost et al. (2003) and Bischoff (2005) can also be seen by the formula proposed by the author (Mota). An advantage of this formula is that at this load level it is always conservative. Table 4.7 shows the statistical analysis of each of the formulas at the service load level. The formulas are conservative if the 95% confidence interval is less than one. The formula given by Bischoff (2005) is the most accurate for GFRP-RC beams with a mean value of 1.01. However, the formula given by Mota is quite comparable in accuracy and is conservative over the entire 95% confidence interval.

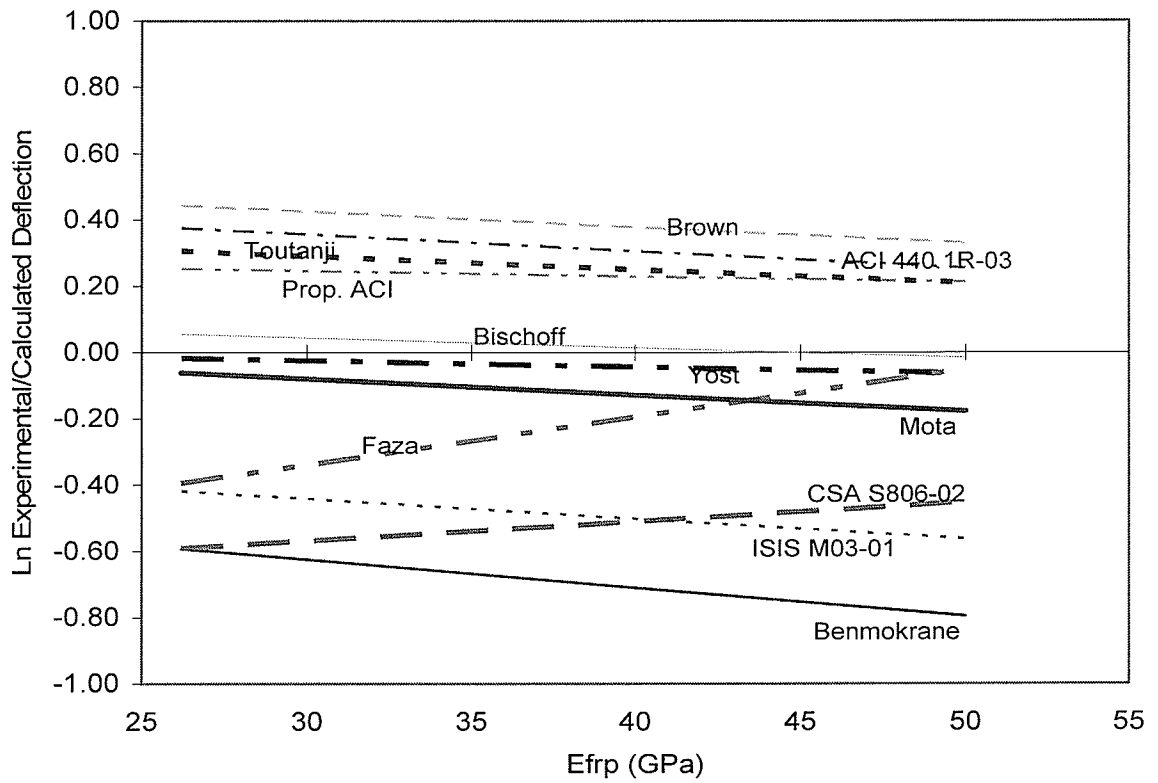


Figure 4.18 - Effect of Modulus on Deflection Prediction at Service for GFRP-RC

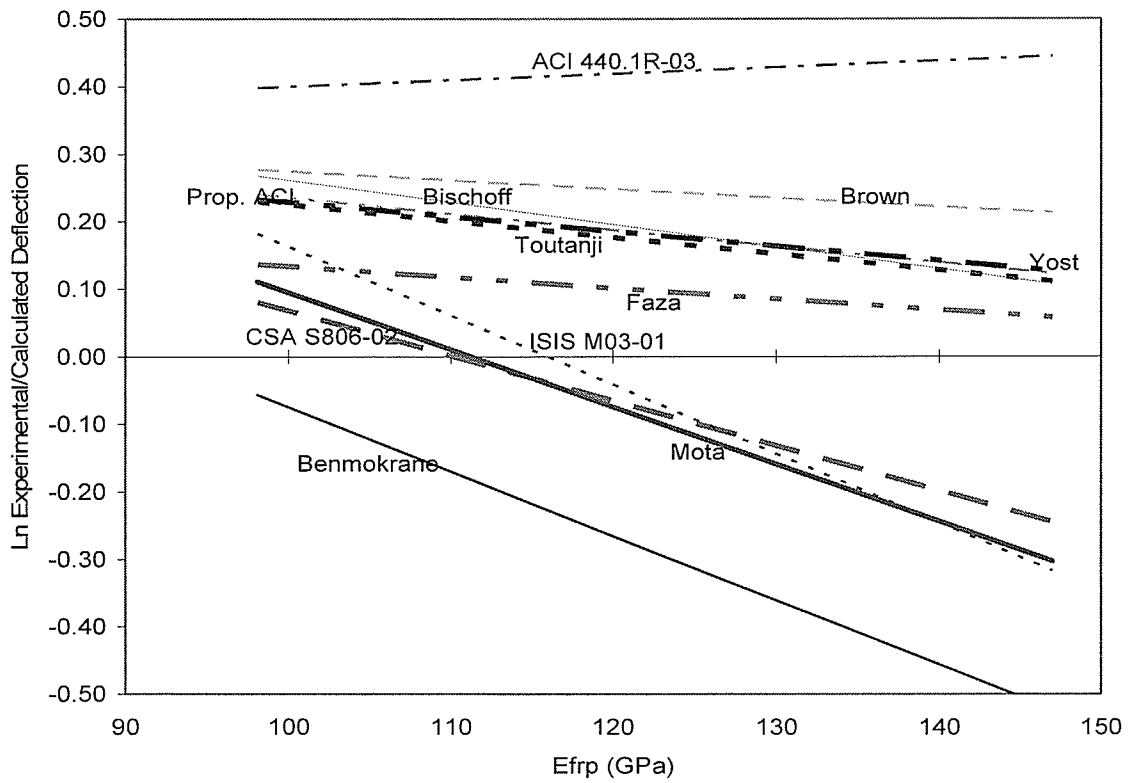


Figure 4.19 - Effect of Modulus on Deflection Prediction at Service for CFRP-RC

Table 4.7 - Statistical Analysis of the Predicted Deflections at Service

Method	Statistical Property	Experimental / Calculated Deflection			
		GFRP-RC	CFRP-RC	AFRP-RC	All Members
	Sample size	67	41	2	110
Faza & GangaRao (1992)	mean	0.81	1.10	1.92	0.92
	variation	0.94	0.36	1.24	0.79
	95 % conf. (-)	0.69	1.00	0.63	0.83
	95 % conf. (+)	0.95	1.21	5.87	1.03
Benmokrane et al. (1996)	mean	0.49	0.72	0.52	0.57
	variation	0.74	0.46	0.05	0.69
	95 % conf. (-)	0.43	0.64	0.49	0.52
	95 % conf. (+)	0.56	0.81	0.56	0.63
Brown & Bartholomew (1996)	mean	1.45	1.27	1.49	1.38
	variation	0.95	0.67	1.71	0.85
	95 % conf. (-)	1.24	1.09	0.37	1.23
	95 % conf. (+)	1.70	1.49	5.93	1.55
Toutanji & Saafi (2000)	mean	1.28	1.17	1.39	1.24
	variation	0.96	0.67	1.77	0.85
	95 % conf. (-)	1.09	1.00	0.34	1.11
	95 % conf. (+)	1.50	1.37	5.71	1.39
ISIS M03-01 (2001)	mean	0.60	0.90	0.69	0.70
	variation	0.73	0.50	0.02	0.70
	95 % conf. (-)	0.53	0.79	0.67	0.63
	95 % conf. (+)	0.68	1.02	0.71	0.77
CSA S806-02 (2002)	mean	0.59	0.90	1.05	0.70
	variation	0.78	0.41	0.81	0.71
	95 % conf. (-)	0.51	0.81	0.46	0.63
	95 % conf. (+)	0.68	1.00	2.39	0.77
ACI 440.1R-03 (2003)	mean	1.35	1.53	1.35	1.42
	variation	0.80	0.59	0.89	0.72
	95 % conf. (-)	1.17	1.33	0.56	1.28
	95 % conf. (+)	1.55	1.76	3.26	1.57
Yost et al. (2003)	mean	0.95	1.19	1.37	1.04
	variation	0.77	0.41	0.53	0.66
	95 % conf. (-)	0.83	1.07	0.76	0.95
	95 % conf. (+)	1.09	1.32	2.47	1.14
Proposed ACI 440.1R (2004)	mean	1.24	1.19	1.87	1.23
	variation	0.84	0.41	1.16	0.69
	95 % conf. (-)	1.07	1.07	0.64	1.12
	95 % conf. (+)	1.43	1.32	5.44	1.36
Bischoff (2005)	mean	1.01	1.19	1.25	1.08
	variation	0.71	0.51	0.91	0.64
	95 % conf. (-)	0.89	1.05	0.51	0.98
	95 % conf. (+)	1.14	1.35	3.04	1.18
Mota	mean	0.87	0.88	1.14	0.88
	variation	0.77	0.44	0.51	0.65
	95 % conf. (-)	0.76	0.79	0.64	0.80
	95 % conf. (+)	1.00	0.98	2.02	0.97

From the trend lines for the deflection ratio versus the modulus of elasticity for CFRP-RC beams at the service load level, a different trend can be seen. Figure 4.19 shows that the accuracy of the methods by Bischoff (2005), Yost et al. (2003), the Proposed ACI 440.1R (2004), Faza and GangaRao (1991), and Toutanji and Saafi (2000) have a lesser variance with the modulus of elasticity of the CFRP than do the methods proposed by ISIS M03-01 (2001), CSA S806-02 (2002), or Mota. Although the accuracy of these latter formulas does seem to vary with the modulus of the CFRP, they do have the advantage of giving conservative deflection estimates. Table 4.7 shows that the formula proposed by Faza and GangaRao (1992) is the most accurate formula for CFRP-RC beams. However, the formulas given by the CSA S806-02 (2002) and ISIS M03-01 (2001) are similar in accuracy and have the benefit of giving conservative deflection estimates. It can also be seen that the formula given by Mota gives very comparable results and is also conservative over its entire 95% confidence interval.

Table 4.7 demonstrates the accuracy of each of the formulas for the AFRP-RC beams present in the database. The CSA S806-02 (2002) equation is the most accurate equation for calculating the deflection of AFRP-RC beams at the service load level. However, given that there were only 2 AFRP-RC members in the database, the central limit theorem does not apply here, and this information should be taken lightly.

Given that the method proposed by Yost et al. (2003) over predicts the deflection of GFRP-RC and under predicts the deflection of CFRP-RC, it is no coincidence that when looking at the entire dataset at the service load level, this method performs the most

accurately as shown in Table 4.7. This trend can also be seen in the formula given by Faza and GangaRao (1992), which also gives accurate results when looking at the entire dataset. However, if consistency of a formula is the key, the formula proposed by Mota was found to satisfy this criterion the best. This formula was both accurate and conservative at this load level. Thus, the use of the Mota formula for calculating the service load deflection of FRP-RC beams is recommended.

Other areas of concern in predicting the deflection at service load are revealed by Figures 4.20 and 4.21, which show the trend lines of each of the equations plotted against the beam slenderness ratio, a/d , and relative reinforcement ratio, ρ/ρ_{bal} , respectively. It can be seen that the accuracy of all of the formulas presented varies as either the slenderness ratio or relative reinforcement ratio changes. The latter is of less concern as FRP-RC tends to usually be only slightly over-reinforced for economic purposes. However, the effect of the slenderness ratio on deflection prediction needs further investigation. It should also be noticed that the formulas proposed by Faza and GangaRao (1992) and Mota are the least affected by either of these relationships.

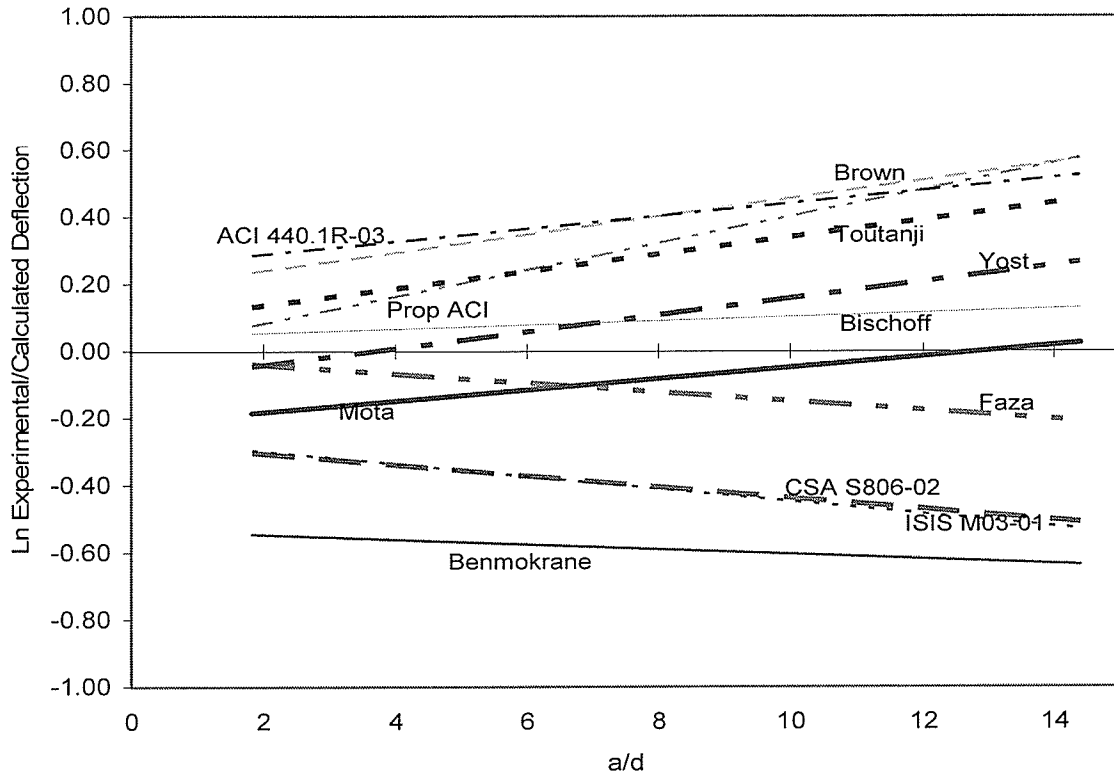


Figure 4.20 - Effect of Slenderness on Deflection Prediction at Service

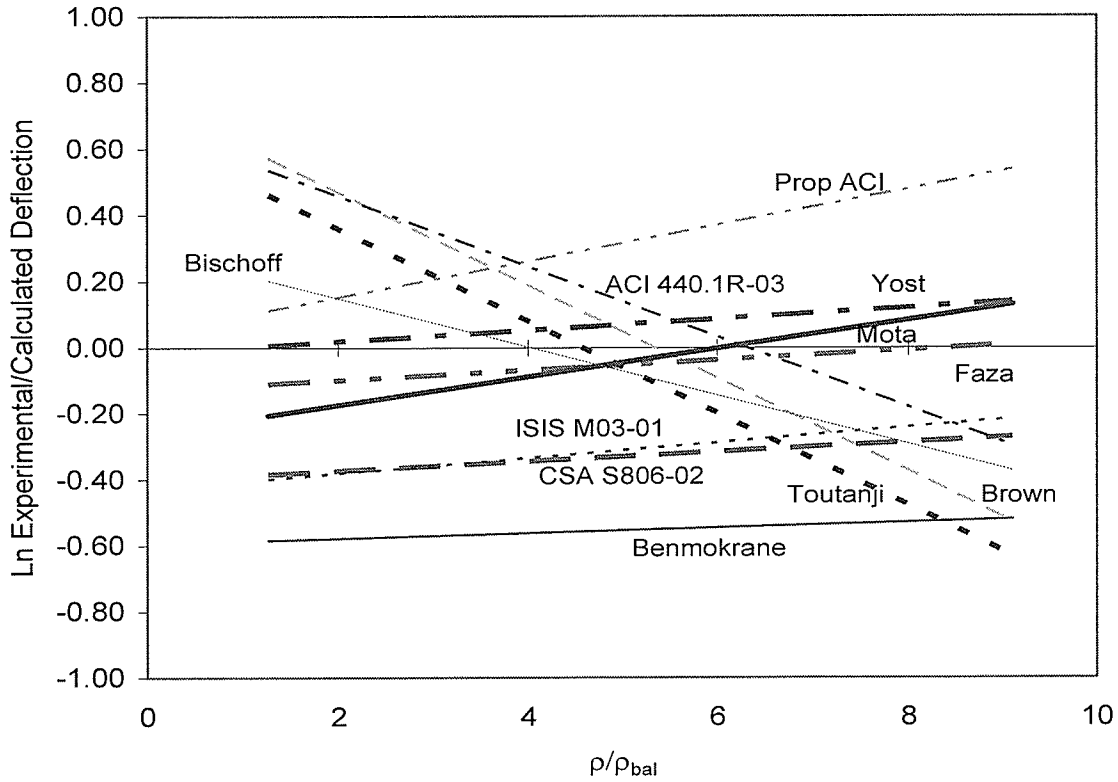


Figure 4.21 - Effect of Relative Reinforcement Ratio on Deflection Prediction at Service

4.5.3 - Deflection Analysis at Load Levels close to Cracking

The trend lines of the log of experimental over calculated deflection, at a load level of $1.1P_{cr}$, were plotted with respect to the modulus of elasticity of GFRP in Figure 4.22. Figure 4.22 shows that the Proposed ACI 440.1R (2004), Yost et al. (2003), and Mota formulas are all quite accurate at predicting the deflection of GFRP-RC beams at a load of $1.1P_{cr}$. The figure indicates that the accuracy of these formulas, with a minor exception to that of the Proposed ACI 440.1R (2004), does not vary with the value for modulus of elasticity of the GFRP. The advantage to the formula given by Mota is that it is always conservative for these types of members, while the other two equations tend to be slightly unconservative at this load level. All other equations tend to be far less accurate at this load level. Table 4.8 shows the statistical analysis of each of the formulas at this load. As mentioned above, the formula given by Yost et al. (2003) is the most accurate. However, the formula given by Mota is quite comparable in accuracy and is conservative over its entire 95% confidence interval.

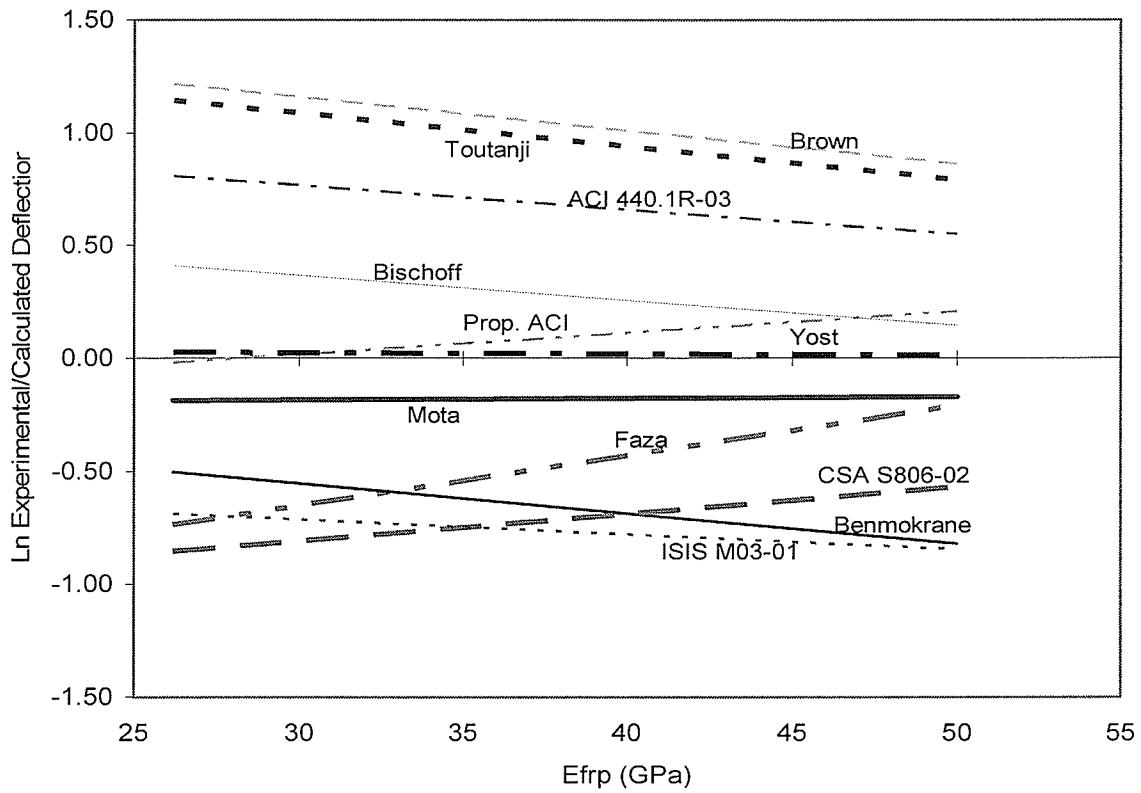


Figure 4.22 - Effect of Modulus on Deflection Prediction at $1.1P_{cr}$ for GFRP-RC

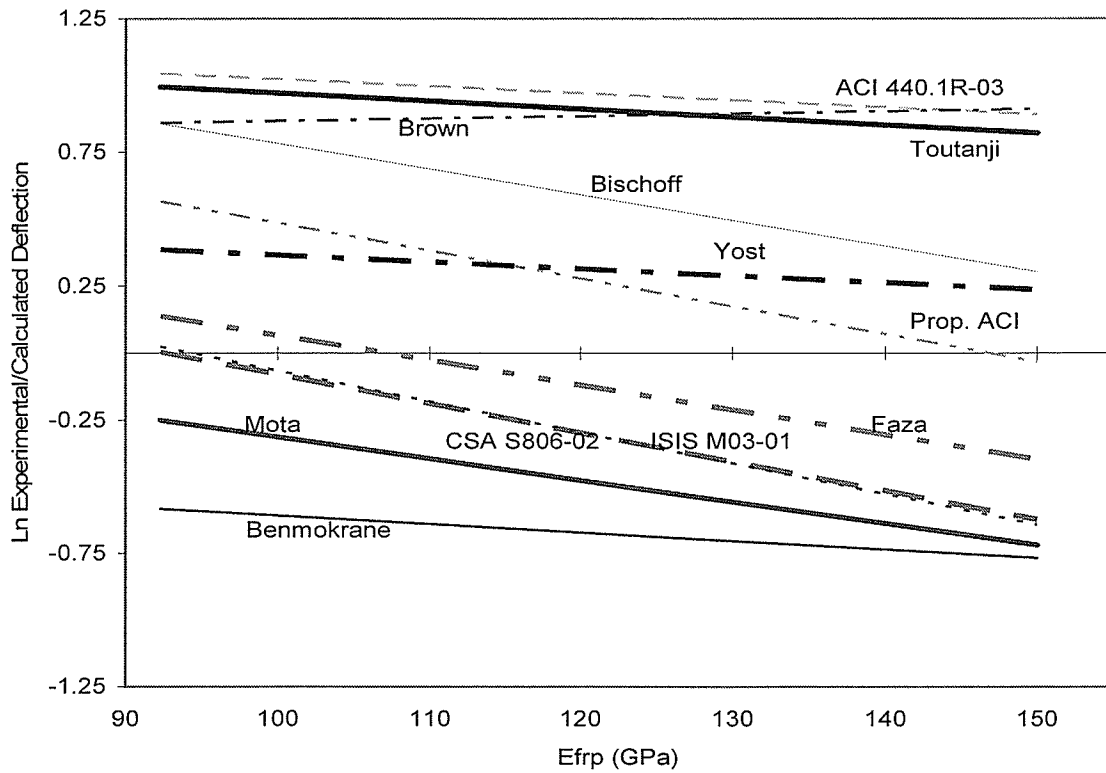


Figure 4.23 - Effect of Modulus on Deflection Prediction at $1.1P_{cr}$ for CFRP-RC

Table 4.8 - Statistical Analysis of the Predicted Deflections at $1.1P_{cr}$

Method	Statistical Property	Experimental / Calculated Deflection				All Members
		GFRP-RC	CFRP-RC	$\rho > \rho_{bal}$	$\rho < \rho_{bal}$	
	Sample size	139	56	165	32	197
Faza & GangaRao (1992)	mean	0.64	0.83	0.70	0.68	0.70
	variation	1.21	0.53	1.02	1.29	1.06
	95 % conf. (-)	0.56	0.74	0.63	0.51	0.63
	95 % conf. (+)	0.73	0.93	0.78	0.91	0.77
Benmokrane et al. (1996)	mean	0.50	0.51	0.43	1.19	0.50
	variation	1.24	1.02	0.82	1.65	1.17
	95 % conf. (-)	0.44	0.42	0.39	0.85	0.45
	95 % conf. (+)	0.57	0.61	0.47	1.67	0.56
Brown & Bartholomew (1996)	mean	2.75	2.67	2.28	6.83	2.72
	variation	1.28	1.14	0.86	1.67	1.23
	95 % conf. (-)	2.40	2.19	2.07	4.86	2.43
	95 % conf. (+)	3.15	3.26	2.51	9.60	3.04
Toutanji & Saafi (2000)	mean	2.56	2.51	2.13	6.34	2.54
	variation	1.27	1.14	0.86	1.68	1.22
	95 % conf. (-)	2.23	2.06	1.94	4.51	2.27
	95 % conf. (+)	2.93	3.06	2.34	8.92	2.84
ISIS M03-01 (2001)	mean	0.46	0.69	0.50	0.60	0.51
	variation	1.01	0.70	0.84	1.60	0.97
	95 % conf. (-)	0.41	0.60	0.46	0.43	0.46
	95 % conf. (+)	0.52	0.79	0.55	0.84	0.56
CSA S806-02 (2002)	mean	0.50	0.69	0.55	0.56	0.55
	variation	1.09	0.51	0.90	1.34	0.97
	95 % conf. (-)	0.44	0.62	0.50	0.42	0.50
	95 % conf. (+)	0.57	0.77	0.61	0.75	0.60
ACI 440.1R-03 (2003)	mean	1.94	2.53	1.75	5.23	2.09
	variation	1.28	1.14	0.86	1.79	1.25
	95 % conf. (-)	1.69	2.07	1.59	3.67	1.87
	95 % conf. (+)	2.22	3.09	1.92	7.46	2.34
Yost et al. (2003)	mean	1.01	1.38	1.01	1.80	1.11
	variation	1.16	0.81	0.89	1.71	1.09
	95 % conf. (-)	0.89	1.18	0.92	1.27	1.00
	95 % conf. (+)	1.15	1.61	1.11	2.54	1.23
Proposed ACI 440.1R (2004)	mean	1.11	1.22	1.20	0.93	1.15
	variation	1.26	0.65	1.00	1.52	1.09
	95 % conf. (-)	0.97	1.07	1.08	0.68	1.04
	95 % conf. (+)	1.27	1.39	1.33	1.28	1.27
Bischoff (2005)	mean	1.29	1.70	1.30	1.97	1.39
	variation	1.00	0.84	0.80	1.63	0.97
	95 % conf. (-)	1.15	1.45	1.19	1.41	1.27
	95 % conf. (+)	1.44	1.99	1.43	2.76	1.53
Mota	mean	0.83	0.59	0.74	0.84	0.76
	variation	1.09	0.65	0.92	1.45	1.00
	95 % conf. (-)	0.73	0.52	0.67	0.62	0.69
	95 % conf. (+)	0.94	0.67	0.82	1.15	0.84

Trend lines for the log of the deflection ratio versus the modulus of elasticity for CFRP-RC were plotted at a load of $1.1P_{cr}$ and are shown in Figure 4.23. In Figure 4.23, there was initially an outlier with a modulus of elasticity greater than 150 GPa which was removed from the analysis so as to not skew the trend lines. It can be seen that the accuracy of all of the formulas presented tends to have a dependence on the modulus of elasticity of the reinforcement for CFRP-RC. The dependence of the method proposed by ACI 440.1R (2004) on the modulus of elasticity of the CFRP is quite similar to the method proposed by Faza and Ganga Rao (1992). However, the formula proposed by Faza and Ganga Rao (1992) conservatively estimates deflection larger than the experimental deflection. Meanwhile, the CSA S806-02 (2002) and ISIS M03-01 (2001) methods are even more conservative than Faza and Ganga Rao's (1992) formula. It can also be seen in Figure 4.23 that the equation given by Mota does not predict the deflection of CFRP-RC beams well at the load level of $1.1P_{cr}$. However, this method does still give conservative results at the load level which is important. Table 4.8 shows that the formula given by Faza and Ganga Rao (1992) is the most accurate for predicting the deflection of CFRP-RC beams at this load level. The formula given by the Proposed ACI 440.1R (2004) is also accurate at this load level but gives deflection predictions that are not conservative, which is undesired. The formula presented by Faza and Ganga Rao (1992) on the other hand is consistently conservative.

It was previously found by the ACI 440.1R (2004) that the relative reinforcement ratio affects the deflection of FRP-RC. Figure 4.24 plots the log of experimental over calculated deflection for over-reinforced members and clearly shows that all of the

methods have varying accuracy depending on the relative reinforcement ratio. Given that members typically have reinforcement ratios that are less than 2.5 times the balanced reinforcement ratio, the method given by Yost et al. (2003) is performing most accurately for beams which are over-reinforced. These results are verified in Table 4.8 with the equation by Yost et al. (2003) having an average ratio of 1.01. This method is the most accurate and consistently conservative at reinforcement ratios of up to $2.5\rho_{bal}$, while the formula given by Mota is conservative up to $5\rho_{bal}$. The CSA S806-02 (2002), ISIS M03-01 (2001), and Faza and Ganga Rao (1992) formulas, are conservative for nearly the entire range of reinforcement ratios, and become increasingly accurate as the reinforcement ratio is increased.

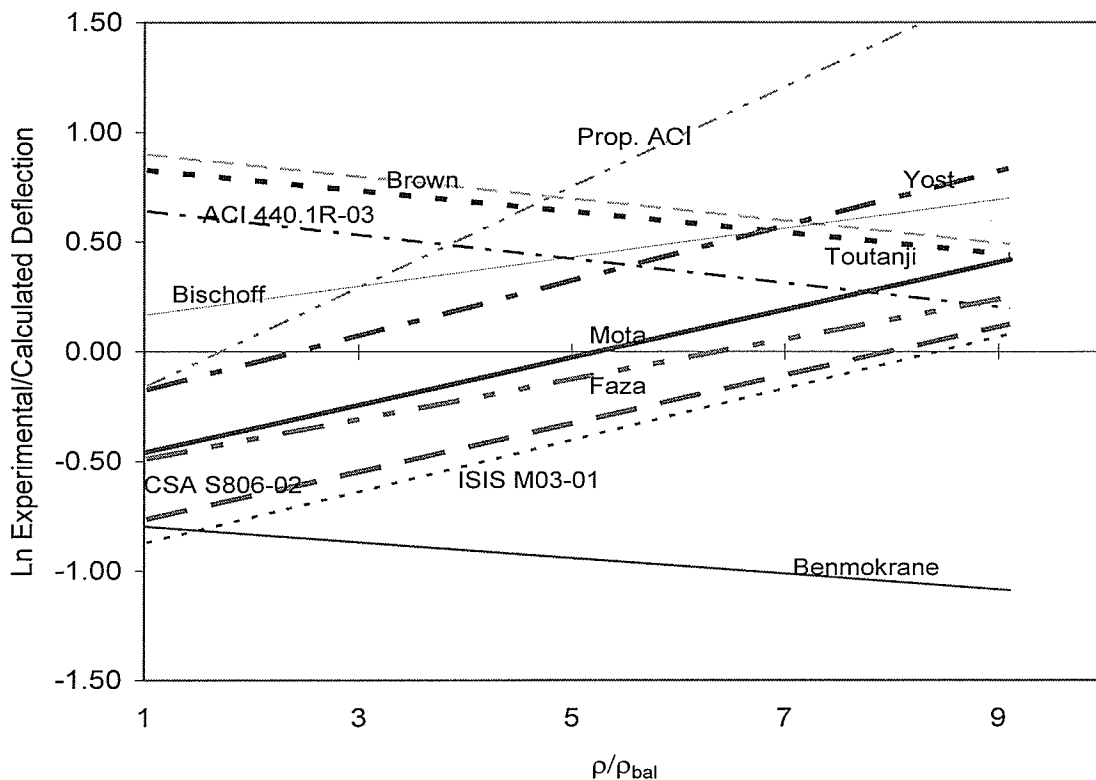


Figure 4.24 - Effect of Relative Reinforcement Ratio on Deflection Prediction for Over-Reinforced Members at 1.1Pcr

When a similar plot for members which are under-reinforced in Figure 4.25 is examined, it appears that the formula of the Proposed ACI 440.1R (2004) is quite precise at calculating the deflection at $1.1P_{cr}$ for under-reinforced members, regardless of the relative reinforcement ratio. Similar results can also be seen for the equation given by Mota, only this formula gives slightly more conservative results than that of the Proposed ACI 440.1R (2004). This is verified by Table 4.8, which shows that both formulas are not only accurate, but also have confidence intervals which are nearly always conservative.

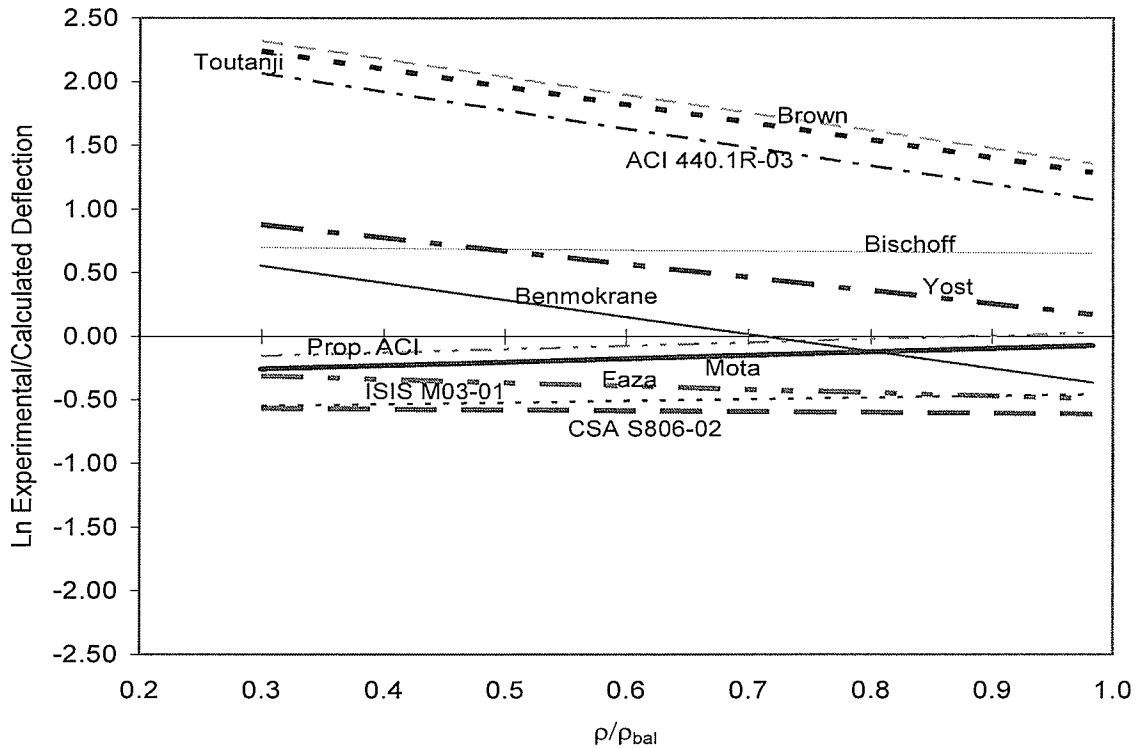


Figure 4.25 - Effect of Relative Reinforcement Ratio on Deflection Prediction for Under-Reinforced Members at $1.1P_{cr}$

It has been shown that the accuracies of the deflection formulas are dependent on both the reinforcement ratio as well as on the type of reinforcement used. For this reason, a further statistical analysis has been completed separating the over-reinforced from the under-reinforced members, and reinforced with either GFRP or CFRP. In Table 4.8, the

formulas presented by Yost et al. (2003) and the Proposed ACI 440.1R (2004) give satisfactory results for calculating the deflection of GFRP-RC beams. The performance of each of these equations with respect to the reinforcement ratio was investigated, as shown in Table 4.9. The Yost et al. (2003) equation is more precise for over-reinforced beams, while the formula of the Proposed ACI 440.1R (2004) is more accurate for under-reinforced beams. It can also be seen that the equation given by Benmokrane et al. is also accurate for GFRP-RC under-reinforced members. Table 4.9 shows that the Faza and GangaRao (1992) formula is quite accurate at forecasting the deflection of both over-reinforced and under-reinforced CFRP-RC members and is conservative for much of the 95% confidence intervals. The CSA S806-02 (2002) equation also performs satisfactorily for CFRP-RC, which indicates that moment-curvature based methods perform well for CFRP-RC, mainly due to the larger stiffness of the beams after cracking compared to GFRP-RC. It should be pointed out that the method of the CSA S806-02 (2002) does not incorporate tension stiffening into its model. It is assumed that if tension stiffening was added to the CSA S806-02 (2002), the results would improve dramatically for GFRP-RC beams. This will become clearer as these beams are analyzed at higher load levels, where tension stiffening does not play an important role, and the level of conservatism in these methods decreases. It can also be noted from viewing Table 4.9 that the method given by Mota gives very accurate results, which are still conservative at this load level for almost all reinforcement schemes. The one area of concern with the equation given by Mota is that it is overly conservative for CFRP-RC beams which are over-reinforced at this load level.

Table 4.9 - Further Analysis of the Predicted Deflections at $1.1P_{cr}$

Method	Statistical Property	Experimental / Calculated Deflection			
		GFRP-RC		CFRP-RC	
		$\rho > \rho_{bal}$	$\rho < \rho_{bal}$	$\rho > \rho_{bal}$	$\rho < \rho_{bal}$
	Sample size	115	24	48	8
Faza & GangaRao (1992)	geometric mean	0.65	0.61	0.81	0.94
	variation	1.15	1.52	0.55	0.35
	95 % confidence (-)	0.57	0.42	0.72	0.76
	95 % confidence (+)	0.75	0.88	0.92	1.16
Benmokrane et al. (1996)	geometric mean	0.43	1.06	0.42	1.69
	variation	0.90	1.93	0.67	0.60
	95 % confidence (-)	0.38	0.69	0.36	1.22
	95 % confidence (+)	0.48	1.63	0.49	2.34
Brown & Bartholomew (1996)	geometric mean	2.33	6.07	2.16	9.69
	variation	0.92	1.95	0.74	0.67
	95 % confidence (-)	2.07	3.94	1.85	6.79
	95 % confidence (+)	2.63	9.36	2.53	13.82
Toutanji & Saafi (2000)	geometric mean	2.17	5.62	2.03	9.06
	variation	0.92	1.94	0.74	0.69
	95 % confidence (-)	1.93	3.65	1.74	6.30
	95 % confidence (+)	2.44	8.65	2.37	13.03
ISIS M03-01 (2001)	geometric mean	0.45	0.48	0.63	1.18
	variation	0.87	1.69	0.66	0.43
	95 % confidence (-)	0.40	0.32	0.55	0.92
	95 % confidence (+)	0.50	0.71	0.73	1.51
CSA S806-02 (2002)	geometric mean	0.50	0.48	0.66	0.88
	variation	1.00	1.52	0.51	0.37
	95 % confidence (-)	0.44	0.33	0.59	0.71
	95 % confidence (+)	0.57	0.69	0.74	1.09
ACI 440.1R-03 (2003)	geometric mean	1.64	4.28	2.03	9.56
	variation	0.92	1.96	0.72	0.62
	95 % confidence (-)	1.46	2.77	1.74	6.84
	95 % confidence (+)	1.85	6.61	2.37	13.36
Yost et al. (2003)	geometric mean	0.93	1.47	1.19	3.28
	variation	0.97	1.87	0.62	0.54
	95 % confidence (-)	0.82	0.96	1.04	2.43
	95 % confidence (+)	1.05	2.24	1.36	4.42
Proposed ACI 440.1R (2004)	geometric mean	1.18	0.81	1.19	1.36
	variation	1.13	1.76	0.68	0.48
	95 % confidence (-)	1.03	0.54	1.03	1.04
	95 % confidence (+)	1.35	1.22	1.38	1.78
Bischoff (2005)	geometric mean	1.23	1.57	1.48	3.93
	variation	0.85	1.67	0.66	0.68
	95 % confidence (-)	1.10	1.06	1.28	2.75
	95 % confidence (+)	1.38	2.32	1.70	5.62
Mota	geometric mean	0.83	0.81	0.55	0.90
	variation	0.96	1.76	0.62	0.46
	95 % confidence (-)	0.73	0.54	0.48	0.69
	95 % confidence (+)	0.94	1.22	0.63	1.17

4.5.4 - Deflection Analysis at 50% of Failure Load

The log of experimental over calculated deflection was plotted in Figure 4.26 with respect to the modulus of elasticity of GFRP at a load level of 50% of the experimental failure load. Figure 4.26 shows that the equations are all quite accurate at predicting the deflection of GFRP-RC beams at this load level. However, the figure indicates that the accuracy of the formulas typically varies with the modulus of elasticity of the GFRP. Here, many of the formulas are conservative at predicting the deflection for lower values of the modulus and unconservative for higher values of the modulus. Only the formulas given by the CSA S806-02 (2002), ISIS M03-01 (2001), and Benmokrane et al. (1996) give conservative estimates for all values of the modulus of elasticity. Table 4.10 shows the statistical analysis of each of the formulas at this load. It can be seen that the formula given by Mota is the most accurate with an average ratio of 1.00. However, upon reviewing Figure 4.26, it can be seen that the formula over-predicts the deflection for GFRP-RC beams with a modulus less than 40 GPa, and under-predicts the deflection of the GFRP-RC beams with a modulus higher than 40 GPa. The same applies to the equation proposed by Bischoff (2005) which is accurate when looking at the results of Table 4.10. Thus, the equation given by ISIS M03-01 (2001) is a better equation for predicting the deflection of GFRP-RC beams at a load level of $0.5P_{\max}$ since it is not only accurate, but also conservative.

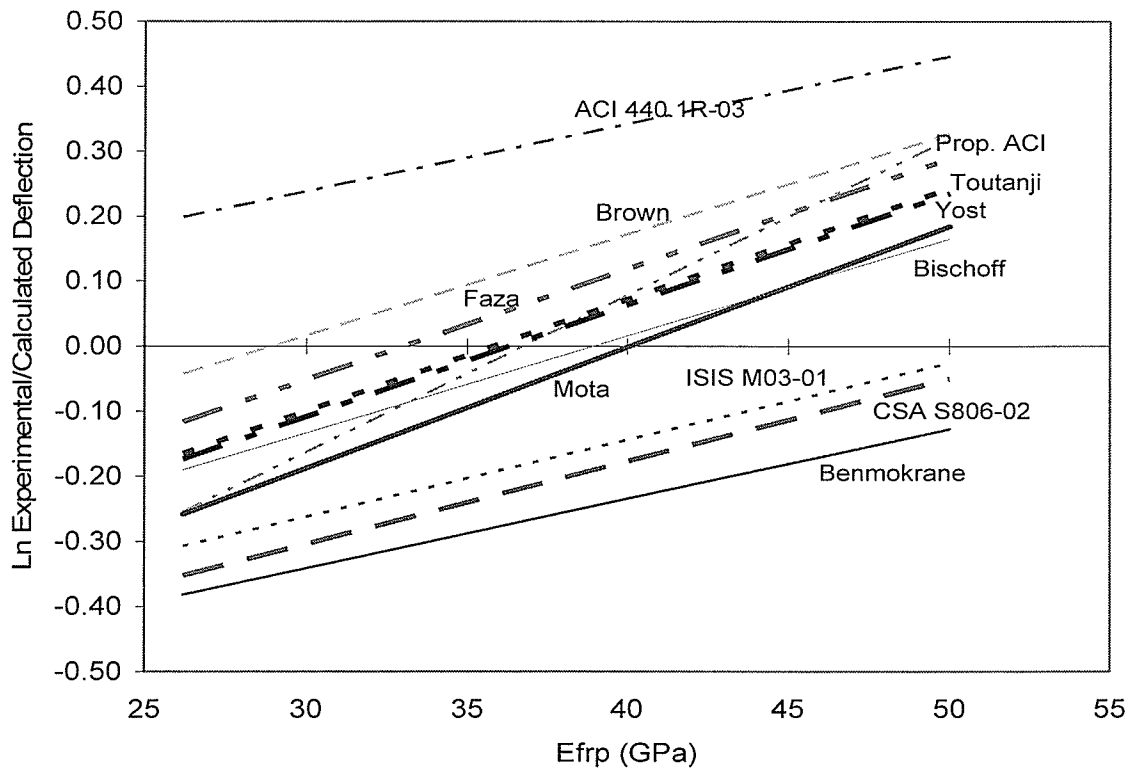


Figure 4.26 - Effect of Modulus on Deflection Prediction at $0.5P_{max}$ for GFRP-RC

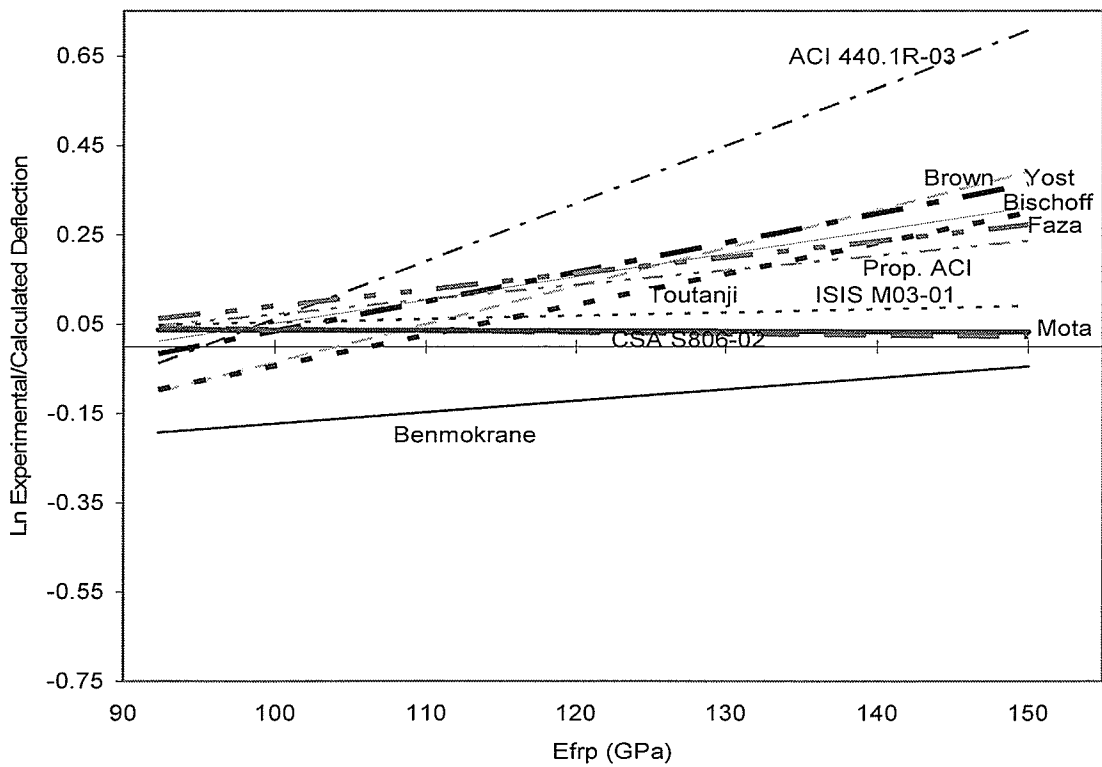


Figure 4.27 - Effect of Modulus on Deflection Prediction at $0.5P_{max}$ for CFRP-RC

Table 4.10 - Statistical Analysis of the Predicted Deflections at $0.5P_{max}$

Method	Statistical Property	Experimental / Calculated Deflection				All Members
		GFRP-RC	CFRP-RC	$\rho > \rho_{bal}$	$\rho < \rho_{bal}$	
	Sample size	139	56	165	32	197
Faza & GangaRao (1992)	mean	1.13	1.28	1.10	1.65	1.17
	variation	0.58	0.91	0.30	1.96	0.68
	95 % conf. (-)	1.05	1.08	1.06	1.13	1.09
	95 % conf. (+)	1.22	1.52	1.14	2.40	1.26
Benmokrane et al. (1996)	mean	0.80	0.96	0.73	1.71	0.84
	variation	0.68	1.08	0.32	1.94	0.80
	95 % conf. (-)	0.73	0.79	0.70	1.18	0.77
	95 % conf. (+)	0.87	1.16	0.76	2.48	0.91
Brown & Bartholomew (1996)	mean	1.20	1.30	1.02	3.15	1.22
	variation	0.82	1.12	0.35	1.76	0.90
	95 % conf. (-)	1.09	1.07	0.97	2.22	1.12
	95 % conf. (+)	1.33	1.58	1.07	4.48	1.33
Toutanji & Saafi (2000)	mean	1.07	1.23	0.94	2.76	1.12
	variation	0.79	1.15	0.34	1.90	0.90
	95 % conf. (-)	0.98	1.01	0.90	1.91	1.02
	95 % conf. (+)	1.19	1.50	0.98	3.99	1.23
ISIS M03-01 (2001)	mean	0.87	1.14	0.86	1.43	0.94
	variation	0.65	0.98	0.34	2.21	0.76
	95 % conf. (-)	0.80	0.95	0.82	0.95	0.87
	95 % conf. (+)	0.95	1.36	0.90	2.14	1.02
CSA S806-02 (2002)	mean	0.84	1.09	0.84	1.33	0.90
	variation	0.65	1.00	0.33	2.35	0.77
	95 % conf. (-)	0.77	0.91	0.80	0.87	0.83
	95 % conf. (+)	0.91	1.31	0.88	2.02	0.97
ACI 440.1R-03 (2003)	mean	1.42	1.61	1.23	3.64	1.47
	variation	0.72	1.02	0.35	1.35	0.81
	95 % conf. (-)	1.30	1.34	1.17	2.71	1.35
	95 % conf. (+)	1.55	1.94	1.29	4.89	1.60
Yost et al. (2003)	mean	1.07	1.31	1.00	2.16	1.13
	variation	0.60	0.94	0.30	1.65	0.71
	95 % conf. (-)	0.99	1.10	0.96	1.54	1.05
	95 % conf. (+)	1.16	1.56	1.04	3.03	1.22
Proposed ACI 440.1R (2004)	mean	1.09	1.24	1.04	1.69	1.13
	variation	0.61	0.92	0.33	1.94	0.70
	95 % conf. (-)	1.01	1.05	1.00	1.16	1.05
	95 % conf. (+)	1.18	1.47	1.09	2.46	1.22
Bischoff (2005)	mean	1.02	1.28	0.97	1.92	1.09
	variation	0.59	1.00	0.30	1.89	0.73
	95 % conf. (-)	0.95	1.07	0.94	1.33	1.01
	95 % conf. (+)	1.11	1.54	1.01	2.77	1.17
Mota	mean	1.00	1.09	0.94	1.63	1.03
	variation	0.60	1.00	0.31	2.00	0.72
	95 % conf. (-)	0.92	0.91	0.90	1.11	0.95
	95 % conf. (+)	1.08	1.31	0.98	2.39	1.11

Trend lines for the log of the deflection ratio versus the modulus of elasticity for CFRP-RC were plotted at a load of $0.5P_{max}$, and are shown in Figure 4.27, excluding the outlier point with a modulus of 174 GPa. It can be seen that the accuracy of many of the formulas varies with the modulus of the CFRP reinforcement at this load level, with the exceptions of Mota, ISIS M03-01 (2001) and the CSA S806-02 (2002). It can also be seen that the equations by Mota and the CSA S806-02 (2002) are quite accurate at predicting the deflection of CFRP-RC at this load level. However, only Benmokrane et al. (1996) is conservative for all reinforcement types. Table 4.10 shows that the equations given by Mota, the CSA S806-02 (2002) and Benmokrane et al. (1996) are all accurate but only the one given by Benmokrane et al. (1996) is conservative for predicting the deflection of CFRP-RC beams at this load level.

Figure 4.28 plots the log of experimental over calculated deflection for over-reinforced members. The trend lines in Figure 4.28 show that all of the methods have varying accuracy depending on the relative reinforcement ratio. Since members typically have reinforcement ratios that are less than 2.5 times the balanced reinforcement ratio, the methods of Toutanji and Saafi (2000), Yost et al. (2003), Bischoff (2005), and Mota are performing most accurately for over-reinforced beams. The methods of the CSA S806-02 (2002) and ISIS M03-01 (2001) are also performing accurately at this load level and are conservative up to $5\rho_{bal}$. These results are verified in Table 4.10 which shows that the method proposed by Yost et al. (2003) is the most accurate and consistently conservative at reinforcement ratios of up to $2.5\rho_{bal}$, while the Bischoff formula is conservative up to

$3.5\rho_{bal}$, the Mota formula is conservative up to $4.5\rho_{bal}$ and the formula proposed by Toutanji and Saafi (2000) is conservative at all reinforcement ratios.

When a similar plot for members which are under-reinforced is examined, as in Figure 4.29, less satisfactory results are arrived at and it appears that all of the equations have a greater difficulty in accurately predicting the deflection at $0.5P_{max}$ for under-reinforced members. This is verified by Table 4.10, which shows that none of the formulas have a conservative average experimental to theoretical deflection ratio. It can also be seen that the CSA S806-02 (2002) equation is performing the most accurately at this load level, with an average deflection ratio of 1.33.

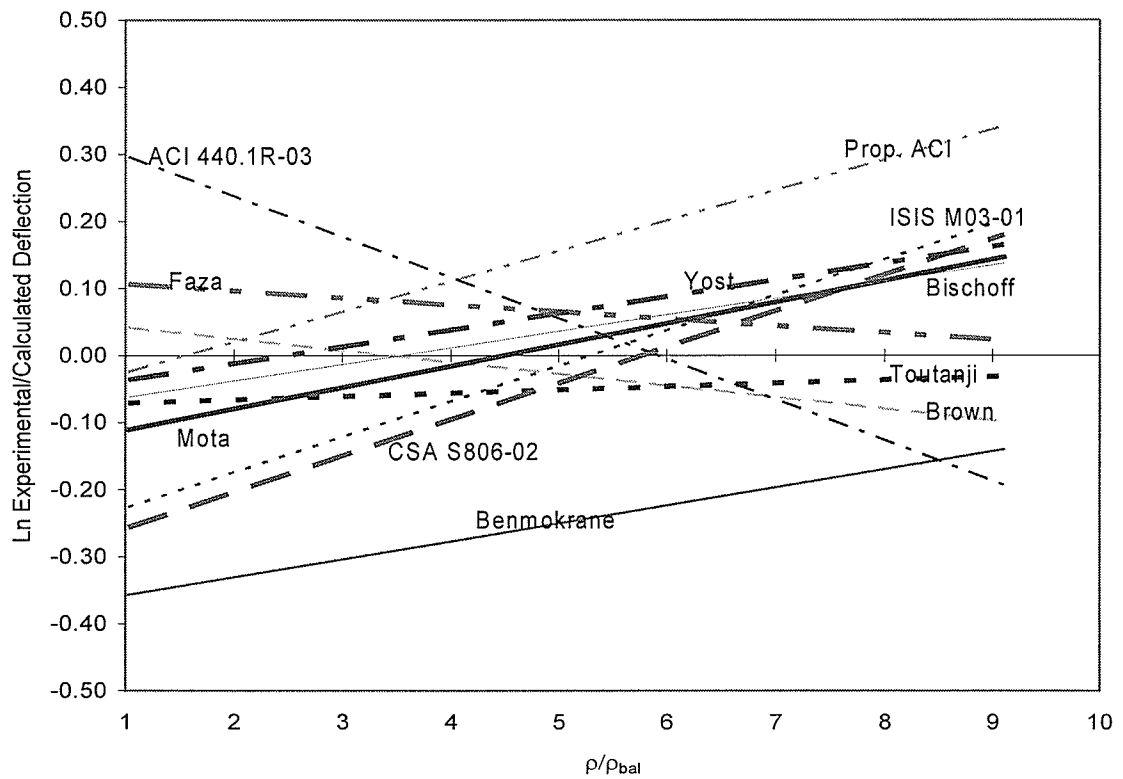


Figure 4.28 - Effect of Relative Reinforcement Ratio on Deflection Prediction for Over-Reinforced Members at $0.5P_{max}$

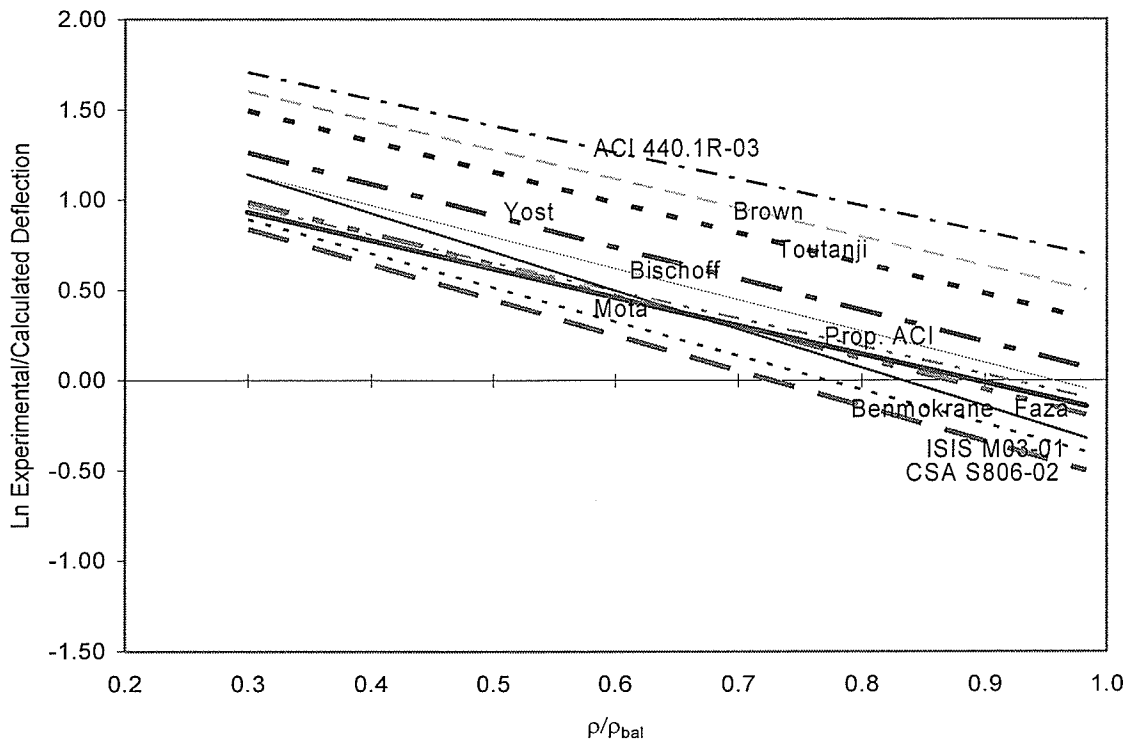


Figure 4.29 - Effect of Relative Reinforcement Ratio on Deflection Prediction for Under-Reinforced Members at $0.5P_{max}$

A further statistical analysis has been completed separating the over-reinforced from the under-reinforced members reinforced with either CFRP or GFRP in Table 4.11. It can be seen that the results are much more accurate for the over-reinforced beams than for the under-reinforced beams. The formulas given by Toutanji and Saafi (2000), Bischoff (2005), and Mota are accurate and conservative for the over-reinforced beams, regardless of whether they are GFRP-RC or CFRP-RC. However, when looking at the under-reinforced beams, the results are varied and the CSA S806-02 (2002) gives the most accurate results at this load level. It must be noted however that none of the equations give conservative deflection estimates for the under-reinforced beams at this load level.

Table 4.11 - Further Analysis of the Predicted Deflections at $0.5P_{max}$

Method	Statistical Property	Experimental / Calculated Deflection			
		GFRP-RC		CFRP-RC	
		$\rho > \rho_{bal}$	$\rho < \rho_{bal}$	$\rho > \rho_{bal}$	$\rho < \rho_{bal}$
	Sample size	115	24	48	8
Faza & GangaRao (1992)	geometric mean	1.08	1.40	1.13	2.66
	variation	0.30	1.52	0.31	3.23
	95 % confidence (-)	1.03	0.97	1.05	0.98
	95 % confidence (+)	1.13	2.03	1.22	7.23
Benmokrane et al. (1996)	geometric mean	0.71	1.44	0.80	2.88
	variation	0.29	1.51	0.36	3.01
	95 % confidence (-)	0.68	1.00	0.73	1.10
	95 % confidence (+)	0.74	2.08	0.87	7.54
Brown & Bartholomew (1996)	geometric mean	1.02	2.64	1.02	5.29
	variation	0.37	1.53	0.31	2.15
	95 % confidence (-)	0.96	1.82	0.94	2.39
	95 % confidence (+)	1.08	3.83	1.10	11.72
Toutanji & Saafi (2000)	geometric mean	0.93	2.28	0.97	4.89
	variation	0.34	1.61	0.33	2.40
	95 % confidence (-)	0.88	1.55	0.89	2.09
	95 % confidence (+)	0.98	3.35	1.05	11.42
ISIS M03-01 (2001)	geometric mean	0.82	1.16	0.98	2.73
	variation	0.31	1.76	0.35	3.14
	95 % confidence (-)	0.78	0.77	0.90	1.02
	95 % confidence (+)	0.86	1.74	1.07	7.31
CSA S806-02 (2002)	geometric mean	0.80	1.08	0.95	2.46
	variation	0.30	1.86	0.36	3.52
	95 % confidence (-)	0.76	0.71	0.87	0.86
	95 % confidence (+)	0.84	1.64	1.04	7.00
ACI 440.1R-03 (2003)	geometric mean	1.21	3.01	1.28	6.41
	variation	0.36	1.16	0.33	1.44
	95 % confidence (-)	1.14	2.21	1.18	3.45
	95 % confidence (+)	1.28	4.10	1.39	11.89
Yost et al. (2003)	geometric mean	0.96	1.76	1.09	3.94
	variation	0.29	1.32	0.31	2.18
	95 % confidence (-)	0.92	1.26	1.01	1.77
	95 % confidence (+)	1.01	2.46	1.18	8.78
Proposed ACI 440.1R (2004)	geometric mean	1.03	1.42	1.08	2.84
	variation	0.34	1.52	0.31	3.00
	95 % confidence (-)	0.98	0.98	1.00	1.09
	95 % confidence (+)	1.09	2.06	1.17	7.42
Bischoff (2005)	geometric mean	0.94	1.50	1.06	4.03
	variation	0.28	1.44	0.31	2.46
	95 % confidence (-)	0.90	1.05	0.98	1.71
	95 % confidence (+)	0.99	2.14	1.15	9.51
Mota	geometric mean	0.93	1.42	0.95	2.46
	variation	0.29	1.52	0.36	3.53
	95 % confidence (-)	0.89	0.98	0.87	0.86
	95 % confidence (+)	0.97	2.06	1.04	7.01

4.5.5 - Deflection Analysis at 80% of Failure Load

The log of experimental over calculated deflection was plotted in Figure 4.30 with respect to the modulus of elasticity of GFRP at a load level of 80% of the experimental failure load. The equations are typically accurate at predicting the deflection of GFRP-RC beams at this load level but the accuracy of the formulas typically varies with the value for modulus of elasticity of the GFRP. None of the formulas are conservative at predicting the deflection for higher values of the modulus. The CSA S806-02 (2002), ISIS M03-01 (2001), Bischoff (2005), and Mota formulas tend to vary the least with the modulus and are also accurate. Table 4.12 shows the statistical analysis of each of the formulas at this load. The formulas given by the CSA S806-02 (2002), ISIS M03-01 (2001), Bischoff (2005), and Mota are the most accurate equations at this load level, with the CSA S806-02 (2002) equation also having the benefit of being conservative.

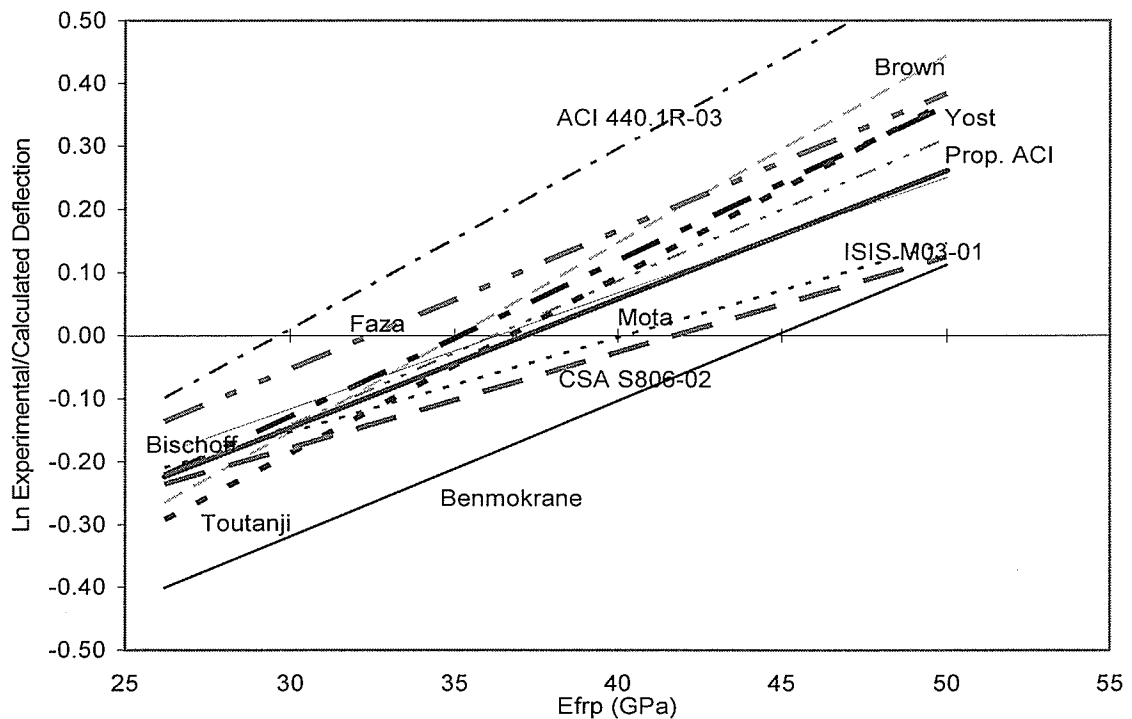


Figure 4.30 - Effect of Modulus on Deflection Prediction at $0.8P_{max}$ for GFRP-RC

Table 4.12 - Statistical Analysis of the Predicted Deflections at $0.8P_{max}$

Method	Statistical Property	Experimental / Calculated Deflection				All Members
		GFRP-RC	CFRP-RC	$\rho > \rho_{bal}$	$\rho < \rho_{bal}$	
	Sample size	139	56	165	32	197
Faza & GangaRao (1992)	mean	1.18	1.18	1.18	1.22	1.18
	variation	0.29	0.25	0.22	0.49	0.27
	95 % conf. (-)	1.13	1.11	1.14	1.06	1.14
	95 % conf. (+)	1.23	1.25	1.22	1.40	1.22
Benmokrane et al. (1996)	mean	0.91	0.96	0.89	1.13	0.92
	variation	0.33	0.32	0.20	0.70	0.33
	95 % conf. (-)	0.87	0.89	0.87	0.94	0.88
	95 % conf. (+)	0.95	1.03	0.92	1.36	0.96
Brown & Bartholomew (1996)	mean	1.17	1.23	1.07	2.02	1.18
	variation	0.64	0.56	0.21	1.60	0.61
	95 % conf. (-)	1.08	1.09	1.04	1.45	1.10
	95 % conf. (+)	1.27	1.38	1.10	2.81	1.26
Toutanji & Saafi (2000)	mean	1.10	1.19	1.04	1.68	1.13
	variation	0.56	0.49	0.20	1.43	0.54
	95 % conf. (-)	1.02	1.07	1.01	1.24	1.06
	95 % conf. (+)	1.18	1.32	1.07	2.29	1.20
ISIS M03-01 (2001)	mean	1.00	1.13	1.06	0.91	1.03
	variation	0.22	0.27	0.20	0.38	0.25
	95 % conf. (-)	0.97	1.06	1.03	0.81	1.00
	95 % conf. (+)	1.03	1.20	1.09	1.02	1.06
CSA S806-02 (2002)	mean	0.98	1.09	1.04	0.86	1.01
	variation	0.22	0.27	0.20	0.35	0.24
	95 % conf. (-)	0.95	1.02	1.01	0.78	0.98
	95 % conf. (+)	1.01	1.16	1.07	0.95	1.04
ACI 440.1R-03 (2003)	mean	1.35	1.42	1.20	2.77	1.37
	variation	0.68	0.67	0.23	1.47	0.67
	95 % conf. (-)	1.24	1.24	1.16	2.02	1.28
	95 % conf. (+)	1.47	1.62	1.24	3.79	1.47
Yost et al. (2003)	mean	1.13	1.23	1.10	1.49	1.16
	variation	0.35	0.37	0.20	0.78	0.36
	95 % conf. (-)	1.08	1.13	1.07	1.22	1.11
	95 % conf. (+)	1.19	1.34	1.13	1.82	1.21
Proposed ACI 440.1R (2004)	mean	1.09	1.15	1.12	1.06	1.11
	variation	0.25	0.26	0.21	0.43	0.25
	95 % conf. (-)	1.05	1.08	1.09	0.94	1.08
	95 % conf. (+)	1.13	1.22	1.15	1.20	1.15
Bischoff (2005)	mean	1.07	1.20	1.10	1.12	1.11
	variation	0.22	0.31	0.20	0.48	0.25
	95 % conf. (-)	1.04	1.12	1.07	0.98	1.07
	95 % conf. (+)	1.11	1.29	1.14	1.29	1.14
Mota	mean	1.06	1.09	1.08	1.02	1.07
	variation	0.24	0.27	0.20	0.42	0.24
	95 % conf. (-)	1.02	1.02	1.05	0.90	1.04
	95 % conf. (+)	1.10	1.16	1.11	1.15	1.10

Trend lines for the log of the deflection ratio versus the modulus of elasticity for CFRP-RC were plotted at a load of $0.8P_{max}$, and are shown in Figure 4.31. In Figure 4.31, the outlier with a modulus of elasticity of 174 GPa has been removed from the analysis to not skew the trend lines. Here, many of the equations predict the deflection similarly with trend lines close to each other. Only the equation given by Benmokrane et al. (1996) gives accurate results that are also conservative. This formula also has the added benefit of having little variance in its accuracy with the modulus of elasticity of the CFRP. Table 4.12 verifies these results and shows that the equation by Benmokrane et al (1996) is the only formula with an average deflection ratio less than 1.0. This equation is quite accurate at this load level with an average deflection ratio of 0.96.

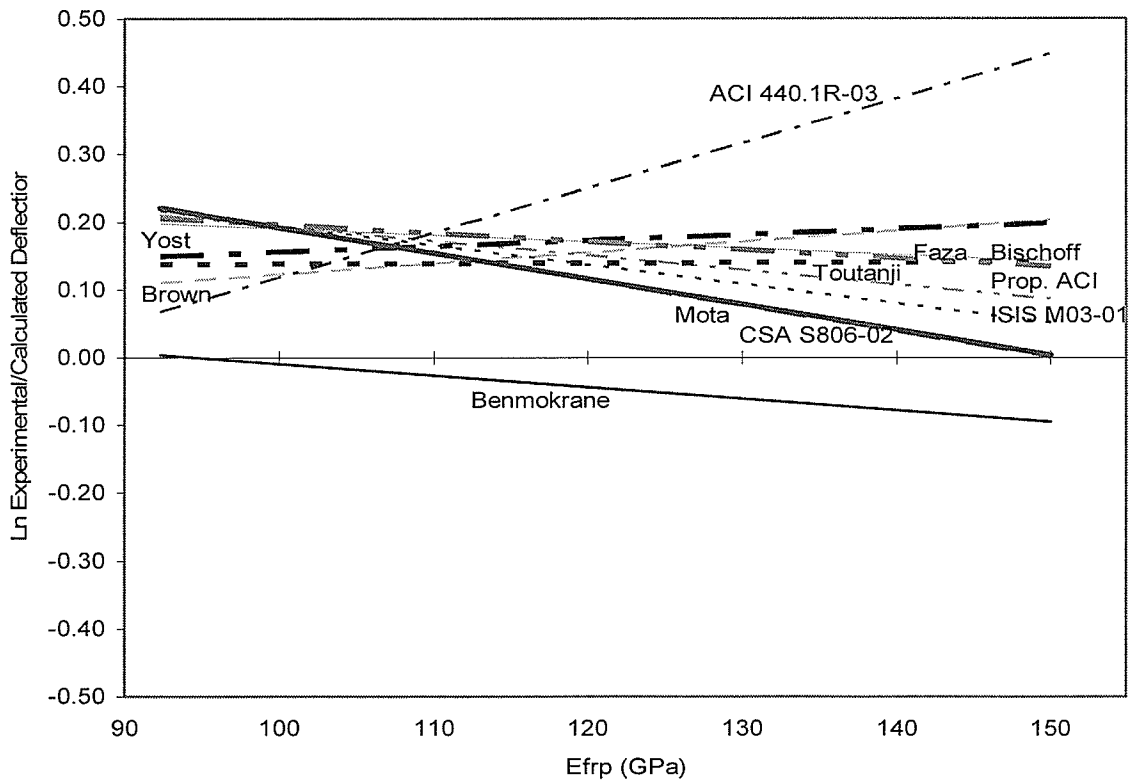


Figure 4.31 - Effect of Modulus on Deflection Prediction at $0.8P_{max}$ for CFRP-RC

Figure 4.32 plots the log of experimental over calculated deflection for over-reinforced members. The trend lines in Figure 4.32 show that most of the methods under predict the deflection at any relative reinforcement ratio, as they have trend lines that are entirely above the x-axis. Here, the only method which gives conservative deflection estimates at this load level is given by Benmokrane et al. (1996). These results are verified in Table 4.12, which shows that the equation by Benmokrane et al. (1996) is the only equation that gives conservative deflection estimates at this load level. However, it must also be noted that the accuracies of all of the formulas are excellent at this load level, even though the results show that the formulas are unconservative.

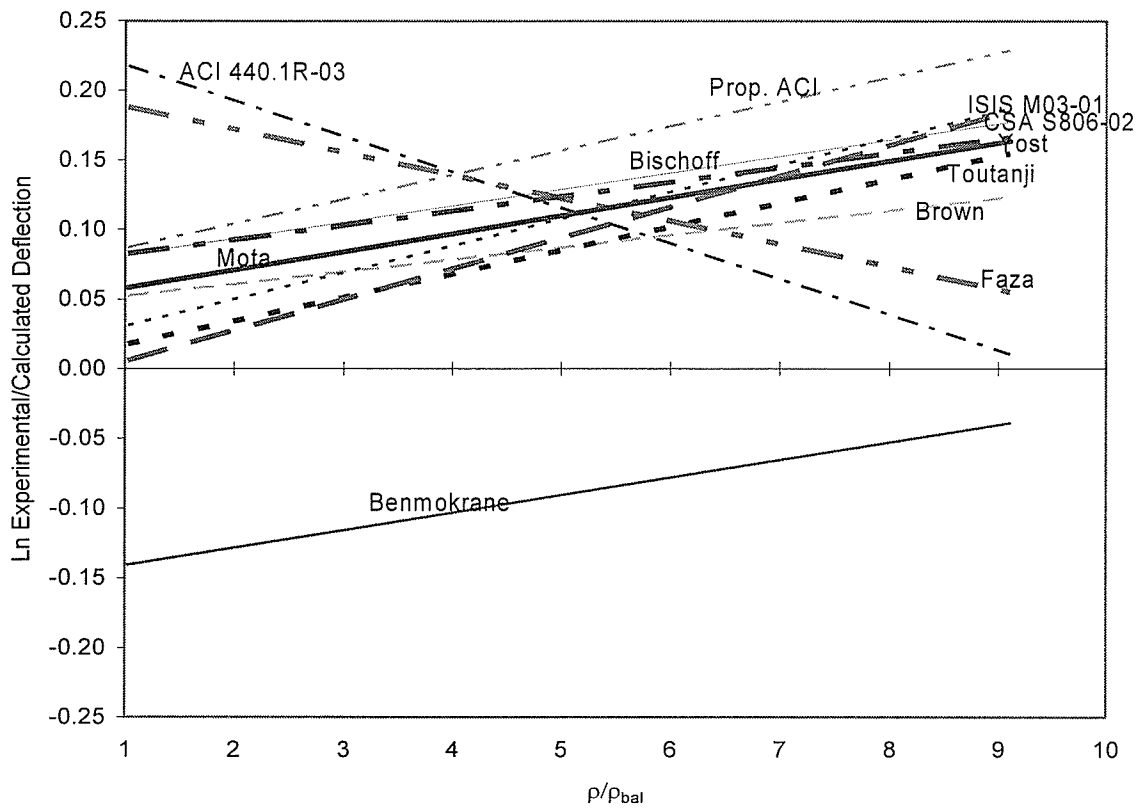


Figure 4.32 - Effect of Relative Reinforcement Ratio on Deflection Prediction for Over-Reinforced Members at $0.8P_{max}$

When a similar plot for members which are under-reinforced is examined, as in Figure 4.33, the results show that the equations given by the Proposed ACI 440.1R (2004), Bischoff (2005), and Mota are accurate at predicting the deflection at $0.8P_{max}$ for under-reinforced members. The formulas given by ISIS M03-01 (2001) and the CSA S806-02 (2002) are also giving accurate results here and have the added benefit of being conservative at all reinforcement ratios. This is later verified by Table 4.12.

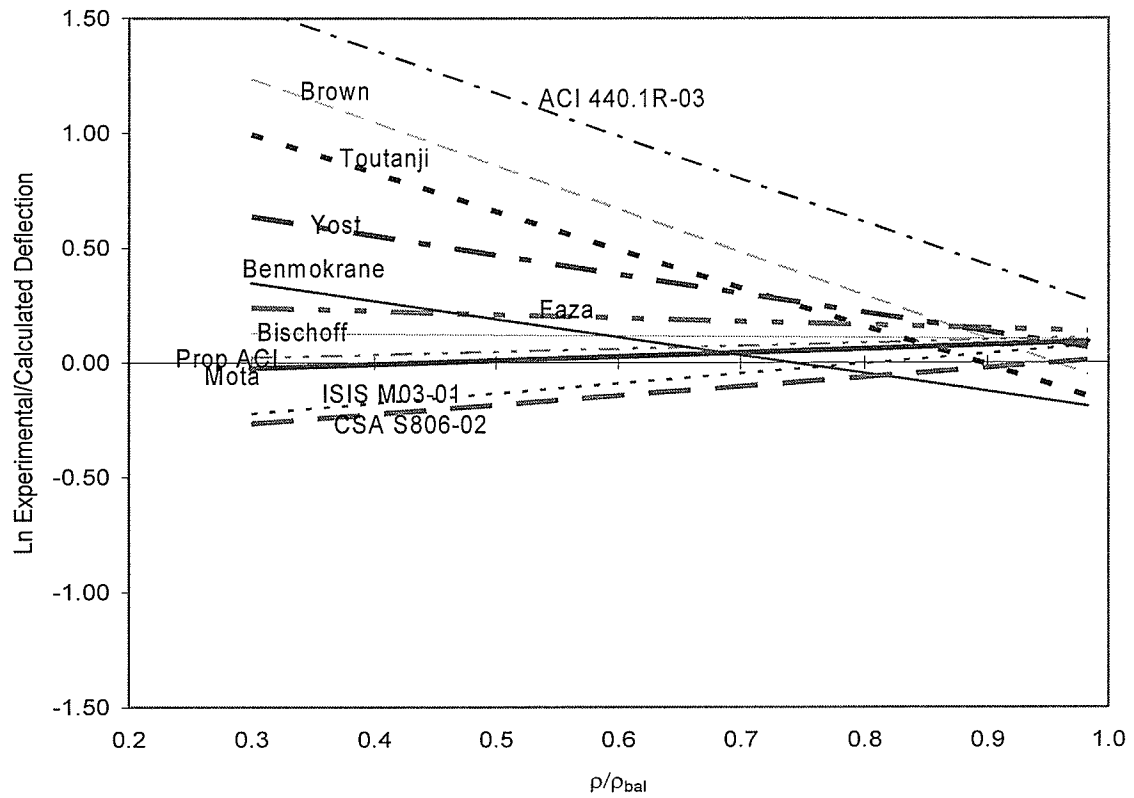


Figure 4.33 - Effect of Relative Reinforcement Ratio on Deflection Prediction for Under-Reinforced Members at $0.8P_{max}$

A further statistical analysis has been completed separating the over-reinforced from the under-reinforced members reinforced with either CFRP or GFRP in Table 4.13. It can be seen that although the majority of the equations are giving accurate deflection predictions for the over-reinforced beams at this load level, only the equation by Benmokrane et al.

(1996) gives conservative deflection estimates. This trend can be seen for both the over-reinforced GFRP-RC and CFRP-RC beams. When viewing the accuracy of the equations for the under-reinforced members at this load level, it can be seen that the CSA S806-02 (2002), ISIS M03-01 (2002), the Proposed ACI 440.1R (2004), and Mota formulas are all giving more accurate results compared to the other methods. Here, the CSA S806-02 (2002) is conservative for both GFRP-RC and CFRP-RC beams, while the equation by ISIS M03-01 (2001) is only conservative for GFRP-RC beams, and the equation by Mota is only conservative for CFRP-RC beams.

Table 4.13 - Further Analysis of the Predicted Deflections at $0.8P_{max}$

Method	Statistical Property	Experimental / Calculated Deflection			
		GFRP-RC		CFRP-RC	
		$\rho > \rho_{bal}$	$\rho < \rho_{bal}$	$\rho > \rho_{bal}$	$\rho < \rho_{bal}$
	Sample size	115	24	48	8
Faza & GangaRao (1992)	geometric mean	1.17	1.24	1.19	1.14
	variation	0.20	0.57	0.26	0.20
	95 % confidence (-)	1.13	1.04	1.11	1.00
	95 % confidence (+)	1.21	1.49	1.27	1.29
Benmokrane et al. (1996)	geometric mean	0.87	1.13	0.94	1.14
	variation	0.15	0.77	0.28	0.48
	95 % confidence (-)	0.85	0.90	0.88	0.87
	95 % confidence (+)	0.89	1.42	1.01	1.50
Brown & Bartholomew (1996)	geometric mean	1.05	1.95	1.12	2.22
	variation	0.17	1.74	0.28	1.26
	95 % confidence (-)	1.02	1.30	1.04	1.26
	95 % confidence (+)	1.08	2.92	1.20	3.91
Toutanji & Saafi (2000)	geometric mean	1.02	1.62	1.11	1.88
	variation	0.16	1.56	0.28	1.14
	95 % confidence (-)	0.99	1.11	1.04	1.11
	95 % confidence (+)	1.05	2.36	1.19	3.19
ISIS M03-01 (2001)	geometric mean	1.03	0.85	1.13	1.10
	variation	0.16	0.38	0.28	0.26
	95 % confidence (-)	1.00	0.75	1.05	0.94
	95 % confidence (+)	1.06	0.97	1.21	1.29
CSA S806-02 (2002)	geometric mean	1.01	0.82	1.11	0.98
	variation	0.16	0.37	0.28	0.22
	95 % confidence (-)	0.98	0.72	1.04	0.85
	95 % confidence (+)	1.04	0.93	1.19	1.12
ACI 440.1R-03 (2003)	geometric mean	1.18	2.59	1.23	3.39
	variation	0.22	1.55	0.26	1.29
	95 % confidence (-)	1.14	1.78	1.15	1.91
	95 % confidence (+)	1.22	3.77	1.31	6.02
Yost et al. (2003)	geometric mean	1.08	1.42	1.16	1.73
	variation	0.17	0.81	0.26	0.67
	95 % confidence (-)	1.05	1.12	1.09	1.21
	95 % confidence (+)	1.11	1.80	1.24	2.47
Proposed ACI 440.1R (2004)	geometric mean	1.10	1.04	1.16	1.11
	variation	0.18	0.48	0.26	0.24
	95 % confidence (-)	1.07	0.89	1.09	0.96
	95 % confidence (+)	1.13	1.22	1.24	1.29
Bischoff (2005)	geometric mean	1.08	1.04	1.17	1.41
	variation	0.16	0.44	0.27	0.47
	95 % confidence (-)	1.05	0.90	1.09	1.08
	95 % confidence (+)	1.11	1.20	1.25	1.85
Mota	geometric mean	1.07	1.04	1.11	0.96
	variation	0.16	0.48	0.28	0.19
	95 % confidence (-)	1.04	0.89	1.04	0.85
	95 % confidence (+)	1.10	1.22	1.19	1.08

Chapter 5 - Summary and Conclusions

5.1 - Experimental Program

Shear and deflection behaviour of FRP-RC beams was examined through an experimental investigation. A total of seven beams were tested monotonically under 4-point bending: two reinforced with steel and five reinforced with CFRP. The shear span to depth ratio of the beams was greater than 2.5 for all specimens, to minimize the effect of arching action and no stirrups were provided in any of the beams to ensure that a shear failure occurred. The testing allowed for a comparison between the behaviour of steel reinforced concrete beams and CFRP-RC beams. The laboratory testing was also used to determine which code formulas are the most accurate at predicting the concrete shear capacity and the load deflection response for FRP-RC beams. The following conclusions were noted as a result of the laboratory testing:

1. Since the moment of inertia of steel RC is higher when compared to CFRP-RC, concrete beams reinforced with steel have stiffer load deflection responses than similarly FRP reinforced concrete beams. This lower moment of inertia is as a result of the higher neutral axis immediately after cracking which can be found in FRP-RC members when compared against similarly reinforced steel RC members.
2. Beams reinforced with steel have a higher concrete shear capacity than similar ones reinforced with FRP. This results largely from the larger crack widths and raised neutral axis in FRP reinforced concrete beams when compared to similarly steel

reinforced beams. This reduces the amount of aggregate interlock present between the concrete cracks and also the amount of uncracked concrete which can carry shear forces. To a lesser degree, the reduction in dowel action when using FRP also contributes to the reduction in shear capacity when compared to steel reinforced concrete.

3. As the reinforcement ratio is increased, the ultimate failure load is typically increased but the ultimate deflection is decreased.

4. The equation for determining the cracking moment of a reinforced concrete beam used by the CSA A23.3-94 (1998) often over predicts the experimental cracking moment. The empirical nature of the formula and the lack of important variables present in the equation may need to be revisited. Such variables include both shrinkage and the age of the concrete.

5. The equation presented by the JSCE (1997) best predicted the concrete contribution to the shear resistance of the FRP reinforced concrete beams tested in this program. The formula was not only accurate but was also conservative.

6. The dependence of the deflection equations on the cracking moment resulted in none of the deflection equations performing particularly well for the entire load deflection response of the beams tested in the laboratory. Given that the equation presented by the CSA S806-02 (2002) was the only equation that gave conservative

deflection predictions, this formula best predicted the load-deflection response of the tested beams.

7. The proposed deflection equation predicted the post-cracking behaviour of the tested beams well. The equation was typically accurate, while still yielding conservative deflection estimates. The pre-cracking behaviour was not predicted well as a result of the poor cracking load predictions.

5.2 - Parametric Study

A parametric study was completed using published papers of other authors to add to the number of members analyzed. Load versus deflection graphs were manually replicated and input into the program, as well as any geometric and material properties. The database consisted of 197 FRP-RC beams which were used to analyze the load deflection behaviour. It also contained 89 beams which contained no stirrups and failed in shear, to analyze the concrete contribution to shear. Beams reinforced with CFRP, GFRP and AFRP were found in this database, however the majority were GFRP-RC beams. The parametric study allowed for a detailed analysis of existing deflection and shear formulas to be performed. The following conclusions were made as a result of the parametric study:

1. The accuracy of the deflection equations improved when the moment due to the self weight of the members was included in the analysis.

2. The most meaningful method for performing the statistical analysis was found to be applying a log transformation to the ratios of the experimental to calculated deflection or shear ratios. A log transformation was employed to give equal weight to those ratios which were below one and those which were above one. Without performing this transformation, more weight is given to the ratios above one and information is lost when statistics is applied.

3. The accuracy of the deflection ratios was highly dependent on the accuracy of the calculated cracking moment. The primary variable here was the modulus of rupture. Upon performing a statistical analysis on various equations for predicting the modulus of rupture, it was found that the CSA A23.3-94 (1998), NZS 3101 (1995) and AS 3600 (1994) codes provided the most accurate equation. This is contrary to the findings of the experimental program, which showed that this formula often over-predicted the cracking moment. Thus, a further analysis of the formula given by the CSA A23.3-94 (1998), NZS 3101 (1995) and AS 3600 (1994) codes is recommended to improve its accuracy for all cases.

4. The accuracy of the deflection equations varies at different loads. Given that the service conditions are only explicitly stated in ISIS M03-01 (2001), an analysis was performed at various loads to encompass the entire load range. This will allow the designer to choose the deflection formula which works best at their chosen service conditions. Results show that at higher loads, most of the methods perform well. However, at lower loads, major discrepancies were found between individual methods.

5. At the service load given by ISIS M03-01 (2001), the formulas proposed by Yost et al. (2003) and Bischoff (2005) were sufficiently accurate for predicting the deflection of GFRP-RC members, while the formulas of the CSA S806-02 (2002) and ISIS M03-01 (2001) were the most accurate for predicting the deflection of CFRP-RC members.

6. The equation proposed by Mota was accurate for CFRP-RC and GFRP-RC and resulted in conservative deflection estimates. The slenderness ratio and relative reinforcement ratio was found to affect most of the deflection ratios. However, the formula proposed by Mota was affected the least by either of these relationships and is thus believed to work very well at the service load level.

7. At a load of $1.1P_{cr}$, it was found that both the relative reinforcement ratio and the type of reinforcement affect the accuracy of each of the deflection equations. Here, it was found that for GFRP-RC, the formula given by Yost et al. (2003) performed the most accurately for those members which were over-reinforced, while the Proposed ACI 440.1R (2004), Benmokrane et al. (1996), and Mota equations performed the most accurately for the under-reinforced members. For the CFRP-RC members, it was found that the formula given by Faza and GangaRao (1992) performed accurately and conservatively at this load level, regardless of the relative reinforcement ratio. The most consistent equation at this load level was given by Mota. However, the Mota formula struggled in producing accurate results for predicting the deflection of over-reinforced CFRP-RC members at this load level, and rather, produced overly-conservative

deflection estimates. Thus, the use of the equation given by Faza and GangaRao (1992) is recommended for these members.

8. At loads of $50\%P_{MaxExp}$ and $80\%P_{MaxExp}$, almost all of the formulas performed accurately. However, none of the methods was able to accurately calculate the deflection of the under-reinforced CFRP-RC members at a load of 50% of the experimental failure load. Further research is needed in this area as the database had a very limited number of these members.

9. The formula developed by Mota accounts for the type of reinforcement, as well as the relative reinforcement ratio. The formula works well and gives accurate results at the service load level as well as at the load $1.1P_{cr}$, while still maintaining a form which is easily recognizable by designers.

10. The formula given by the JSCE (1997) tends to be the most consistent formula for predicting the concrete contribution to the shear capacity. The equation gives reasonably accurate results and its accuracy does not vary greatly with the type of FRP used, the effective depth of the member, the slenderness ratio, or the concrete strength. The formula given by the JSCE (1997) gives conservative results for all cases mentioned. The accuracy of this formula was verified in the experimental work, as it gave the most accurate shear predictions but was still conservative in its predictions. Thus, the use of the JSCE (1997) code equation is recommended for predicting the concrete contribution to shear of FRP-RC members.

References

American Concrete Institute, ACI 440.1R-03 (2003). *Guide for the design and construction of concrete reinforced with FRP bars*, ACI Committee 440, Farmington Hills, Michigan, 42

American Concrete Institute (2004). *Proposed Revisions to 'Guide for the design and construction of concrete reinforced with FRP bars'*, ACI Committee 440, Farmington Hills, Michigan, 35

ACI Standard 318-99 (1999). *Building code requirements for structural concrete*, American Concrete Institute, Farmington Hills, Michigan.

Al-Salloum, Y.A., Alsayed, S.H. and Almusallam, T.H. (1996). "Evaluation of Service Load Deflection for Beams Reinforced by GFRP Bars." Proceedings of the ACMBS-2 Conference, Montreal, 165-172

Abdalla, H. and El-Badry, M.M. (1996). "Deflection of Concrete Slabs Reinforced with Advanced Composite Materials." Proceedings of the ACMBS-2 Conference, Montreal, 201-208

Alkhrdaji, T., Ombres, L. and Nanni, A. (1996). "*Flexural Behavior of One-Way Concrete Slabs Reinforced with Deformed GFRP Bars.*" Proceedings of the ACMBS-2 Conference, Montreal, 217-224

Alkhrdaji, T., Wideman, M., Belarbi, A. and Nanni, A. (2001). "*Shear strength of RC beams and slabs.*" Composites in Construction, J. Figueiras, L. Juvandes and R. Faria, eds., A.A. Balkema Publishers, Lisse, Netherlands, 409-414

Almusallam, T.H., Al-Salloum, Y.A., Alsayed, S.H. and Amjad, M.A. (1997). "*Behaviour of Concrete Beams Doubly Reinforced by FRP Bars.*" Proceedings of the FRPRCS-3 Conference, Sapporo, Japan, 471-478

Alsayad, S.H, Al-Salloum, Y.A. and Almusallam, T.H. (1996). "*Evaluation of Shear Stresses in Concrete Beams Reinforced by FRP Bars.*" Proceedings of the ACMBS-II Conference, El-Badry, CSCE, Montreal, 173-179.

Alsayad, S.H, Almusallam, T.H. and Al-Salloum, Y.A. (1995). "*Flexural Behaviour of Concrete Elements Reinforced by GFRP Bars.*" Proceedings of the FRPRCS-2 Conference, Taerwe, L., ed., Ghent, 219-226

Benmokrane, B. and Masmoudi, R. (1996). "FRP C-Bar Reinforcing Rod for Concrete Structures." Proceedings of the ACMBS-2 Conference, Montreal, 181-188

Benmokrane, B., Chaallal, O. and Masmoudi, R. (1996). “*Flexural response of concrete beams reinforced with FRP reinforcing bars.*” ACI Structural Journal, 91(2), 46-55.

Bischoff, P. (2005). “*A Rational Proposal for Predicting Beam Deflection.*” Proceedings of the 33rd Annual General Conference of the Canadian Society for Civil Engineering, CSCE, Toronto, Ontario

Brown, V.L. and Bartholomew, C.L. (1996). “*Long-term deflections of GFRP-reinforced concrete beams.*” Proceedings of the ICCI Conference, Tucson, Arizona, 389-400

CSA Canadian Standard A23.3-94 (1998). *Concrete design handbook*, 2nd ed., Canadian Standards Association, Rexdale, Ontario

CSA Canadian Standard S806-02 (2002). *Design and construction of building components with fibre-reinforced polymers*, Canadian Standards Association, Toronto, Ontario, 177.

CEB-FIP MC-90 (1990). *Model code for concrete structures (MC-90)*, Comité Euro-International du Béton – Fédération International de la Précontrainte, Thomas Telford, London, England.

Choi, B. S., Scanlon, A. and Johnson, P. A. (2004). "Monte Carlo simulation of immediate and time-dependent deflections of reinforced concrete beams and slabs." *ACI Structural Journal*, 101(5), 633-641.

Cosenza, E., Greco, C., Manfredi, G. and Pecce, M. (1997). "Flexural Behaviour of Concrete Beams Reinforced with Fiber Reinforced Plastic (FRP) Bars." Proceedings of the FRPRCS-3 Conference, Sapporo, Japan, 463-470

Deitz, D. (1998). "GFRP Reinforced Concrete Bridge Decks." PhD. Thesis, University of Kentucky, Lexington, Kentucky

Duranovic, N., Pilakoutas, K. and Waldron, P. (1997). "Tests on Concrete Beams Reinforced with Glass Fibre Reinforced Plastic Bars." Proceedings of the FRPRCS-3 Conference, Sapporo, Japan, 479-485

El-Salakawy, E.F., Kassem, C. and Benmokrane, B. (2003). "Flexural Behaviour of Bridge Deck Slabs Reinforced with FRP Composite Bars." Proceedings of the FRPRCS-6 Conference, World Scientific Publishing Company, Singapore, 1291-1300

El-Sayad, A., El-Salakawy, E. and Benmokrane, B. (2004). "Evaluation of Concrete Shear Strength for Beams Reinforced with FRP Bars." Proceedings of the 5th SSP of the CSCE Conference, CSCE, Saskatoon, ST-224

Farahmand, F. (1996). "*Effect of GFRP on Concrete Contribution to Shear.*" MSc. Thesis, University of Manitoba, Winnipeg

Faza, S.S. and GangaRao, H.V.S. (1992). "*Pre- and post-cracking deflection behaviour of concrete beams reinforced with fibre-reinforced plastic rebars.*" Proceedings of the ACMBS Conference, CSCE, 151-160.

Fernando, L. (2001). "*The Serviceability of Concrete Beams Reinforced with FRP.*" BSc. Thesis, University of Manitoba, Winnipeg, Manitoba, 16-26

Ghali, A., Hall, T. and Bobey, W. (2001) "*Minimum thickness of concrete members reinforced with fibre reinforced polymer bars.*" Canadian Journal of Civil Engineering, 28, 583-592.

Guadagnini, M., Pilakoutas, K., and Waldron, P. (2001). "*Investigation on Shear Carrying Mechanisms in FRP RC Beams.*" Proceedings of the FRPRCS-5 Conference, Thomas Telford, London, 949-958

Gross, S. P., Dinehart, D. W. and Yost, J. R. (2004) "*Experimental Tests on High Strength Concrete Beams Reinforced with CFRP bars.*" Proceedings of the ACMBS-4 Conference, Calgary

Hall, T.S. (2000). “*Deflections of Concrete Members Reinforced with Fibre Reinforced Polymer (FRP) Bars.*” MSc. Thesis, University of Calgary, Calgary, Alberta

Jawara, A. (1999). “Low Heat High Performance Concrete for Glass Fiber Reinforced Polymer Reinforcement.” MSc. Thesis, University of Manitoba, Winnipeg, Manitoba

JSCE (1997). *Recommendation for design and construction of concrete structures using continuous fiber reinforcing materials*, Research Committee on Continuous Fiber Reinforcing Materials, A. Machida Ed., Japan Society of Civil Engineers, Tokyo, Japan, 325

Kassem, C., El-Salakawy, E. and Benmokrane, B. (2003). “*Deflection Behaviour of Concrete Beams Reinforced with Carbon FRP Composite Bars.*” Deflection Control for the Future, ACI Special Publication SP-210, Gardner, J. Ed., ACI, MI, 65-92

Kobayashi, K., Rahman, H., and Fujisaki, T. (1997). “*Crack Width Prediction for Nefmac-Reinforced Flexural Members.*” Proceedings of the FRPRCS-3 Conference, Sapporo, Japan, 447-454

Légeron, F. and Paultre, P. (2000). “*Prediction of Modulus of Rupture of Concrete.*” ACI Materials Journal, Vol. 90, No. 3, 193-200

MacGregor, J.G. and Bartlett, F.M. (2000). "Reinforced Concrete: Mechanics and Design." Prentice Hall Canada Inc. Scarborough, Ontario

Maruyama, K. and Zhao, W. (1996). "*Size Effect in Shear Behavior of FRP Reinforced Concrete Beams.*" Proceedings of the ACMBS-2 Conference, Montreal, 227-234

Matthys, S. and Taerwe, L. (1995). "*Loading Tests on Concrete Slabs Reinforced with FRP Grids.*" Proceedings of the FRPRCS-2 Conference, Taerwe, L., ed., Ghent, 352-359.

Michaluk, C., Rizkalla, S., Tadros, C., and Benmokrane, B. (1998). "*Flexural Behaviour of One-Way Concrete Slabs Reinforced by Fiber Plastic Reinforcements.*" ACI Structural Journal, 95(3), 353-365.

Mota (2004), "Concrete Beam Laboratory." Unpublished lab tests performed at the Univeristy of Manitoba, Winnipeg, Manitoba

Najjar, S., Pilakoutas, K., and Waldron, P. (1997). "*Finite Element Analysis of GFRP Reinforced Concrete Beams.*" Proceedings of the FRPRCS-3 Conference, Sapporo, Japan, 519-526

Nawy, E.G. and Neuwerth, A.M. (1977). "*Fiberglass Reinforced Concrete Slabs and Beams.*" ACI Structural Journal, 421-439.

Newhook, J., Ghali, A. and Tadros, G. (2002) "*Concrete flexural members reinforced with fiber reinforced polymer: design for cracking and deformability.*" Canadian Journal of Civil Engineering, 29, 125-134.

OHBDC (1992). "*Ontario Highway Bridge Design Code, 3rd Edition.*" Ministry of Transportation, Downsview, Ontario

Oluokun, F.A. (1991). "*Prediction of Concrete Tensile Strength from its Compressive Strength: An Evaluation of Existing Relations for Normal Weight Concrete.*" ACI Materials Journal, Vol. 88, No. 3, 302-309

Pecce, M., Manfredi, G. and Cosenza, E. (2000). "*Experimental Response and Code Models of GFRP RC Beams in Bending.*" Journal of Composites for Construction Vol. 4, ASCE, 182-190

Raphael, J.M. (1984). "*Tensile Strength of Concrete.*" ACI Journal, Vol. 81, No. 2, 158-165

Razaqpur, A.G., Svecova, D. and Cheung, M.S. (2000). "*Rational method for calculating deflection of fiber-reinforced polymer reinforced beams.*" ACI Structural Journal, 97(1),175-184.

Razaqpur, A., Isgor, B., Greenway, S., and Selley, A. (2004). "Concrete Contribution to the Shear Resistance of FRP Reinforced Concrete Members." ASCE Composites in Construction Journal, September/October, 452-460.

Razaqpur, A., Isgor, B., Greenway, S., and Selley, A. (2004). "Proposed Shear Design Method for FRP Reinforced Concrete Members without Stirrups." Manuscript submitted to the ACI Structural Journal

Reda Taha, M.M. and Hassanain, M.A. (2003). "Estimating the error in calculating deflections of HPC slabs: A parametric study using the theory of error propagation." Deflection Control for the Future, ACI Special Publication SP-210, Gardner, J. Ed., ACI, MI, 65-92.

Rizkalla, S. and Mufti, A. (2001). "Reinforcing concrete structures with fibre reinforced polymers - Design Manual No. 3", ISIS Canada, Winnipeg, Manitoba.

Standards Australia, AS 3600-1994 (1994). "Concrete Structures." Standards Association of Australia, Homebush, Australia

Standards New Zealand, NZS 3101 (1995). "The Design of Concrete Structures." Standards New Zealand, Wellington, New Zealand

Swamy, N. and Aburawi, M. (1997). "*Structural Implications of Using GFRP Bars as Concrete Reinforcement.*" Proceedings of the FRPRCS-3 Conference, Sapporo, Japan, 503-510

Tariq, M. (2003). "*Effects of Flexural Reinforcement Properties on Shear Strength of Concrete Beams.*" Masters Thesis, Dalhousie University, Halifax

Theriault, M. and Benmokrane, B. (1997). "*Theoretical and experimental investigation on crack width, deflection and deformability of concrete beams reinforced with FRP rebars.*" Proceedings of the Annual Conference of the Canadian Society for Civil Engineering, CSCE, Sherbrooke, Quebec, 151-160.

Toutanji, H.A. and Saafi, M. (2000). "*Flexural behavior of concrete beams reinforced with glass fiber-reinforced polymer (GFRP) bars.*" ACI Structural Journal, 97(5), 712-719.

Tureyen, A.K. and Frosch, R.J. (2002). "*Shear Tests of FRP-Reinforced Concrete Beams without Stirrups.*" ACI Structural Journal, 99(4), 427-434.

Vogel, H.M. (2005). "*Thermal Compatibility and Bond Strength of FRP Reinforcement in Prestressed Concrete Applications.*" MSc. Thesis, University of Manitoba, Winnipeg, Manitoba, 21-24

Yost, J., Goodspeed, H., and Schmeckpeper, R. (2001). "*Flexural Performance of Concrete Beams Reinforced with FRP Grids.*" Journal of Composites for Construction Vol. 5, ASCE, 18-25

Yost, J.R, Gross, S.P and Dinehart, D.W. (2001). "*Shear Strength of Normal Strength Concrete Beams Reinforced with Deformed GFRP Bars.*" Journal of Composites for Construction, ASCE, 268-275.

Yost, J.R, Gross, S.P and Dinehart, D.W. (2003). "*Effective moment of inertia for glass fiber-reinforced polymer-reinforced concrete beams.*" ACI Structural Journal, 100(6), 732-739.

Zhao, W. and Maruyama, K. (1995). "*Shear behavior of concrete beams reinforced by FRP rods as longitudinal and shear reinforcement.*" Proceedings of the FRPRCS-2 Conference, Taerwe, L., ed., Ghent, 352-359.

Zhao, W., Pilakoutas, K. and Waldron, P. (1997). "*FRP Reinforced Concrete: Cracking Behaviour and Determination.*" Proceedings of the FRPRCS-3 Conference, Sapporo, Japan, 439-446

Zhao, W., Pilakoutas, K. and Waldron, P. (1997). "*FRP Reinforced Concrete: Calculations for Deflections.*" Proceedings of the FRPRCS-3 Conference, Sapporo, Japan, 511-518

**Appendix I – Properties of Members used in the
Parametric Study**

AFRP-RC Deflection Members

Members Tested by Tureyen and Frosch (2002)

Beam #	L (mm)	a (mm)	b (mm)	h (mm)	d (mm)	f'_c (MPa)	E_{frp} (GPa)	f_{frpu} (MPa)	# bars	d_b (mm)	Stirrups Present	Failure Mode
V-A-1	2448	1224	457	406.4	360.4	40.33	47	1419	8	15.9	No	Shear
V-A-2	2448	1224	457	426.7	360.4	42.61	47	1419	16	15.9	No	Shear

CFRP-RC Deflection Members

Members Tested by El-Salakawy, Kassem and Benmokrane (2003)

Beam #	L (mm)	a (mm)	b (mm)	h (mm)	d (mm)	f'_c (MPa)	E_{frp} (GPa)	f_{frpu} (MPa)	# bars	d_b (mm)	Stirrups Present	Failure Mode
S-C1	2500	1000	1000	200	165.25	40	114	1536	9	9.5	No	Shear
S-C2B	2500	1000	1000	200	165.25	40	114	1536	18	9.5	No	Shear
S-C3B	2500	1000	1000	200	162.1	40	114	1536	27	9.5	No	Shear

Members Tested by El-Sayad, El-Salakawy, and Benmokrane (2004)

Beam #	L (mm)	a (mm)	b (mm)	h (mm)	d (mm)	f'_c (MPa)	E_{frp} (GPa)	f_{frpu} (MPa)	# bars	d_b (mm)	Stirrups Present	Failure Mode
CN-1	2750	1000	250	400	326	50	128	1536	10	9.5	No	Shear
CN-2	2750	1000	250	400	326	44.6	134	986	8	12.7	No	Shear
CN-3	2750	1000	250	400	326	43.6	134	986	11	12.7	No	Shear

Members Tested by Fernando (2001)

Beam #	L (mm)	a (mm)	b (mm)	h (mm)	d (mm)	f'_c (MPa)	E_{frp} (GPa)	f_{frpu} (MPa)	# bars	d_b (mm)	Stirrups Present	Failure Mode
FRP-1	2300	850	165	250	199	41.25	147	2250	1	10	Yes	Compression
FRP-3	2300	850	165	250	195	41.25	147	2250	3	10	Yes	Compression
FRP-4	2300	850	165	250	199	41.25	147	2250	4	10	Yes	Compression

Members Tested by Gross, Dinehart, and Yost (2004)

Beam #	L (mm)	a (mm)	b (mm)	h (mm)	d (mm)	f' _c (MPa)	E _{frp} (GPa)	f _{frpu} (MPa)	# bars	d _b (mm)	Stirrups Present	Failure Mode
11-2-1	1970	910	89	172	143	81.4	139	2640	2	6.35	No	Shear
11-2-2	1970	910	89	172	143	81.4	139	2640	2	6.35	No	Shear
11-2-3	1970	910	89	172	143	81.4	139	2640	2	6.35	No	Shear
11-3-1	1970	910	121	172	141	81.4	139	2640	2	9.525	No	Shear
11-3-2	1970	910	121	172	141	81.4	139	2640	2	9.525	No	Shear
11-3-3	1970	910	121	172	141	81.4	139	2640	2	9.525	No	Shear
8-2-1	1970	910	127	172	143	60.3	139	2640	2	6.35	No	Shear
8-2-2	1970	910	127	172	143	60.3	139	2640	2	6.35	No	Shear
8-2-3	1970	910	127	172	143	60.3	139	2640	2	6.35	No	Shear
8-3-1	1970	910	159	172	141	61.8	139	2640	2	9.525	No	Shear
8-3-2	1970	910	159	172	141	61.8	139	2640	2	9.525	No	Shear
8-3-3	1970	910	159	172	141	61.8	139	2640	2	9.525	No	Shear

Members Tested by Kassem, El-Salakawy, and Benmokrane (2003)

Beam #	L (mm)	a (mm)	b (mm)	h (mm)	d (mm)	f' _c (MPa)	E _{frp} (GPa)	f _{frpu} (MPa)	# bars	d _b (mm)	Stirrups Present	Failure Mode
CB-4	2750	875	200	300	236	39.8	122	1988	4	9	Yes	Compression
CB-6	2750	875	200	300	236	44.8	122	1988	6	9	Yes	Compression
CB-8	2750	875	200	300	236	44.8	122	1988	8	9	Yes	Compression
IS-4	2750	875	200	300	235.5	40.4	114	1506	4	9.5	Yes	Balanced
IS-6	2750	875	200	300	235.5	39.3	114	1506	6	9.5	Yes	Compression
IS-8	2750	875	200	300	235.5	39.3	114	1506	8	9.5	Yes	Compression

Member Tested by Kobayashi, Rahman and Fujisaki (1997)

Beam #	L (mm)	a (mm)	b (mm)	h (mm)	d (mm)	f' _c (MPa)	E _{frp} (GPa)	f _{frpu} (MPa)	A _{frp} (mm ²)	Stirrups Present	Failure Mode
C-120-M	1800	600	400	120	90	39.4	92.3	1800	144.8	No	Shear

Members Tested by Maruyama and Zhao (1996)

Beam #	L (mm)	a (mm)	b (mm)	h (mm)	d (mm)	f' _c (MPa)	E _{frp} (GPa)	f _{frpu} (MPa)	A _{frp} (mm ²)	Stirrups Present	Failure Mode
No.26	1250	625	150	300	250	34	100	1200	390	Yes	Shear
No.30	2500	1250	300	580	500	29.5	100	1200	1560	Yes	Shear

Members Tested by Matthys and Taerwe (1995)

Beam #	L (mm)	a (mm)	b (mm)	h (mm)	d (mm)	f' _c (MPa)	E _{frp} (GPa)	f _{frpu} (MPa)	A _{frp} (mm ²)	Stirrups Present	Failure Mode
C1	4000	1000	1000	120	96	30.4	98.1	1180	274.4	No	Balanced
C2	4000	1000	1000	120	95	29.6	98.1	1180	1000	No	Compression
C3	4000	1000	1000	150	126	28	98.1	1180	650	No	Compression

Beam #	L (mm)	a (mm)	b (mm)	h (mm)	d (mm)	f' _c (MPa)	E _{frp} (GPa)	f _{frpu} (MPa)	# bars	d _b (mm)	Stirrups Present	Failure Mode
CS	4000	1000	1000	120	98	27.2	150	2300	9	5	No	Tension

Member Tested by Michaluk, Rizkalla, Tadros and Benmokrane (1995)

Beam #	L (mm)	a (mm)	b (mm)	h (mm)	d (mm)	f' _c (MPa)	E _{frp} (GPa)	f _{frpu} (MPa)	# bars	d _b (mm)	Stirrups Present	Failure Mode
LL-200-C	3000	1000	1000	200	158	66.3	147	1970	6	8	No	Bond

Members Tested by Razaqpur, Isgor, Greenway, and Selley (2004)

Beam #	L (mm)	a (mm)	b (mm)	h (mm)	d (mm)	f' _c (MPa)	E _{frp} (GPa)	f _{frpu} (MPa)	# bars	d _b (mm)	Stirrups Present	Failure Mode
BA1	2000	410	200	250	225	40.5	145	2250	7	8	No	Shear
BA3	2000	800	200	250	225	40.5	145	2250	4	8	No	Shear
BA4	2000	1012.5	200	250	225	40.5	145	2250	4	8	No	Shear
BR1	2000	600	200	250	225	40.5	145	2250	2	8	No	Shear
BR2	2000	600	200	250	225	49	145	2250	4	8	No	Shear
BR3	2000	600	200	250	225	40.5	145	2250	5	8	No	Shear
BR4	2000	600	200	250	225	40.5	145	2250	7	8	No	Shear

Members Tested by Tariq (2003)

Beam #	L (mm)	a (mm)	b (mm)	h (mm)	d (mm)	f' _c (MPa)	E _{frp} (GPa)	f _{frpu} (MPa)	# bars	d _b (mm)	Stirrups Present	Failure Mode
R-C007Na	2500	950	130	380	310	34.49	120	1596	4	9.5	No	Shear
R-C007Nb	2500	950	130	380	310	34.49	120	1596	4	9.5	No	Shear
R-C010Na	2500	1150	130	380	310	43.21	120	1596	6	9.5	No	Shear
R-C010Nb	2500	1150	130	380	310	43.21	120	1596	6	9.5	No	Shear
R-C015Na	2500	1150	130	380	310	34.05	120	1596	9	9.5	No	Shear
R-C015Nb	2500	1150	130	380	310	34.05	120	1596	9	9.5	No	Shear

Members Tested by Zhao and Maruyama (1995)

Beam #	L (mm)	a (mm)	b (mm)	h (mm)	d (mm)	f_c (MPa)	E_{frp} (GPa)	f_{frpu} (MPa)	# bars	d_b (mm)	Stirrups Present	Failure Mode
No.18	1300	500	150	300	250	34.3	105	1124	2	19	Yes	Shear
No.19	2300	1000	150	300	250	34.3	105	1124	2	19	Yes	Shear
No.5	1800	750	150	300	250	34.3	105	1124	2	19	Yes	Compression

GFRP-RC Deflection Members

Members Tested by Abdalla and El-Badry (1996)

Beam #	L (mm)	a (mm)	b (mm)	h (mm)	d (mm)	f _c (MPa)	E _{frp} (GPa)	f _{frpu} (MPa)	# bars	d _b (mm)	Stirrups Present	Failure Mode
I-150-A	3000	1400	1000	150	112	63.9	42.2	692	11	8	No	Tension
I-150-B	3000	1400	1000	150	112	66.3	42.2	692	17	8	No	Tension

Members Tested by Alkhrdaji, Ombres and Nanni (2000)

Beam #	L (mm)	a (mm)	b (mm)	h (mm)	d (mm)	f _c (MPa)	E _{frp} (GPa)	f _{frpu} (MPa)	# bars	d _b (mm)	Stirrups Present	Failure Mode
SB1	2438.4	914.4	254	101.6	76.2	25.51	41.37	830	5	9.525	No	Compression
SB3	2438.4	914.4	254	101.6	76.2	25.51	41.37	800	2	12.7	No	Compression
SB5	2438.4	914.4	254	101.6	76.2	25.51	41.37	800	4	12.7	No	Compression
SB6	2438.4	914.4	254	101.6	63.5	25.51	41.37	800	3	12.7	No	Compression
SB7	2438.4	914.4	254	101.6	76.2	25.51	39.99	780	2	15.875	No	Compression

Members Tested by Almusallam, Al-Salloum, Alsayad and Amjad (1997)

Beam #	L (mm)	a (mm)	b (mm)	h (mm)	d (mm)	f _c (MPa)	E _{frp} (GPa)	f _{frpu} (MPa)	# bars	d _b (mm)	Stirrups Present	Failure Mode
COMP-00	2500	1150	200	240	190.6	35.4	43.37	886	4	12.7	Yes	Compression
COMP-25	2500	1150	200	240	190.6	35.4	43.37	886	4	12.7	Yes	Compression
COMP-50	2500	1150	200	240	190.6	36.5	43.37	886	4	12.7	Yes	Compression
COMP-75	2500	1150	200	240	190.6	36.5	43.37	886	4	12.7	Yes	Compression

Members Tested by Al-Salloum, Alsayed and Almusallam (1996)

Beam #	L (mm)	a (mm)	b (mm)	h (mm)	d (mm)	f' _c (MPa)	E _{frp} (GPa)	f _{frpu} (MPa)	# bars	d _b (mm)	Stirrups Present	Failure Mode
II	2700	1250	200	210	157.5	31.3	35.6	700	4	19	Yes	Compression
III	2700	1250	200	260	210.7	31.3	43.4	886	4	12.7	Yes	Compression
IV	2700	1250	200	300	247.5	40.7	35.6	700	2	19	Yes	Compression
V	2700	1250	200	250	197.5	40.7	35.6	700	4	19	Yes	Compression

Members Tested by Alsayed, Al-Salloum and Almusallam (1996)

Beam #	L (mm)	a (mm)	b (mm)	h (mm)	d (mm)	f' _c (MPa)	E _{frp} (GPa)	f _{frpu} (MPa)	# bars	d _b (mm)	Stirrups Present	Failure Mode
Group B	2200	1000	200	360	309.5	35.53	35.63	700	3	19.05	Yes	Shear
Group D	2200	1000	200	360	309.5	35.53	35.63	700	3	19.05	Yes	Shear

Members Tested by Alsayed, Almusallam and Al-Salloum (1995)

Beam #	L (mm)	a (mm)	b (mm)	h (mm)	d (mm)	f' _c (MPa)	E _{frp} (GPa)	f _{frpu} (MPa)	# bars	d _b (mm)	Stirrups Present	Failure Mode
Group II	2700	1250	200	210	157.5	31.3	50	620	4	19	Yes	Compression
Group III	2700	1250	200	260	210.7	31.3	50	740	4	12.7	Yes	Compression

Members Tested by Benmokrane and Masmoudi (1996)

Beam #	L (mm)	a (mm)	b (mm)	h (mm)	d (mm)	f' _c (MPa)	E _{frp} (GPa)	f _{frpu} (MPa)	# bars	d _b (mm)	Stirrups Present	Failure Mode
CB2B	3000	1300	200	300	262.5	52	38	773	2	14.9	Yes	Compression
CB3B	3000	1300	200	300	262.5	52	38	773	3	14.9	Yes	Compression
CB4B	3000	1300	200	300	240	45	38	773	4	14.9	Yes	Compression
CB6B	3000	1300	200	300	240	45	38	773	6	14.9	Yes	Compression

Members Tested by Benmokrane, Chaallal and Masmoudi (1996)

Beam #	L (mm)	a (mm)	b (mm)	h (mm)	d (mm)	f' _c (MPa)	E _{frp} (GPa)	f _{frpu} (MPa)	# bars	d _b (mm)	Stirrups Present	Failure Mode
ISO 1-2	3000	1000	200	300	260	43	45	690	2	19.1	Yes	Compression
ISO 3-4	3000	1000	200	550	511	43	45	690	2	19.1	Yes	Tension

Members Tested by Brown and Bartholomew (1996)

Beam #	L (mm)	a (mm)	b (mm)	h (mm)	d (mm)	f' _c (MPa)	E _{frp} (GPa)	f _{frpu} (MPa)	# bars	d _b (mm)	Stirrups Present	Failure Mode
D1	1675	685	102	152	115	35	41.4	550	2	9.5	Yes	Compression
D2	1675	685	102	152	102.5	35	41.4	550	2	9.5	Yes	Compression

Member Tested by Cosenza, Greco, Manfredi and Pecce (1997)

Beam #	L (mm)	a (mm)	b (mm)	h (mm)	d (mm)	f' _c (MPa)	E _{frp} (GPa)	f _{frpu} (MPa)	# bars	d _b (mm)	Stirrups Present	Failure Mode
C5	3400	1200	500	180	145	30	42	886	7	12.7	Yes	Compression

Member Tested by Duranovic, Pilakoutas and Waldron (1997)

Beam #	L (mm)	a (mm)	b (mm)	h (mm)	d (mm)	f _c (MPa)	E _{frp} (GPa)	f _{frpu} (MPa)	# bars	d _b (mm)	Stirrups Present	Failure Mode
GB10	2300	767	150	250	210	39.8	45	886	3	13.5	Yes	Compression

Members Tested by El-Salakawy, Kassem and Benmokrane (2003)

Beam #	L (mm)	a (mm)	b (mm)	h (mm)	d (mm)	f _c (MPa)	E _{frp} (GPa)	f _{frpu} (MPa)	# bars	d _b (mm)	Stirrups Present	Failure Mode
S-G1	2500	1000	1000	200	162.05	40	40	570	7	15.9	No	Shear
S-G2B	2500	1000	1000	200	162.05	40	40	570	14	15.9	No	Shear
S-G3B	2500	1000	1000	200	156.75	40	40	570	21	15.9	No	Shear

Members Tested by El-Sayed, El-Salakawy and Benmokrane (2004)

Beam #	L (mm)	a (mm)	b (mm)	h (mm)	d (mm)	f _c (MPa)	E _{frp} (GPa)	f _{frpu} (MPa)	# bars	d _b (mm)	Stirrups Present	Failure Mode
GN-1	2750	1000	250	400	326	50	39	608	10	9.5	No	Shear
GN-2	2750	1000	250	400	326	44.6	42	754	5	15.9	No	Shear
GN-3	2750	1000	250	400	326	43.6	42	754	7	15.9	No	Shear

Member Tested by Guadagnini, Pilakoutas and Waldron (2001)

Beam #	L (mm)	a (mm)	b (mm)	h (mm)	d (mm)	f _c (MPa)	E _{frp} (GPa)	f _{frpu} (MPa)	# bars	d _b (mm)	Stirrups Present	Failure Mode
GB43	2300	750	150	250	223	50.4	45	750	3	13.5	No	Shear

Members Tested by Hall (2000)

Beam #	L (mm)	a (mm)	b (mm)	h (mm)	d (mm)	f' _c (MPa)	E _{frp} (GPa)	f _{frpu} (MPa)	# bars	d _b (mm)	Stirrups Present	Failure Mode
Sh-G-2-S	3200	1067	280	180	158	31.8	42	680	2	15	No	Bond
Sh-G-3-S	3200	1067	280	180	158	30	42	680	3	15	No	Compression

Members Tested by Jawara (1999)

Beam #	L (mm)	a (mm)	b (mm)	h (mm)	d (mm)	f' _c (MPa)	E _{frp} (GPa)	f _{frpu} (MPa)	# bars	d _b (mm)	Stirrups Present	Failure Mode
LG0.5-1	3700	1300	150	350	300	82	34	532	2	12	Yes	Tension
LG0.5-2	3700	1300	150	350	300	82	34	532	2	12	Yes	Tension
LG1.5-1	3700	1300	150	350	300	82	34	532	6	12	Yes	Tension
LG1.5-2	3700	1300	150	350	300	82	34	532	6	12	Yes	Tension
NG0.5-1	3700	1300	150	350	300	38	34	532	2	12	Yes	Tension
NG1.5-1	3700	1300	150	350	300	38	34	532	6	12	Yes	Compression

Members Tested by Matthys and Taerwe (1995)

Beam #	L (mm)	a (mm)	b (mm)	h (mm)	d (mm)	f' _c (MPa)	E _{frp} (GPa)	f _{frpu} (MPa)	A _{frp} (mm ²)	Stirrups Present	Failure Mode
H1	4000	1000	1000	120	95	96.7	36.3	520	621.6	No	Tension
H2	4000	1000	1000	120	89	29.3	36.3	520	3350	No	Compression
H3	4000	1000	1000	150	122	26.3	36.3	520	1561	No	Compression

Members Tested by Michaluk, Rizkalla, Tadros and Benmokrane (1995)

Beam #	L (mm)	a (mm)	b (mm)	h (mm)	d (mm)	f' _c (MPa)	E _{frp} (GPa)	f _{frpu} (MPa)	# bars	d _b (mm)	Stirrups Present	Failure Mode
I-150A	3000	1000	1000	150	106	63.9	41.3	690	4	12.7	No	Tension
I-150B	3000	1000	1000	150	104	66.3	41.3	690	4	15.9	No	Tension
I-150C	3000	1000	1000	150	104	66.0	41.3	690	5	15.9	No	Shear
I-200C	3000	1000	1000	200	154	66.0	41.3	690	6	15.9	No	Shear

Members Tested by Mota (2004)

Beam #	L (mm)	a (mm)	b (mm)	h (mm)	d (mm)	f' _c (MPa)	E _{frp} (GPa)	f _{frpu} (MPa)	# bars	d _b (mm)	Stirrups Present	Failure Mode
D3 #4	2700	900	200	400	347.5	45.15	40	691	2	25	Yes	Compression
D3 #5	2700	900	200	400	355	45.15	40	691	2	10	Yes	Tension

Member Tested by Najjar, Pilakoutas and Waldron (1997)

Beam #	L (mm)	a (mm)	b (mm)	h (mm)	d (mm)	f' _c (MPa)	E _{frp} (GPa)	f _{frpu} (MPa)	# bars	d _b (mm)	Stirrups Present	Failure Mode
GB6	2300	767	150	250	220	31.8	45	1000	3	13.5	No	Shear

Member Tested by Nawy and Neuwerth (1997)

Beam #	L (mm)	a (mm)	b (mm)	h (mm)	d (mm)	f' _c (MPa)	E _{frp} (GPa)	f _{frpu} (MPa)	# bars	d _b (mm)	Stirrups Present	Failure Mode
BF9	3050	1067	127	304.8	273.05	29.65	26.2	724	6	12.7	Yes	Compression

Members Tested by Pecce, Manfredi and Cosenza (1997)

Beam #	L (mm)	a (mm)	b (mm)	h (mm)	d (mm)	f' _c (MPa)	E _{frp} (GPa)	f _{frpu} (MPa)	# bars	d _b (mm)	Stirrups Present	Failure Mode
F1	3400	1200	500	185	145	30	42	770	7	12.7	Yes	Tension
F2	3400	1200	500	185	145	30	42	770	4	12.7	Yes	Tension
F3	3400	1200	500	185	145	30	42	770	7	12.7	Yes	Tension

Members Tested by Swamy and Aburawi (1997)

Beam #	L (mm)	a (mm)	b (mm)	h (mm)	d (mm)	f' _c (MPa)	E _{frp} (GPa)	f _{frpu} (MPa)	# bars	d _b (mm)	Stirrups Present	Failure Mode
F-1-GF	2100	700	154	254	222.2	42	34	586	3	15	Yes	Compression
F-2-GF	2100	700	154	254	222.2	42	34	586	3	15	Yes	Shear
F-3-GF	2100	700	154	254	222.2	42	34	586	3	15	No	Shear

Members Tested by Tariq (2003)

Beam #	L (mm)	a (mm)	b (mm)	h (mm)	d (mm)	f' _c (MPa)	E _{frp} (GPa)	f _{frpu} (MPa)	# bars	d _b (mm)	Stirrups Present	Failure Mode
R-G007Na	2500	950	160	380	346	34.49	42	674	2	15.9	No	Shear
R-G007Nb	2500	950	160	380	346	34.49	42	674	2	15.9	No	Shear
R-G010Na	2500	1150	160	380	346	43.21	42	674	3	15.9	No	Shear
R-G010Nb	2500	1150	160	380	346	43.21	42	674	3	15.9	No	Shear
R-G015Na	2500	1150	160	380	325	34.05	42	674	4	15.9	No	Shear
R-G015Nb	2500	1150	160	380	325	34.05	42	674	4	15.9	No	Shear

Members Tested by Theriault and Benmokrane (1997)

Beam #	L (mm)	a (mm)	b (mm)	h (mm)	d (mm)	f' _c (MPa)	E _{frp} (GPa)	f _{frpu} (MPa)	# bars	d _b (mm)	Stirrups Present	Failure Mode
BC2H	1500	500	130	180	147.85	57.2	38	773	2	12.3	Yes	Compression
BC2Ha	1500	500	130	180	151	57.2	38	773	2	12.3	Yes	Compression
BC2N	1500	500	130	180	147.85	53.1	38	773	2	12.3	Yes	Shear
BC2V	1500	500	130	180	147.85	97.4	38	773	2	12.3	Yes	Compression
BC4H	1500	500	130	180	129.2	53.9	38	773	4	12.3	Yes	Compression
BC4N	1500	500	130	180	129.2	46.2	38	773	4	12.3	Yes	Shear
BC4V	1500	500	130	180	129.2	93.5	38	773	4	12.3	Yes	Compression

Members Tested by Toutanji and Saafi (2000)

Beam #	L (mm)	a (mm)	b (mm)	h (mm)	d (mm)	f' _c (MPa)	E _{frp} (GPa)	f _{frpu} (MPa)	# bars	d _b (mm)	Stirrups Present	Failure Mode
GB1	2800	1200	180	300	268	35	40	695	2	12.7	Yes	Compression
GB2	2800	1200	180	300	268	35	40	695	3	12.7	Yes	Compression
GB3	2800	1200	180	300	255	35	40	695	4	12.7	Yes	Compression

Members Tested by Tureyen and Frosch (2002)

Beam #	L (mm)	a (mm)	b (mm)	h (mm)	d (mm)	f' _c (MPa)	E _{frp} (GPa)	f _{frpu} (MPa)	# bars	d _b (mm)	Stirrups Present	Failure Mode
V-G1-1	2448	1224	457	406.4	360.4	39.71	40.5	606	8	15.9	No	Shear
V-G1-2	2448	1224	457	426.7	360.4	42.26	40.5	606	16	15.9	No	Shear
V-G2-1	2448	1224	457	406.4	360.4	39.85	37.6	592	8	15.9	No	Shear
V-G2-2	2448	1224	457	426.7	360.4	42.54	37.6	592	16	15.9	No	Shear

Members Tested by Yost, Goodspeed and Schmeckpeper (2001)

Beam #	L (mm)	a (mm)	b (mm)	h (mm)	d (mm)	f' _c (MPa)	E _{frp} (GPa)	f _{frpu} (MPa)	A _{frp} (mm ²)	Stirrups Present	Failure Mode
Lab1FRP1	1778	787	381	203	179	27.6	41.4	830	80	No	Tension
Lab1FRP2	1778	787	381	203	179	27.6	41.4	830	80	No	Tension
Lab1FRP3	1778	787	381	203	179	27.6	41.4	830	80	No	Tension
Lab2FRP1	1778	787	318	216	192	27.6	41.4	830	80	No	Tension
Lab2FRP2	1778	787	318	216	192	27.6	41.4	830	80	No	Tension
Lab2FRP3	1778	787	318	216	192	27.6	41.4	830	80	No	Tension
Lab3FRP	1778	787	305	216	192	38.0	41.4	830	160	No	Shear
Lab4FRP	1778	787	203	152	124	27.6	41.4	830	320	No	Compression
Lab5FRP	1778	787	191	152	124	27.6	41.4	830	320	No	Compression

Members Tested by Yost, Gross and Dinehart (2003)

Beam #	L (mm)	a (mm)	b (mm)	h (mm)	d (mm)	f' _c (MPa)	E _{frp} (GPa)	f _{frpu} (MPa)	# bars	d _b (mm)	Stirrups Present	Failure Mode
1a-HL	2895.6	1295.4	254	184.15	138.18	79.497	40.3	690	2	15.875	No	Not Reported
1a-HS	2133.6	914.4	203.2	285.75	225.55	79.634	40.3	690	2	19.05	No	Not Reported
1a-NL	2895.6	1295.4	254	184.15	139.7	40.334	40.3	690	2	12.7	No	Not Reported
1a-NS	2133.6	914.4	228.6	285.75	225.55	36.335	40.3	690	2	19.05	No	Shear
1b-HL	2895.6	1295.4	254	184.15	138.18	79.497	40.3	690	2	15.875	No	Not Reported
1b-HS	2133.6	914.4	203.2	285.75	225.55	79.634	40.3	690	2	19.05	No	Not Reported
1b-NL	2895.6	1295.4	254	184.15	139.7	40.334	40.3	690	2	12.7	No	Not Reported
1b-NS	2133.6	914.4	228.6	285.75	225.55	36.335	40.3	690	2	19.05	No	Shear

Members Tested by Yost, Gross and Dinehart (2003) (continued)

Beam #	L (mm)	a (mm)	b (mm)	h (mm)	d (mm)	f' _c (MPa)	E _{frp} (GPa)	f _{frpu} (MPa)	# bars	d _b (mm)	Stirrups Present	Failure Mode
1c-HL	2895.6	1295.4	254	184.15	138.18	79.497	40.3	690	2	15.875	No	Not Reported
1c-HS	2133.6	914.4	203.2	285.75	225.55	79.634	40.3	690	2	19.05	No	Not Reported
1c-NL	2895.6	1295.4	254	184.15	139.7	40.334	40.3	690	2	12.7	No	Not Reported
1c-NS	2133.6	914.4	228.6	285.75	225.55	36.335	40.3	690	2	19.05	No	Shear
2a-HL	2895.6	1295.4	190.5	184.15	138.18	79.497	40.3	690	2	15.875	No	Not Reported
2a-HS	2133.6	914.4	152.4	285.75	225.55	79.634	40.3	690	2	19.05	No	Not Reported
2a-NL	2895.6	1295.4	304.8	184.15	138.18	40.334	40.3	690	2	15.875	No	Not Reported
2a-NS	2133.6	914.4	228.6	285.75	225.55	36.335	40.3	690	3	19.05	No	Shear
2b-HL	2895.6	1295.4	190.5	184.15	138.18	79.497	40.3	690	2	15.875	No	Not Reported
2b-HS	2133.6	914.4	152.4	285.75	225.55	79.634	40.3	690	2	19.05	No	Not Reported
2b-NL	2895.6	1295.4	304.8	184.15	138.18	40.334	40.3	690	2	15.875	No	Not Reported
2b-NS	2133.6	914.4	228.6	285.75	225.55	36.335	40.3	690	3	19.05	No	Shear
2c-HL	2895.6	1295.4	190.5	184.15	138.18	79.497	40.3	690	2	15.875	No	Not Reported
2c-HS	2133.6	914.4	152.4	285.75	225.55	79.634	40.3	690	2	19.05	No	Not Reported
2c-NL	2895.6	1295.4	304.8	184.15	138.18	40.334	40.3	690	2	15.875	No	Not Reported
2c-NS	2133.6	914.4	228.6	285.75	225.55	36.335	40.3	690	3	19.05	No	Shear
3a-HL	2895.6	1295.4	152.4	184.15	138.18	79.497	40.3	690	2	15.875	No	Not Reported
3a-HS	2133.6	914.4	165.1	285.75	223.77	79.634	40.3	690	2	22.225	No	Not Reported
3a-NL	2895.6	1295.4	241.3	184.15	138.18	40.334	40.3	690	2	15.875	No	Not Reported
3a-NS	2133.6	914.4	254	285.75	223.77	36.335	40.3	690	3	22.225	No	Shear

Members Tested by Yost, Gross and Dinehart (2003) (continued)

Beam #	L (mm)	a (mm)	b (mm)	h (mm)	d (mm)	f _c (MPa)	E _{frp} (GPa)	f _{frpu} (MPa)	# bars	d _b (mm)	Stirrups Present	Failure Mode
3b-HL	2895.6	1295.4	152.4	184.15	138.18	79.497	40.3	690	2	15.875	No	Not Reported
3b-HS	2133.6	914.4	165.1	285.75	223.77	79.634	40.3	690	2	22.225	No	Not Reported
3b-NL	2895.6	1295.4	241.3	184.15	138.18	40.334	40.3	690	2	15.875	No	Not Reported
3b-NS	2133.6	914.4	254	285.75	223.77	36.335	40.3	690	3	22.225	No	Shear
3c-HL	2895.6	1295.4	152.4	184.15	138.18	79.497	40.3	690	2	15.875	No	Not Reported
3c-NL	2895.6	1295.4	241.3	184.15	138.18	40.334	40.3	690	2	15.875	No	Not Reported
3c-NS	2133.6	914.4	254	285.75	223.77	36.335	40.3	690	3	22.225	No	Shear
4a-HL	2895.6	1295.4	177.8	184.15	138.18	79.497	40.3	690	2	19.05	No	Not Reported
4a-HS	2133.6	914.4	203.2	285.75	223.77	79.634	40.3	690	3	22.225	No	Not Reported
4a-NL	2895.6	1295.4	203.2	184.15	138.18	40.334	40.3	690	2	15.875	No	Not Reported
4a-NS	2133.6	914.4	228.6	285.75	223.77	36.335	40.3	690	3	22.225	No	Shear
4b-HL	2895.6	1295.4	177.8	184.15	138.18	79.497	40.3	690	2	19.05	No	Not Reported
4b-HS	2133.6	914.4	203.2	285.75	223.77	79.634	40.3	690	3	22.225	No	Not Reported
4b-NL	2895.6	1295.4	203.2	184.15	138.18	40.334	40.3	690	2	15.875	No	Not Reported
4b-NS	2133.6	914.4	228.6	285.75	223.77	36.335	40.3	690	3	22.225	No	Shear
4c-HL	2895.6	1295.4	177.8	184.15	138.18	79.497	40.3	690	2	19.05	No	Not Reported
4c-HS	2133.6	914.4	203.2	285.75	223.77	79.634	40.3	690	3	22.225	No	Not Reported
4c-NL	2895.6	1295.4	203.2	184.15	138.18	40.334	40.3	690	2	15.875	No	Not Reported
4c-NS	2133.6	914.4	228.6	285.75	223.77	36.335	40.3	690	3	22.225	No	Shear

Members Tested by Zhao, Pilakoutas and Waldron (1997)

Beam #	L (mm)	a (mm)	b (mm)	h (mm)	d (mm)	f_c (MPa)	E_{frp} (GPa)	f_{frpu} (MPa)	# bars	d_b (mm)	Stirrups Present	Failure Mode
GB11	2300	767	150	250	220	39.8	45	1000	3	13.5	Yes	Shear
GB5	2300	767	150	250	220	31.2	45	1000	3	13.5	Yes	Compression

AFRP-RC Shear Members

Members Tested by Tureyen and Frosch (2002)

Beam #	L (mm)	a (mm)	b (mm)	h (mm)	d (mm)	f_c (MPa)	E_{frp} (GPa)	f_{frpu} (MPa)	# bars	d_b (mm)	P_{Max} (kN)
V-A-1	2448	1224	457	406.4	360.4	40.33	47	1419	8	15.9	114.8
V-A-2	2448	1224	457	426.7	360.4	42.61	47	1419	16	15.9	177

CFRP-RC Shear Members

Members Tested by El-Salakawy, Kassem and Benmokrane (2003)

Beam #	L (mm)	a (mm)	b (mm)	h (mm)	d (mm)	f' _c (MPa)	E _{frp} (GPa)	f _{frpu} (MPa)	# bars	d _b (mm)	P _{Max} (kN)
S-C1	2500	1000	1000	200	165.25	40	114	1536	9	9.5	135.715
S-C2B	2500	1000	1000	200	165.25	40	114	1536	18	9.5	163.5
S-C3B	2500	1000	1000	200	162.1	40	114	1536	27	9.5	189.285

Members Tested by El-Sayad, El-Salakawy, and Benmokrane (2004)

Beam #	L (mm)	a (mm)	b (mm)	h (mm)	d (mm)	f' _c (MPa)	E _{frp} (GPa)	f _{frpu} (MPa)	# bars	d _b (mm)	P _{Max} (kN)
CN-1	2750	1000	250	400	326	50	128	1536	10	9.5	77.5
CN-2	2750	1000	250	400	326	44.6	134	986	8	12.7	104
CN-3	2750	1000	250	400	326	43.6	134	986	11	12.7	124.5

Members Tested by Gross, Dinehart, and Yost (2004)

Beam #	L (mm)	a (mm)	b (mm)	h (mm)	d (mm)	f' _c (MPa)	E _{frp} (GPa)	f _{frpu} (MPa)	# bars	d _b (mm)	P _{Max} (kN)
11-2-1	1970	910	89	172	143	81.4	139	2640	2	6.35	8.76
11-2-2	1970	910	89	172	143	81.4	139	2640	2	6.35	11.7
11-2-3	1970	910	89	172	143	81.4	139	2640	2	6.35	8.92
11-3-1	1970	910	121	172	141	81.4	139	2640	2	9.525	14.32
11-3-2	1970	910	121	172	141	81.4	139	2640	2	9.525	15.3
11-3-3	1970	910	121	172	141	81.4	139	2640	2	9.525	16.55
8-2-1	1970	910	127	172	143	60.3	139	2640	2	6.35	14.32
8-2-2	1970	910	127	172	143	60.3	139	2640	2	6.35	12.86
8-2-3	1970	910	127	172	143	60.3	139	2640	2	6.35	14.72
8-3-1	1970	910	159	172	141	61.8	139	2640	2	9.525	19.84
8-3-2	1970	910	159	172	141	61.8	139	2640	2	9.525	23.13
8-3-3	1970	910	159	172	141	61.8	139	2640	2	9.525	17.04

Member Tested by Kobayashi, Rahman and Fujisaki (1997)

Beam #	L (mm)	a (mm)	b (mm)	h (mm)	d (mm)	f' _c (MPa)	E _{frp} (GPa)	f _{frpu} (MPa)	A _{frp} (mm ²)	P _{Max} (kN)
C-120-M	1800	600	400	120	90	39.4	92.3	1800	144.8	32.5

Members Tested by Maruyama and Zhao (1996)

Beam #	L (mm)	a (mm)	b (mm)	h (mm)	d (mm)	f _c (MPa)	E _{frp} (GPa)	f _{frpu} (MPa)	A _{frp} (mm ²)	P _{Max} (kN)
No.23	1250	625	150	300	250	34	100	1200	390	28.5
No.24	1250	625	150	300	250	34	100	1200	390	38

Members Tested by Razaqpur, Isgor, Greenway, and Selley (2004)

Beam #	L (mm)	a (mm)	b (mm)	h (mm)	d (mm)	f _c (MPa)	E _{frp} (GPa)	f _{frpu} (MPa)	# bars	d _b (mm)	P _{Max} (kN)
BA1	2000	410	200	250	225	40.5	145	2250	7	8	96.18
BA3	2000	800	200	250	225	40.5	145	2250	4	8	46.99
BA4	2000	1012.5	200	250	225	40.5	145	2250	4	8	38.45
BR1	2000	600	200	250	225	40.5	145	2250	2	8	36.11
BR2	2000	600	200	250	225	49	145	2250	4	8	46.95
BR3	2000	600	200	250	225	40.5	145	2250	5	8	47.23
BR4	2000	600	200	250	225	40.5	145	2250	7	8	42.71

Members Tested by Tariq (2003)

Beam #	L (mm)	a (mm)	b (mm)	h (mm)	d (mm)	f _c (MPa)	E _{frp} (GPa)	f _{frpu} (MPa)	# bars	d _b (mm)	P _{Max} (kN)
R-C007Na	2500	950	130	380	310	34.49	120	1596	4	9.5	49.17
R-C007Nb	2500	950	130	380	310	34.49	120	1596	4	9.5	45.75
R-C010Na	2500	1150	130	380	310	43.21	120	1596	6	9.5	47.555
R-C010Nb	2500	1150	130	380	310	43.21	120	1596	6	9.5	52.655
R-C015Na	2500	1150	130	380	310	34.05	120	1596	9	9.5	55.855
R-C015Nb	2500	1150	130	380	310	34.05	120	1596	9	9.5	58.29

Members Tested by Zhao and Maruyama (1995)

Beam #	L (mm)	a (mm)	b (mm)	h (mm)	d (mm)	f _c (MPa)	E _{frp} (GPa)	f _{frpu} (MPa)	# bars	d _b (mm)	P _{Max} (kN)
No.1	1800	750	150	300	250	34.3	105	1124	2	19	45
No.15	1800	750	150	300	250	34.3	105	1124	3	19	40.5
No.6	1800	750	150	300	250	34.3	105	1124	4	19	46

GFRP-RC Shear Members

Members Tested by Alkhrdaji, Wideman, Belarbi and Nanni (2001)

Beam #	L (mm)	a (mm)	b (mm)	h (mm)	d (mm)	f' _c (MPa)	E _{frp} (GPa)	f _{frpu} (MPa)	A _{frp} (mm ²)	P _{Max} (kN)
BM7	1500	450	178	330	279	24.1	40	717	1142	53.4
BM8	1500	450	178	330	287	24.1	40	717	393	36.1
BM9	1500	450	178	330	287	24.1	40	717	684	40.05

Members Tested by El-Salakawy, Kassem and Benmokrane (2003)

Beam #	L (mm)	a (mm)	b (mm)	h (mm)	d (mm)	f' _c (MPa)	E _{frp} (GPa)	f _{frpu} (MPa)	# bars	d _b (mm)	P _{Max} (kN)
S-G1	2500	1000	1000	200	162.05	40	40	570	7	15.9	114.285
S-G2B	2500	1000	1000	200	162.05	40	40	570	14	15.9	160.715
S-G3B	2500	1000	1000	200	156.75	40	40	570	21	15.9	165

Members Tested by El-Sayed, El-Salakawy and Benmokrane (2004)

Beam #	L (mm)	a (mm)	b (mm)	h (mm)	d (mm)	f' _c (MPa)	E _{frp} (GPa)	f _{frpu} (MPa)	# bars	d _b (mm)	P _{Max} (kN)
GN-1	2750	1000	250	400	326	50	39	608	10	9.5	70.5
GN-2	2750	1000	250	400	326	44.6	42	754	5	15.9	60
GN-3	2750	1000	250	400	326	43.6	42	754	7	15.9	77.5

Members Tested by Farahmand (1996)

Beam #	L (mm)	a (mm)	b (mm)	h (mm)	d (mm)	f _c (MPa)	E _{frp} (GPa)	f _{frpu} (MPa)	# bars	d _b (mm)	P _{Max} (kN)
Beam#1	2000	1000	200	300	250	31.2	40.3	690	3	10.7	23.7
Beam#2	2000	1000	200	300	250	31.2	40.3	690	2	15.9	25.8
Beam#3	2000	1000	250	300	250	31.2	40.3	690	3	12	32.6
Beam#4	1500	750	200	300	250	35	40.3	690	2	12.7	29.9
Beam#5	1500	750	200	300	250	35	40.3	690	3	12.7	39.3
Beam#6	1500	750	250	300	250	35	40.3	690	4	12.7	37.2
Beam#7	1000	500	200	300	250	31	40.3	690	2	12.7	55.7
Beam#8	1000	500	200	300	250	32.5	40.3	690	3	12.7	57
Beam#9	1000	500	250	300	250	32.5	40.3	690	4	12.7	57

Member Tested by Guadagnini, Pilakoutas and Waldron (2001)

Beam #	L (mm)	a (mm)	b (mm)	h (mm)	d (mm)	f _c (MPa)	E _{frp} (GPa)	f _{frpu} (MPa)	# bars	d _b (mm)	P _{Max} (kN)
GB43	2300	750	150	250	223	50.4	45	750	3	13.5	28.75

Members Tested by Michaluk, Rizkalla, Tadros and Benmokrane (1995)

Beam #	L (mm)	a (mm)	b (mm)	h (mm)	d (mm)	f _c (MPa)	E _{frp} (GPa)	f _{frpu} (MPa)	# bars	d _b (mm)	P _{Max} (kN)
I-150C	3000	1000	1000	150	104	66.0	41.3	690	5	15.9	36.735
I-200C	3000	1000	1000	200	154	66.0	41.3	690	6	15.9	77.78

Member Tested by Najjar, Pilakoutas and Waldron (1997)

Beam #	L (mm)	a (mm)	b (mm)	h (mm)	d (mm)	f _c (MPa)	E _{frp} (GPa)	f _{frpu} (MPa)	# bars	d _b (mm)	P _{Max} (kN)
GB6	2300	767	150	250	220	31.8	45	1000	3	13.5	21.05

Member Tested by Swamy and Aburawi (1997)

Beam #	L (mm)	a (mm)	b (mm)	h (mm)	d (mm)	f _c (MPa)	E _{frp} (GPa)	f _{frpu} (MPa)	# bars	d _b (mm)	P _{Max} (kN)
F-3-GF	2100	700	154	254	222.2	42	34	586	3	15	30

Members Tested by Tariq (2003)

Beam #	L (mm)	a (mm)	b (mm)	h (mm)	d (mm)	f _c (MPa)	E _{frp} (GPa)	f _{frpu} (MPa)	# bars	d _b (mm)	P _{Max} (kN)
R-G007Na	2500	950	160	380	346	34.49	42	674	2	15.9	54.51
R-G007Nb	2500	950	160	380	346	34.49	42	674	2	15.9	63.69
R-G010Na	2500	1150	160	380	346	43.21	42	674	3	15.9	42.755
R-G010Nb	2500	1150	160	380	346	43.21	42	674	3	15.9	45.495
R-G015Na	2500	1150	160	380	325	34.05	42	674	4	15.9	48.69
R-G015Nb	2500	1150	160	380	325	34.05	42	674	4	15.9	44.875

Members Tested by Tureyen and Frosch (2002)

Beam #	L (mm)	a (mm)	b (mm)	h (mm)	d (mm)	f _c (MPa)	E _{frp} (GPa)	f _{frpu} (MPa)	# bars	d _b (mm)	P _{Max} (kN)
V-G1-1	2448	1224	457	406.4	360.4	39.71	40.5	606	8	15.9	108.1
V-G1-2	2448	1224	457	426.7	360.4	42.26	40.5	606	16	15.9	137
V-G2-1	2448	1224	457	406.4	360.4	39.85	37.6	592	8	15.9	94.8
V-G2-2	2448	1224	457	426.7	360.4	42.54	37.6	592	16	15.9	152.6

Members Tested by Yost, Goodspeed and Schmeckpeper (2001)

Beam #	L (mm)	a (mm)	b (mm)	h (mm)	d (mm)	f _c (MPa)	E _{frp} (GPa)	f _{frpu} (MPa)	A _{frp} (mm ²)	P _{Max} (kN)
Lab3FRP1	1778	787	305	216	192	38.0	41.4	830	160	25.6
Lab3FRP2	1778	787	305	216	192	38.0	41.4	830	160	26.7
Lab3FRP3	1778	787	305	216	192	38.0	41.4	830	160	26.7

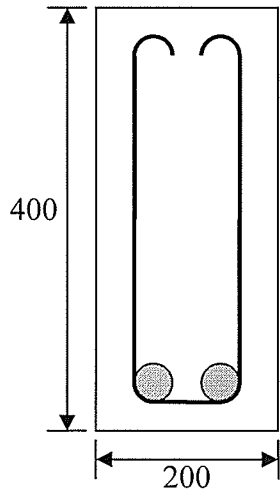
Members Tested by Yost, Gross and Dinehart (2001)

Beam #	L (mm)	a (mm)	b (mm)	h (mm)	d (mm)	f _c (MPa)	E _{frp} (GPa)	f _{frpu} (MPa)	# bars	d _b (mm)	P _{Max} (kN)
2FRPa	2134	914	178	286	225	36.3	40.336	689.5	2	19.05	28.1
2FRPb	2134	914	178	286	225	36.3	40.336	689.5	2	19.05	35
2FRPc	2134	914	178	286	225	36.3	40.336	689.5	2	19.05	32.05
4FRPa	2134	914	178	286	225	36.3	40.336	689.5	4	19.05	43.8
4FRPb	2134	914	178	286	225	36.3	40.336	689.5	4	19.05	45.9
4FRPc	2134	914	178	286	225	36.3	40.336	689.5	4	19.05	46.05

Members Tested by Yost, Gross and Dinehart (2003)

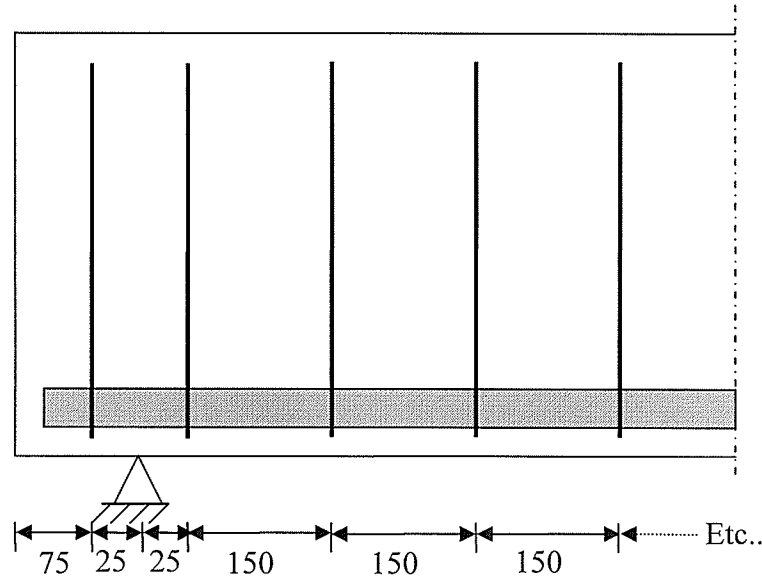
Beam #	L (mm)	a (mm)	b (mm)	h (mm)	d (mm)	f _c (MPa)	E _{frp} (GPa)	f _{frpu} (MPa)	# bars	d _b (mm)	P _{Max} (kN)
1a-NS	2133.6	914.4	228.6	285.75	225.55	36.335	40.3	690	2	19.05	43.14775
1a-NS	2133.6	914.4	228.6	285.75	225.55	36.335	40.3	690	2	19.05	44.48222
1a-NS	2133.6	914.4	228.6	285.75	225.55	36.335	40.3	690	2	19.05	38.25471
2a-NS	2133.6	914.4	228.6	285.75	225.55	36.335	40.3	690	3	19.05	40.2564
2a-NS	2133.6	914.4	228.6	285.75	225.55	36.335	40.3	690	3	19.05	50.2649
2a-NS	2133.6	914.4	228.6	285.75	225.55	36.335	40.3	690	3	19.05	45.59427
3a-NS	2133.6	914.4	254	285.75	223.77	36.335	40.3	690	3	22.225	38.47712
3a-NS	2133.6	914.4	254	285.75	223.77	36.335	40.3	690	3	22.225	52.71143
3a-NS	2133.6	914.4	254	285.75	223.77	36.335	40.3	690	3	22.225	48.93044
4a-NS	2133.6	914.4	228.6	285.75	223.77	36.335	40.3	690	3	22.225	53.60107
4a-NS	2133.6	914.4	228.6	285.75	223.77	36.335	40.3	690	3	22.225	42.48051
4a-NS	2133.6	914.4	228.6	285.75	223.77	36.335	40.3	690	3	22.225	42.25811

Appendix II – Details of Members tested by Mota (2004)

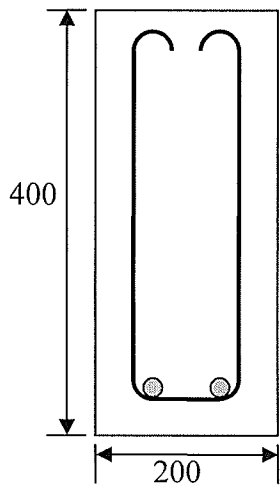


2 – 25 mm
glass bars
10M stirrups

30 mm cover
to stirrups

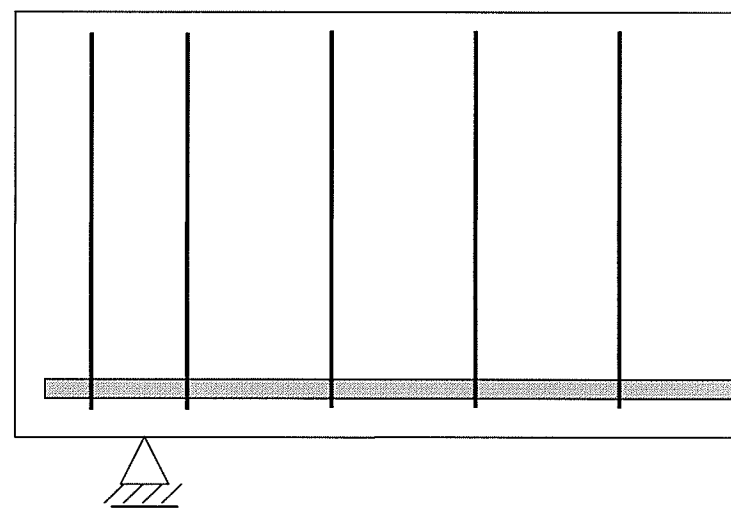


**Beam
D3 #4**

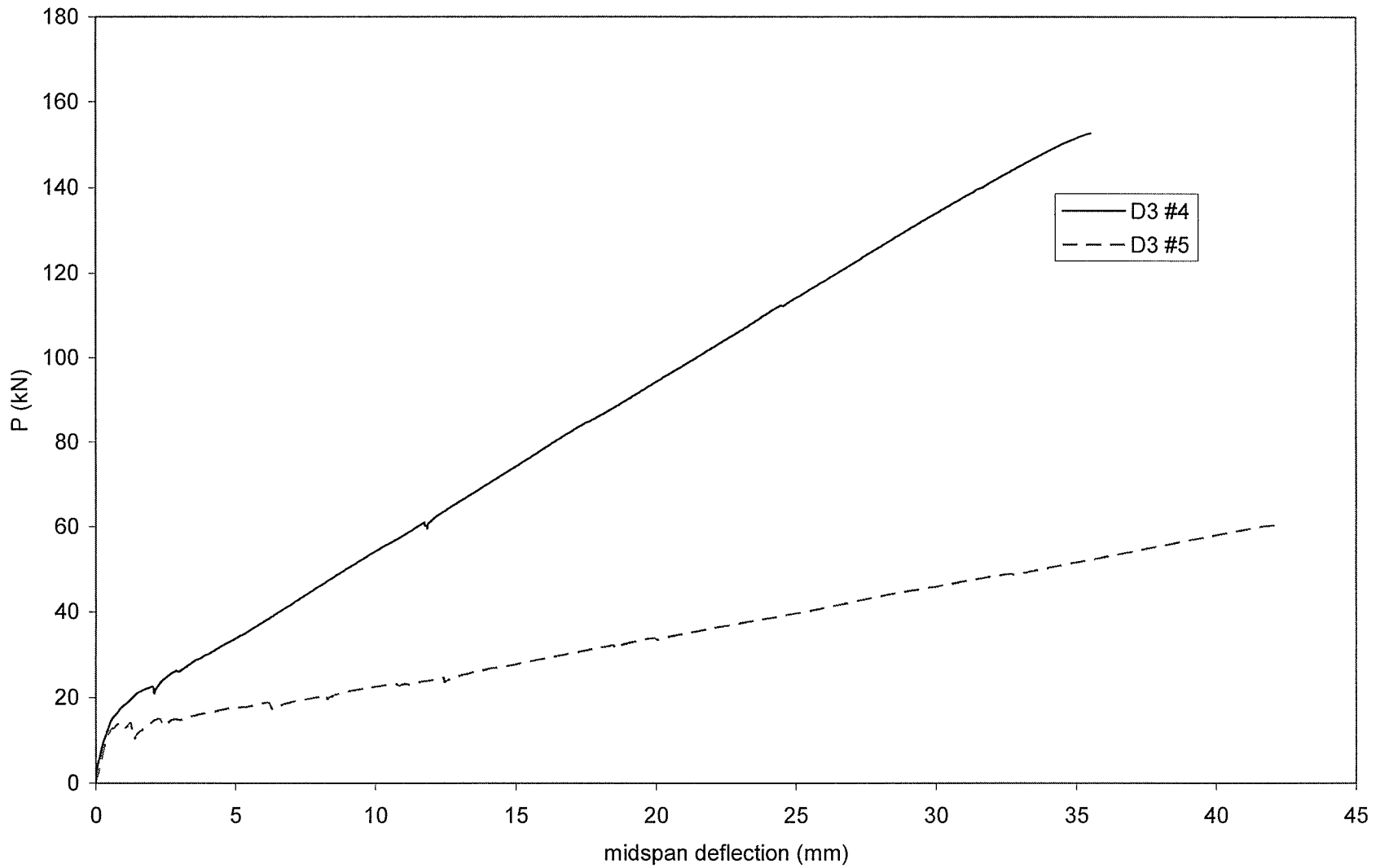


2 – 10 mm
glass bars
10M stirrups

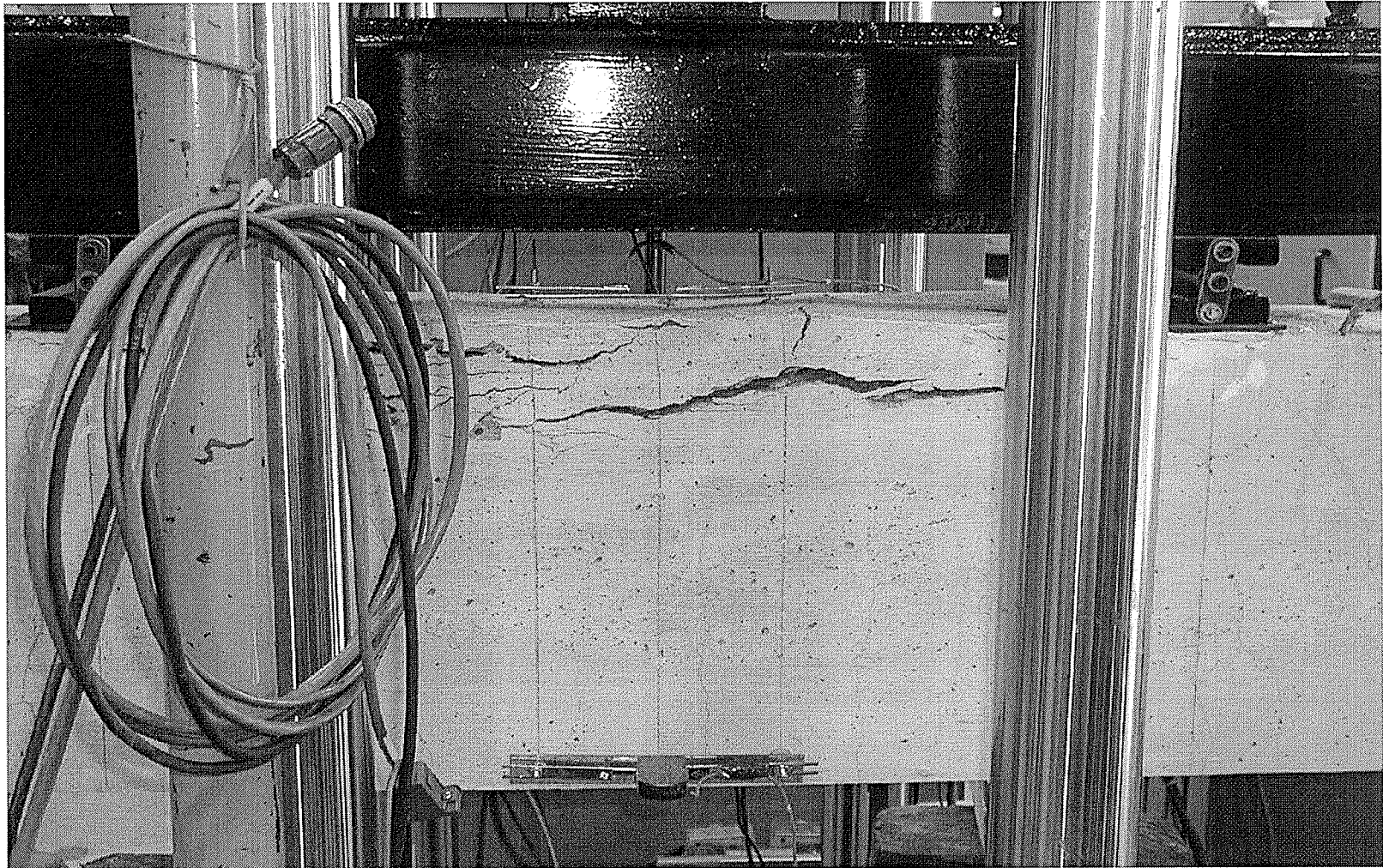
30 mm cover
to stirrups



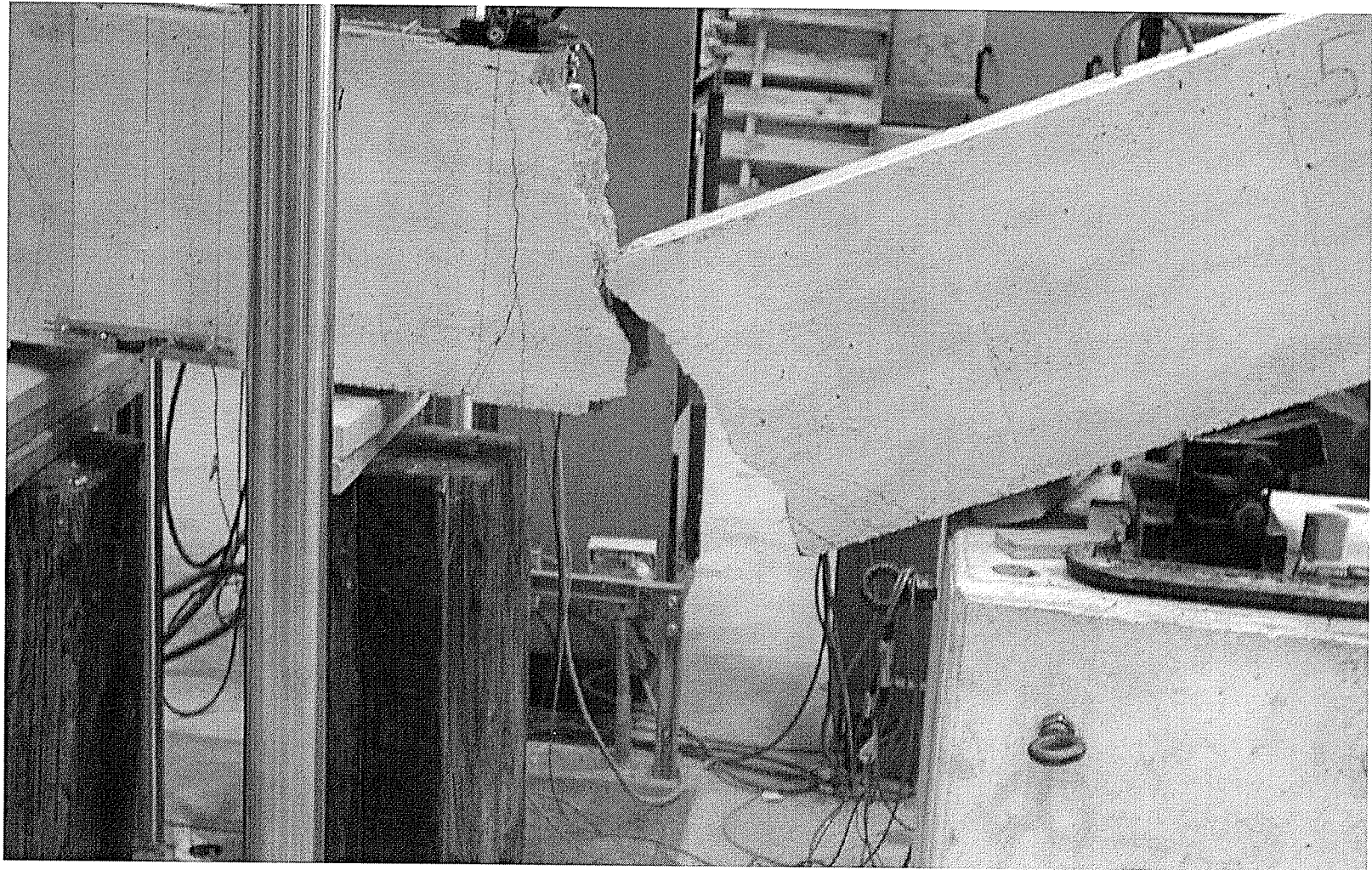
**Beam
D3 #5**



Load-Deflection Behaviour of Beams tested by Mota (2004)



Failure of Beam D3 #4



Failure of Beam D3 #5